



VCU

Virginia Commonwealth University
VCU Scholars Compass

Theses and Dissertations

Graduate School

2018

PROCESSING OF 3'-BLOCKED DNA DOUBLE-STRAND BREAKS BY TYROSYL-DNA PHOSPHODIESTERASE 1, ARTEMIS AND POLYNUCLEOTIDE KINASE/ PHOSPHATASE

Ajinkya S. Kawale
Virginia Commonwealth University

Follow this and additional works at: <https://scholarscompass.vcu.edu/etd>

 Part of the [Biochemistry Commons](#), [Molecular Biology Commons](#), and the [Molecular Genetics Commons](#)

© The Author

Downloaded from

<https://scholarscompass.vcu.edu/etd/5329>

This Dissertation is brought to you for free and open access by the Graduate School at VCU Scholars Compass. It has been accepted for inclusion in Theses and Dissertations by an authorized administrator of VCU Scholars Compass. For more information, please contact libcompass@vcu.edu.

© Ajinkya Kawale 2018
All Rights Reserved

PROCESSING OF 3'-BLOCKED DNA DOUBLE-STRAND BREAKS BY TYROSYL-DNA
PHOSPHODIESTERASE 1, ARTEMIS AND POLYNUCLEOTIDE KINASE/
PHOSPHATASE

A dissertation submitted in partial fulfillment of the requirements for the degree of Doctor of
Philosophy at Virginia Commonwealth University.

Ajinkya Kawale,
MS, Pharmacology and Toxicology, Virginia Commonwealth University, 2015
B.Tech, Biotechnology, Dr. D. Y. Patil University, 2013

Advisor: Dr. Lawrence F. Povirk, Professor, Department of Pharmacology and Toxicology

Virginia Commonwealth University
Richmond, Virginia,
April, 2018.

ACKNOWLEDGEMENTS

Several people have played important roles in helping me reach this stage in my professional career and the little success that I have achieved is a direct extension of all of their hardwork and blessings. First and foremost, I would like to express my sincere gratitude to my PhD Advisor, Dr. Lawrence F. Povirk. He has been a fantastic mentor throughout my time in his lab and has helped me at each and every stage of my graduate career. He is an extremely motivated, determined and an intelligent scientist and has indirectly taught me the importance of those virtues. Even at the dusk of his career, he can be seen working at the bench not only during regular hours, but also on weekends trying to standardize and getting the experiments to work. He is a man of few words and naturally, those few words carry a lot of weight and meaning. It is unfortunate that such a great scientist is laying down his armor. He will be retiring in the coming months and it is a big loss to science and the field of DNA repair. If I get to be 10% of a scientist as he was in his career, I would have done a good job in my professional life.

I would also like to appreciate all my committee members, Dr. Kris Valerie, Dr. Ross Mikkelsen, Dr. Tomasz Kordula and Dr. David Gewirtz. Suggestions provided by all of them have been extremely valuable in providing a definite direction for my project. Their advice in helping me choose a postdoc position was very helpful. Specially, the discussions I have had with Dr. Mikkelsen have been very insightful and fun at the same time. He has been a big supporter of me throughout these years and I am really grateful for that. I would also like to thank Dr. Gail Christie and Dr. Hamid Akbarali for their guidance. Both of them have been very patient in answering all my questions and have given some terrific advice. I would also like to acknowledge Dr. Larisa Litovchick for her guidance and Dr. Jill Bettinger for making me a better public speaker. It would have been impossible for me to continue doing my PhD without the financial support provided by Dr. William Dewey and the Pharmacology and Toxicology department.

If my mind and my intellect have been sharpened by Dr. Povirk, my hands have been trained by my colleagues in the lab, especially, Dr. Konstantin Akopiants. He has been a great colleague and a mentor and has taught me the importance of pessimism in science. Several others who started out as colleagues became friends along the way. I have enjoyed several discussions with Dr. Srilakshmi Chalasani and have almost always ended up on the opposite sides. It has been a pleasure to work alongside her who kept the lab environment lively and jolly.

I have been extremely lucky to have my best friend/fiancée, Varsha Ananthapadmanabhan, through this whole journey and has been my support system for these past three years. I cannot

imagine going through this period without having her on my side. She has a great scientific acumen and has given me some very valuable suggestions that have helped me in my project. Away from work, all the activities that we have done together including skydiving and several hiking trips have really helped in taking my mind away from the studies. I have enjoyed spending time with Dr. Vijay Menon and Dr. Amrita Sule both in and outside the lab environment. I would also like to acknowledge friends who became family along the way; Jacob and Mary Ann Copetilo and their three kids, Ava, Matthew and Gabriel.

My parents, Sudhir and Smita Kawale, have a lion's share in all the success that I have attained in reaching at this position. They have worked hard and have made tremendous sacrifices in their lives to ensure that I get what I want. I would also like to acknowledge the influence of my maternal uncle and aunt, Suhas and Anuradha Bhargave on several decisions that I have taken in my life.

Lastly, I would like to dedicate this dissertation to my grandfather, Madhukar Kawale, who passed away last year. I was unfortunate in not being able to be with him in his last days but he will always remain in my heart.

TABLE OF CONTENTS

LIST OF FIGURES	viii
LIST OF ABBREVIATIONS	xi
ABSTRACT.....	xviii
1. GENERAL INTRODUCTION	1
1.1 Structure of DNA	1
1.2 Historical Perspective on DNA repair.....	2
1.3 Double strand breaks – most lethal of all DNA lesions	6
1.4 DNA damage response.....	11
1.5 Double-strand break repair pathways.....	12
1.6 Non-Homologous End Joining (NHEJ)	13
1.6.1 DSB recognition and complex assembly	14
1.6.2 DSB end-processing	15
1.6.3 DNA end-ligation	16
1.7 Radiomimetic Agents.....	17
1.7.1 Neocarzinostatin (NCS).....	18

1.7.2 Calicheamicin	20
2. INTRODUCTION TO THE THESIS	24
2.1 Tyrosyl-DNA Phosphodiesterase 1 (TDP1).....	24
2.1.1 Discovery.....	25
2.1.2 Structure.....	26
2.1.3 Catalytic Mechanism	27
2.1.4 Role in SSB repair	30
2.1.5 Regulation of TDP1	32
2.1.6 TDP1 in DSB repair	33
2.2 Artemis.....	35
2.2.1 Discovery.....	35
2.2.2 Structure.....	36
2.2.3 Biochemical properties	37
2.2.4 Function in DSB repair.....	39
2.3 Polynucleotide Kinase/ Phosphatase.....	40
2.3.1 Structure.....	41
2.3.2 Function	41
2. 4 Specific Aims	43

3. MATERIALS AND METHODS.....	45
3.1 Cell lines and reagents.....	45
3.1.1 HCT116 cells.....	46
3.1.2 HEK293 and HEK293T cells.....	47
3.1.3 48BR WT and CJ179 Artemis deficient fibroblasts.....	49
3.2 Dilution cloning for selection of clones.....	51
3.3 Growth curve assay.....	51
3.4 TDP1 activity assay.....	51
3.5 Sequencing polyacrylamide gel electrophoresis.....	52
3.6 Cytosol-Nuclear Fractionation.....	52
3.7 Western blot analyses.....	53
3.8 Clonogenic survival assays.....	53
3.9 Mitotic shake-off for G1-phase synchronization.....	54
3.10 Immunofluorescence.....	55
3.11 Cell cycle analysis by flow cytometry.....	55
3.12 Centromere-fluorescence in situ hybridization.....	56
3.13 Transformation.....	57
3.13 Statistics.....	57

4. RESULTS	59
4.1 Generation of TDP1-mutant (shTDP1 and TDP1 ^{-/-}) cell lines.....	59
4.2 TDP1 deficient cells are hypersensitive to ionizing radiation and radiomimetic agents. ...	63
4.3 Generation of TDP1 and Artemis double knockouts	66
4.4 TDP1 and Artemis are epistatic for the repair of 3'-PG DSBs via NHEJ.....	71
4.5 Absence of Artemis but not TDP1 confers a defect in DSB rejoining	77
4.6 Loss of TDP1 but not Artemis leads to misjoining of 3'-PG DSBs.....	85
4.7 Absence of Artemis delays G1-S progression upon DSB induction; this delay is rescued in an additional absence of TDP1.....	91
4.8 Interplay between TDP1/Artemis with the DNA damage response proteins PARP1 and ATM.....	96
4.9 PNKP-deficient cells display enhanced hypersensitivity to NCS.....	100
4.10 Interplay between PNKP and other DNA repair factors.....	103
4.10 PNKP is required for rejoining of 3'-P ended DSBs in cells.	107
5. DISCUSSION	110
6. CONCLUSIONS AND FUTURE PERSPECTIVES	124
7. BIBLIOGRAPHY	127

LIST OF FIGURES

Figure 1-1 Albert Kelner (Left) and Renato Dulbecco (Right)	5
Figure 1-2: DNA Damage response (top) and 53BP1 recruitment at DSB sites(bottom)	8
Figure 1-3: Double-strand break repair pathways	9
Figure 1-4: Non-Homologous End Joining Pathway Schematic	10
Figure 1-5: Structures of enediyne antitumor antibiotics - Calicheamicin (Top) and Neocarzinostatin (bottom)	21
Figure 1-6: Mechanism of NCS action and typical DSB ends formed.....	22
Figure 1-7: NCS and CAL induced bistranded lesions with specific modifications	23
Figure 2-1: Structure of TDP1	28
Figure 2-2: Catalytic mechanism of TDP1 in its canonical function.....	29
Figure 3-1: Lentiviral transfer vector pLSLPw harboring the shRNA against TDP1	50
Figure 4-1- TDP1 expression in HCT116 cells.	61
Figure 4-2: TDP1 expression in HEK293 cells.	62
Figure 4-3: Loss of TDP1 enhances the cytotoxicity of radiomimetic agents in HCT116 cells. .	64
Figure 4-4: Loss of TDP1 enhances the cytotoxicity of radiomimetic agents in HEK293 and HEK293T cells.....	65
Figure 4-5: Characterization of Artemis ^{-/-} shTDP1 cell line.....	68

Figure 4-6: Growth curve.....	69
Figure 4-7: Characterization of HCT116 Artemis ^{-/-} .TDP1 ^{-/-} mutant cells	70
Figure 4-8: TDP1 and Artemis are epistatic for the repair of 3'-PG-ended DSBs	73
Figure 4-9: Cell Cycle Synchronization by Mitotic shakeoff.....	74
Figure 4-10: TDP1 and Artemis are epistatic in the G1-phase for the repair of 3'-PG-ended DSBs	75
Figure 4-11: TDP1 and Artemis are epistatic with DNA-PK for the repair of NCS-induced DSBs.	76
Figure 4-12: Representative confocal images of 53BP1 repair foci in HCT116 WT cells.	79
Figure 4-13: Representative confocal images of 53BP1 repair foci in HCT116 shTDP1#18 cells.	80
Figure 4-14: Representative confocal images of 53BP1 repair foci in HCT116 Artemis ^{-/-} cells.	81
Figure 4-15: Representative confocal images of 53BP1 repair foci in HCT116 Artemis ^{-/-} •shTDP1#2 #2 cells.....	82
Figure 4-16: Artemis-deficient but not TDP1-depleted cells show a DSB rejoining defect	83
Figure 4-17: Dose-dependent increase in 53BP1 foci	84
Figure 4-18: TDP1 depletion leads to misjoining of DSBs.	87
Figure 4-19: Chromosomal Aberrations in HCT116 cells upon NCS treatment.....	88
Figure 4-20: TDP1 deficiency leads to increased chromosomal aberrations in HEK293 cells upon NCS treatment.....	89
Figure 4-21: Chromosomal Aberrations in HEK293 cells upon NCS treatment.....	90

Figure 4-22: G1-S Cell Cycle Progression in HCT116 cells	93
Figure 4-23: G1-S cell cycle progression followed by G2/M arrest in HCT116 cells in the presence of Nocodazole	94
Figure 4-24: G1-S cell cycle progression upon DSB induction by NCS in HCT116 cells.	95
Figure 4-25: Artemis and TDP1 function in parallel with PARP1 in response to NCS-induced DSBs.	98
Figure 4-26: TDP1 and Artemis function in parallel to ATM in response to NCS-induced DSBs.	99
Figure 4-27: Absence of PNKP in nuclear extracts of PNKP ^{-/-} HCT116 cells.	101
Figure 4-28: PNKP-deficient cells are hypersensitive to NCS and radiation.....	102
Figure 4-29: Interplay between PNKP and ATM, DNA-PK and PARP1 in response to NCS-induced DSBs.....	105
Figure 4-30: Confirmation of PARP inhibition using western blotting.....	106
Figure 4-31: PNKP-deficient cells show a defect in 3'-P DSB rejoining.....	108
Figure 4-32: PNKP ^{-/-} cells show increased HR compared to WT cells for repairing 3'-P ended DSBs	109
Figure 5-1: Model of the epistasis between Artemis and TDP1	112

LIST OF ABBREVIATIONS

'	Prime
°C	degrees Centigrade
53BP1	p53 binding protein
A	Adenine
Å	Angstrom
ACV	Acyclovir
AOA4	Ataxia with Oculomotor Apraxia 4
AP	Apurinic/ Apyrimidinic
APE1	Apurinic/ Apyrimidinic Endonuclease 1
APLF	Aprataxin and PNKP-like factor
ATCC	American Type Culture Collection
ATL	Adult T-cell Leukemia
ATM	Ataxia Telangiectasia Mutated
ATR	ATM and Rad3-related
AZT	Zidovudine
BER	Base Excision Repair
BIA	Biochemical Induction Assay

BRCT	Breast Cancer Susceptibility Gene C Terminus
BSA	Bovine Serum Albumin
C	Cytosine
Chk2	Checkpoint Kinase 2
cm	centimeter
CO ₂	Carbon dioxide
CPT	Camptothecin
CtIP	C-terminal binding protein-interacting protein
CTNA	Chain terminating nucleoside analog
Cy5	Cyanine 5
DAPI	4'-6-diamidino-2-phenylindole
DCLRE1C	DNA Cross-Link Repair 1C
ddC	Zalcitabine
DDR	DNA damage response
DMSO	Dimethyl Sulfoxide
DNA	Deoxyribose Nucleic Acid
DNA-PKcs	DNA-dependent Protein Kinase catalytic subunit
DRB	5,6-dichloro-1-β-D-ribofuranosylbenzimidazole
dRP	deoxyribosephosphate
DSBs	Double Strand Breaks
DTT	Dithiothrietol

EDTA	ethylene diamine tetraacetic acid
EPR	Enzymatic Photoreactivation
FBS	Fetal Bovine Serum
FHA	forkhead associated
G	Guanine
G1	Growth 1
G2	Growth 2
GFP	Green Fluorescent Protein
Gy	Gray
H	Histidine
HAc	Acetic Acid
HAD	haloacid dehydrogenase
HEK	Human Embryonic Kidney
HEPES	4-(2-hydroxyethyl)-1-piperazineethanesulfonic acid
HKN	Histidine Lysine Asparagine
HR	Homologous Recombination
IR	Ionising radiation
K	Potassium
KCl	Potassium Chloride
KDa	KiloDalton
M	Molar

MCSZ	Microcephaly with Seizures
MDC1	Mediator of DNA-damage Checkpoint protein 1
MEF	Mouse Embryonic Fibroblast
Mg	Magnesium
Min	minutes
mL	millilitre
MMS	methyl methane sulfonate
MRN	Mre11-Rad50-Nbs1
N ₂	Nitrogen
NaCl	Sodium Chloride
NaVO ₄	Sodium Orthovanadate
NCS	Neocarzinostatin
NCS-Chrom	Neocarzinostatin – chromophore
NHEJ	Non-Homologous End Joining
NP-40	nonyl phenoxy polyethoxy ethanol
Pac	Puromycin N-Acetyl transferase
PARP	Poly (ADP-ribose) polymerase
PBS	Phosphate Buffered Saline
PCR	Polymerase Chain Reaction
PE	Plating Efficiency
PG	phosphoglycolate

PI	Propidium iodide
PIKK	phosphoinositol-3-kinase-like kinase
PLD	Phospholipase D
pM	picomolar
PMSF	phenylmethanesulfonyl fluoride
PMT	photomultiplier tube
PNKP	Polynucleotide Kinase Phosphatase
PTM	post translational modifications
pTyr	phosphotyrosine
R	Arginine
RNF	RING finger protein
ROS	Reactive Oxygen Species
ROS	reactive oxygen species
RPM	rotations per minute
RPMI	Roswell Park Memorial Institute
RS-SCID	Radiosensitive – Severe combined Immunodeficiency
SCAN1	Spinocerebellar Ataxia with Axonal Neuropathy
SDSA	Synthesis-Dependent Strand Annealing
SEM	Standard Error of Mean
SF	Surviving Fraction
shRNA	short hairpin ribonucleic acid

S-phase	Synthesis phase
SSA	Single-Strand Annealing
SSBs	Single Strand Breaks
T	Thymine
TBE	Tris Borate EDTA
TDP1	Tyrosyl-DNA Phosphodiesterase 1
TDP2	Tyrosyl-DNA Phosphodiesterase 2
TEMED	N, N, N', N'-tetramethylethylene diamine
Top 1	Topoisomerase 1
Top1cc	Topoisomerase 1 cleavage complex
TX	Texas
UV	Ultraviolet
V(D)J	Variable (Discrete) Joining
W	Watts
WCE	Whole cell extracts
XLF	XRCC4-like factor
XRCC4	X-Ray Cross Complementing Protein 4
Y	tyrosine
α	Alpha
β	Beta
γ	Gamma

Θ	Theta
λ	Lambda
μ	Mu
μm	micrometer

ABSTRACT**PROCESSING OF 3'-BLOCKED DNA DOUBLE-STRAND BREAKS BY TYROSYL-DNA
PHOSPHODIESTERASE 1, ARTEMIS AND POLYNUCLEOTIDE KINASE/
PHOSPHATASE**

Ajinkya Kawale, MS

A dissertation submitted in partial fulfillment of the requirements for the degree of Doctor of
Philosophy at Virginia Commonwealth University.

Virginia Commonwealth University, 2018.

Advisor: Dr. Lawrence F. Povirk, Professor, Department of Pharmacology and Toxicology

DNA double-strand breaks (DSBs) containing unligatable termini are potent cytotoxic lesions leading to growth arrest or cell death. The Artemis nuclease and tyrosyl-DNA phosphodiesterase (TDP1) are each capable of resolving protruding 3'-phosphoglycolate (PG) termini of DNA double-strand breaks (DSBs). Consequently, a knockout of Artemis and a knockout/knockdown of TDP1 rendered cells sensitive to the radiomimetic agent neocarzinostatin (NCS), which induces 3'-PG-terminated DSBs. Unexpectedly, however, a knockdown or knockout of TDP1 in Artemis-null cells did not confer any greater sensitivity than either deficiency

alone, indicating a strict epistasis between TDP1 and Artemis. Moreover, a deficiency in Artemis, but not TDP1, resulted in a fraction of unrepaired DSBs, which were assessed as 53BP1 foci. Conversely, a deficiency in TDP1, but not Artemis, resulted in a dramatic increase in dicentric chromosomes following NCS treatment. An inhibitor of DNA-dependent protein kinase, a key regulator of the classical nonhomologous end joining (C-NHEJ) pathway sensitized cells to NCS but eliminated the sensitizing effects of both TDP1 and Artemis deficiencies. Moreover, Polynucleotide Kinase/ Phosphatase (PNKP) is known to process 3'-phosphates and 5'-hydroxyls during DSB repair. PNKP-deficiency sensitized both HCT116 and HeLa cells to 3'-phosphate ended DSBs formed upon radiation and radiomimetic drug treatment. The increased cytotoxicity in the absence of PNKP was synonymous with persistent, un-rejoined 3'-phosphate-ended DSBs. However, DNA-PK deficiency sensitized PNKP^{-/-} cells to low doses of NCS suggesting that, in the absence of PNKP, alternative enzyme(s) can remove 3'-phosphates in a DNA-PK-dependent manner. These results suggest that TDP1 and Artemis perform different functions in the repair of terminally blocked DSBs by the C-NHEJ pathway, and that whereas an Artemis deficiency prevents end joining of some DSBs, a TDP1 deficiency tends to promote DSB mis-joining. In addition, loss of PNKP significantly sensitizes cells to 3'-phosphate-ended DSBs due to a defect in 3'-dephosphorylation.

1. GENERAL INTRODUCTION

1.1 Structure of DNA

The discovery of the double-helical structure of DNA was arguably one of the most important breakthroughs that revolutionized biology forever. Linus Pauling, a pioneer and the world's best physical chemist at that time, had just discovered the single-stranded alpha helical structure found in proteins and had diverted his attention to the elucidating the structure of DNA and was at the pole position to finding it out. Pauling soon proposed a tripe helix model of DNA that surprisingly had the bases orienting outwards and the phosphates facing the interior! Soon, it was realized that the like negative charges on the phosphates would repel them and it became apparent that his structure was incorrect.

On April 25th 1953, in their seminal paper, James Watson and Francis Crick laid out the molecular structure of nucleic acids (WATSON & CRICK, 1953). The structure of DNA described by Watson and Crick, who were greatly helped by Rosalind Franklin and Maurice Wilkins, had a double-helix with the phosphates pointing outwards unlike the triple helix put forth by Pauling. The two helical chains are comprised of the sugar phosphate backbone that run antiparallel to one another.

The bases are oriented on the inside of the helix allowing them to hydrogen bond with the corresponding bases on the opposite strand holding the two strands together by purine and pyrimidine bases. The purines (Adenine and Guanine) always pair with their Pyrimidine counterparts (Thymine and Cytosine respectively). The intra-strand distance between each base is 3.4 Å. One helical turn of DNA has 10 bases and is thus, 34 Å long whereas the distance between the two strands is 20 Å. For their discovery of the structure of DNA, James Watson, Francis Crick and Maurice Wilkins were awarded the Nobel Prize in Physiology and Medicine in 1962. At the end of their seminal paper, Watson and Crick made an interesting comment that opened up new avenues for researchers leading to the proposal of not only the basic central dogma of molecular biology comprising of DNA replication, transcription and translation but also other DNA metabolic processes like DNA repair and recombination.

“It has not escaped our notice that the specific pairing we have postulated immediately suggests a possible copying mechanism for the genetic material.”
- Jim Watson & Francis Crick, Nature 1953.

1.2 Historical Perspective on DNA repair

Damaged DNA can be repaired by different types of distinct mechanisms that differ drastically from one another. It is believed that the process of enzymatic photoreactivation (EPR) is the first DNA repair mechanism that evolved in nature. When life was evolving in the primordial soup, one can imagine the important role this process would have played in protecting the DNA of these early organisms from the harmful UV radiation coming from the sun. Incidentally, EPR was also the first DNA repair mechanism to be discovered independently by two American groups in the 1940s, almost a decade prior to the discovery of the structure of DNA (Friedberg, 2008; Friedberg, 2015).

Following the discovery of penicillin, Albert Kelner, working at the Cold Spring Harbor Laboratory, was attempting to identify strains of *Streptomyces* that produced new and more efficacious antibiotics. In an attempt to standardize his experimental system, Kelner was trying to mutagenize *E. coli* and *Streptomyces* cells growing on agar plates by exposing them to different doses of UV radiation. To his great dissatisfaction, he regularly obtained extremely irreproducible survival yields. In a letter to one of his friends, Kelner confided his frustration:

“My first task was to irradiate *E. coli* with UV light to induce mutants, and from the first experiment in October 1946 I ran into difficulty with the reproducibility of survival rates..... I would irradiate a suspension, assay an aliquot for survival, storing the remainder of the suspension at 5 °C until the assay plates grew..... I needed a suspension of irradiated cells whose titer was accurate to about +/- 25% colonies per plate. But irradiation with the same UV dose two days apart gave variations exceeding this limit..... By October or November of 1946, I had acquired a healthy disrespect for the implications of quantitative exactness of the beautiful UV survival curves in the literature.”

-Albert Kelner in a letter to Claude Stanley Rupert, 14 years after his experiments (Friedberg, 2008)

Little did he know, he was onto something spectacular. Upon further examination, Kelner found out the source of his variable results was exposure to fluorescent lights in the laboratory and also further demonstrated that exposure of cells to visible light considerably rescued the viability of UV-irradiated cells.

While Kelner was trying to find an explanation to his enigmatic observations, around 800 miles away at University of Indiana - Bloomington, Renato Dulbecco, a postdoc in the lab of Salvatore Luria, was trying to study bacteriophage replication. While attempting to mutagenize phage-infected cells using UV-radiation, Dulbecco observed a great variation in the surviving fraction of phages obtained from the stacks of agar plates stored on his bench. Quite smartly, he

noticed that plates from top of the stacks showed the greatest number of plaques formed by the phages. An excerpt from the letter written by Luria to Kelner describing Dulbecco's findings is provided below:

“Dulbecco ran into photoreactivation in a most queer way, by forgetting to put off the fluorescent light on a table on which he left a pile of plates with irradiated phage to incubate them at room temperature. Next day the top plate had 100× more plaques than the bottom one, and the intermediate ones had gradually different numbers..... It is a most exciting thing, and I imagine that the bacterial phenomenon you discovered must also be such.”

- Salvadore Luria in a note to Albert Kelner (Friedberg, 2008)

Like Kelner, Dulbecco too realized the presence of a light-dependent mechanism of DNA repair. These serendipitous discoveries led to the identification of the photoreactivation process and was later demonstrated to be catalyzed by a light-dependent photoreactivating enzyme. Interestingly, a young graduate student by the name of James Watson was one of Dulbecco's colleagues who went on to demonstrate that photoreactivation was not observed when cells were exposed to ionizing radiation instead of UV radiation (Friedberg, 2008).

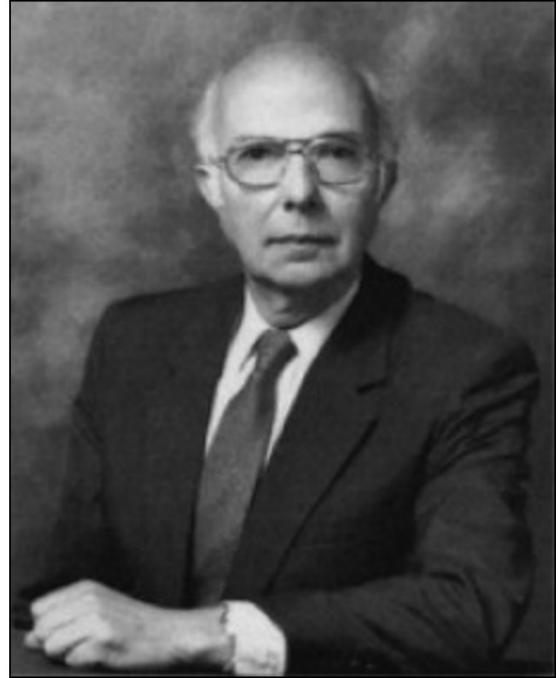


Figure 1-1 Albert Kelner (Left) and Renato Dulbecco (Right)

Adapted from (Friedberg, 2008)

1.3 Double strand breaks – most lethal of all DNA lesions

Since the identification of DNA as the genetic material followed by the discovery of its structure almost 65 years ago, astute investigations have revealed the presence of complex mechanisms that preserve the genetic message encoded by DNA. These remarkable mechanisms protect the integrity of the genome by rapid and efficient repair of the damage induced to DNA and thus, warrant accurate transmission of genetic information over many generations.

Spontaneous endogenous damage constitutes DNA alterations brought about by misincorporation of nucleotides during DNA replication, modification of bases by alkylation or deamination, abasic lesions formed due to depurination and oxidation of bases and single- and double-strand breaks as a result of reactive oxygen species (ROS) formed during normal cell metabolism (Chapman, Taylor, & Boulton, 2012). Exogenous DNA damage can be induced by various physical and chemical sources. Ultraviolet radiation (UV-B) from sunlight is estimated to induce almost 10^5 pyrimidine dimers or photoproducts per cell per day (Ciccia & Elledge, 2010). Ionizing radiation is extremely heterogenous and produces a large number of strand breaks in addition to base damage. The list of chemical agents inducing DNA damage is nearly limitless and includes a variety of drugs used in cancer chemotherapy such as alkylating agents (temozolomide), crosslinking agents (platinum drugs), topoisomerase poisons, radiomimetic drugs, etc.

In contrast to other DNA lesions, DSBs are the most threatening as their defining feature is a physical disruption of the molecular continuity of DNA. The frequency with which DSBs are induced by exogenous sources of radiation is especially very high. Interesting statistical values help put this fact into perspective. Assuming that mammalian cells irradiated with 1 Gy accumulate around 40 DSBs per cell and ~1000 SSBs per cell, an approximately 20-hour flight from Mumbai, India to Richmond, Virginia results in around 0.004 DSBs per cell, a full body CT scan leads to

around 0.3 DSBs per cell, a 2-month space mission results in around 2 DSBs per cell, the Chernobyl incident resulted in around 12 DSBs per cell, external beam radiotherapy results in around 80 DSBs per cell (Ciccica & Elledge, 2010).

However, the potentially lethal damage that DSBs can cause is perhaps more alarming than their sheer numbers. If DSBs are left unrepaired, all the genetic material between the breaks and the telomeres could be potentially lost during mitosis. This could result in large deletions in chromosomes resulting in daughter cells devoid of critical genetic regions and cause cell death. If DSBs are inappropriately repaired, it can cause large sequential alterations and lead to chromosomal aberrations including inversions, deletions and translocations by illegitimate joining of wrong pair of DSBs ends (Deriano & Roth, 2013). The deletions can lead to inactivation of critical tumor suppressor genes leading to neoplastic transformation. Chromosomal translocations can result in gene fusion activating oncogenes and causing transformation of normal cells into cancer cells. A study conducted 10 years ago suggested that gene fusions accounted for around 20% of human cancer morbidity (Mitelman, Johansson, & Mertens, 2007). Given the lethality of DSBs, it is extremely essential for cells to be effectively armored against these lethal lesions. Fortunately, cells have evolved highly orchestrated and complex network of responses to deal with DSBs referred to as the DNA damage response (DDR).

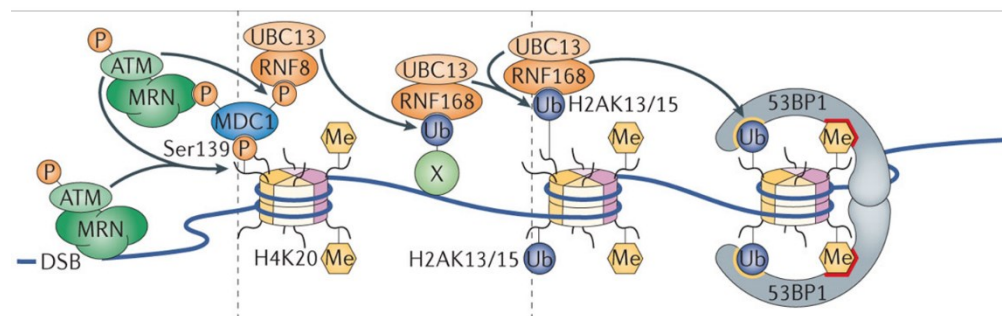
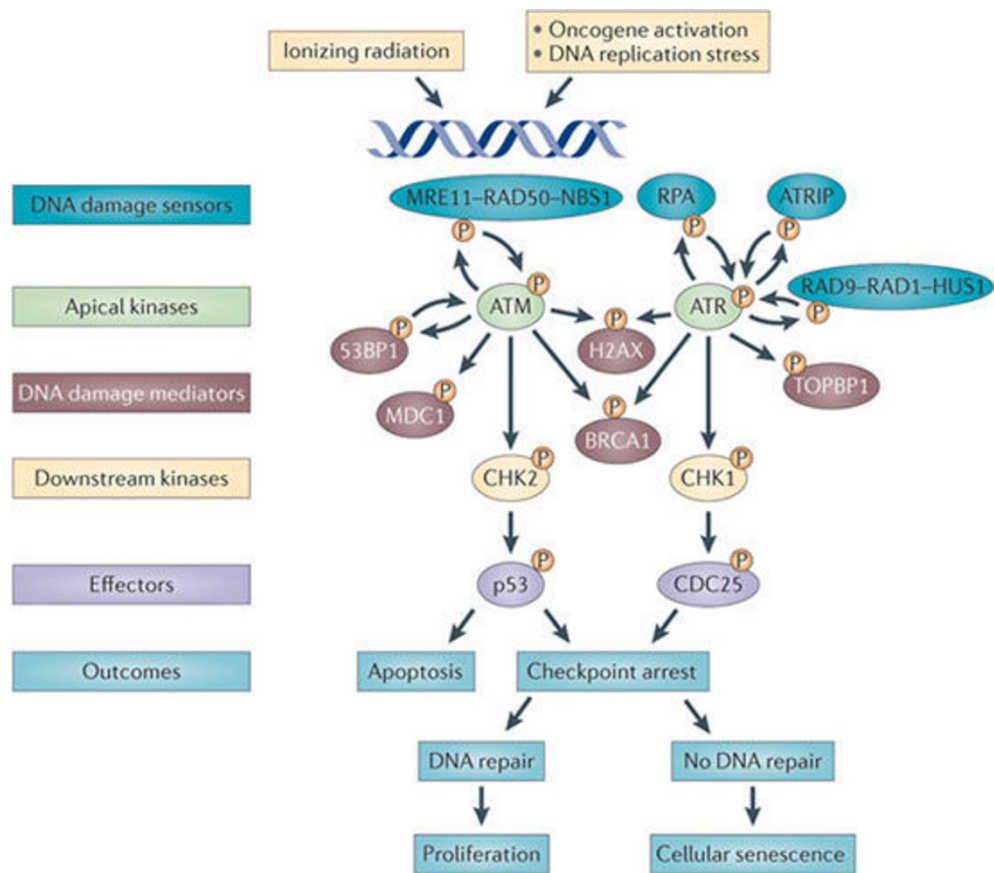


Figure 1-2: DNA Damage response (top) and 53BP1 recruitment at DSB sites (bottom)

The DNA damage response is elicited upon DSB formation that includes a whole host of proteins taking part in different activities ultimately recruiting the effector protein 53BP1. (Panier & Boulton, 2014; Sulli, Di Micco, & d'Adda di Fagagna, 2012)

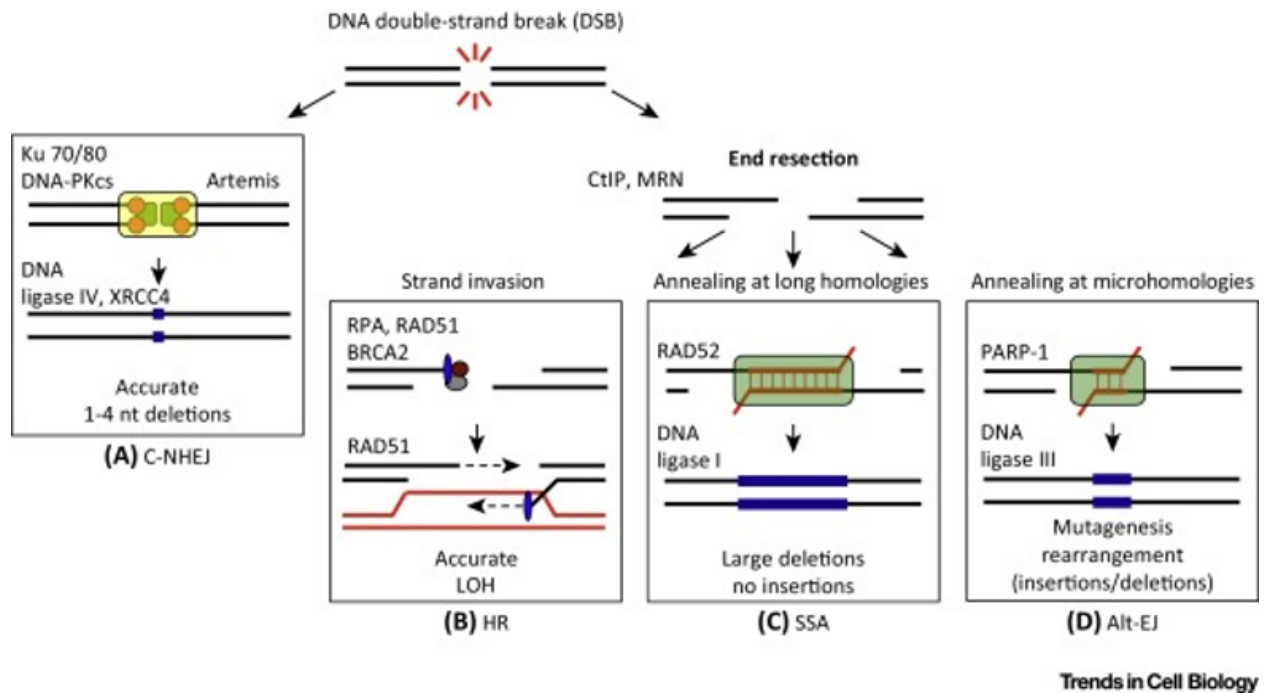


Figure 1-3: Double-strand break repair pathways

DSB induction leads to the activation of DSB repair pathways. Depending on the cell cycle phase and recruitment of certain proteins, specific pathways are activated. cNHEJ is the most dominant pathway active throughout the cell cycle that functions with minima if any resection. If the break is resected, it leads to the channeling of the DSBs to either HR, SSA or A-EJ. (Ceccaldi, Rondinelli, & D'Andrea, 2016)

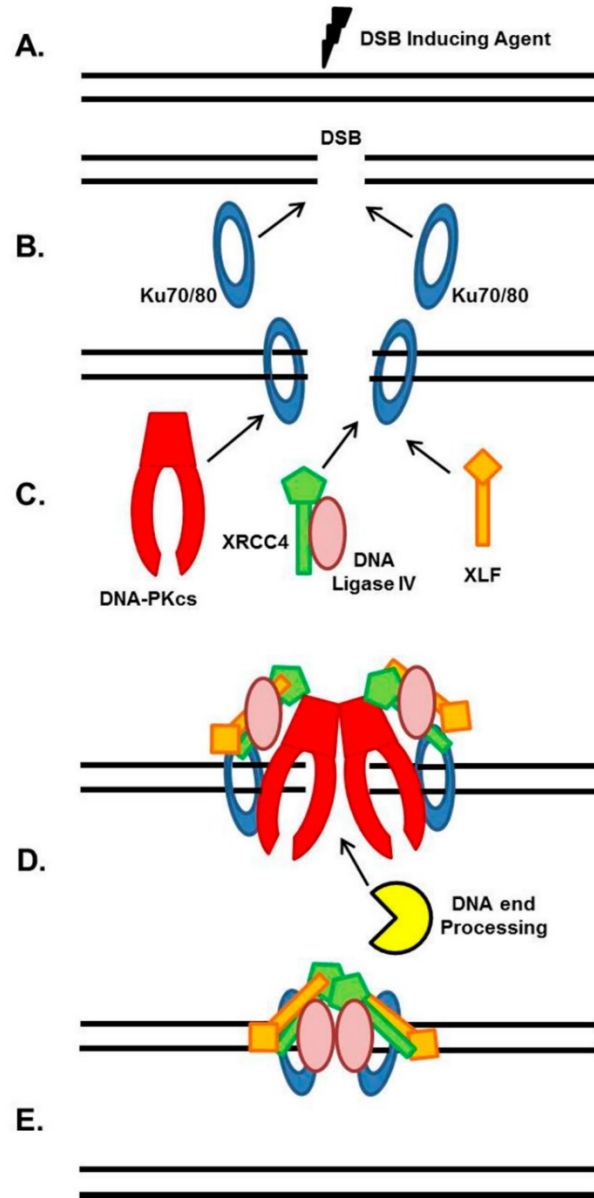


Figure 1-4: Non-Homologous End Joining Pathway Schematic

Upon DSB induction, Ku70/80 immediately binds to the DSB ends and channels the DSBs towards NHEJ. It recruits other proteins in NHEJ including DNA-PKcs, XRCC4/Ligase IV and XLF. This leads to the bridging of DNA ends via a filament mediated by XRCC4 and XLF. Nucleases and polymerases may also be recruited to the DSB sites to process the modified ends. Once the ends have been made ligatable, Ligase IV in association with XRCC4 ligates the ends resealing the break. (Davis & Chen, 2013)

1.4 DNA damage response

For any effective repair system, high sensitivity allowing the rapid detection of even a single lesion is paramount. The DDR is an answer for the high sensitivity detection of DSBs and elicits an orchestrated response downstream for their accurate repair. The DDR is mediated by three key protein belonging to the phosphoinositol-3-kinase-like protein kinases (PIKKs); Ataxia-Telangiectasia Mutated (ATM), ATM and Rad3-related (ATR) and DNA-dependent Protein Kinase (DNA-PK) (Blackford & Jackson, 2017). In addition, Poly (ADP-ribose) polymerase (PARP) family members also play crucial roles in the sensing of DSBs (Price & D'Andrea, 2013). While ATM and DNA-PK are activated in response to DSBs, ATR is activated in response to single-stranded DNA formation at stalled replication forks or at end-resection steps during homologous recombination.

ATM is a serine/threonine kinase which is recruited and activated by the Mre11-Rad50-Nbs1 (MRN) complex at DSB sites (Paull, 2015). Once activated, ATM phosphorylates a plethora of substrate proteins important in DNA repair, cell cycle regulation, transcription and chromatin remodeling among many other processes. A central player in the DNA damage response is the tumor suppressor protein p53. Upon DSB formation, ATM phosphorylates and activates the Checkpoint effector Kinase 2 (Chk2) which then phosphorylates p53. p53 is also phosphorylated directly by ATM and once activated, promotes arrest of cell cycle progression until the damage is repaired (Blackford & Jackson, 2017).

Another key substrate of ATM is the histone variant H2AX. ATM phosphorylates H2AX at the serine 139 position referred to as γ -H2AX over megabase regions surrounding a DSB site. This is an extremely quick response that starts within a minute and peaks by 20 minutes upon DSB formation (Rogakou, Pilch, Orr, Ivanova, & Bonner, 1998). This phosphorylation is a critical event

that signals the physical location of the DSB to the DNA repair machinery. γ -H2AX (pS139) is recognized by mediator of DNA-damage checkpoint protein 1 (MDC1) which is also phosphorylated by ATM leading to the recruitment of the E3-ubiquitin ligase RNF8. RNF8 mediates the recruitment of RNF168 which ubiquitylates histone H2A on lysine 13/15 (H2AK13/K15). The ubiquitylation of H2AK15 leads to the stable recruitment of oligomerized p53-binding protein 1 (53BP1) which also needs mono- and dimethylated H4K20 (Panier & Boulton, 2014). Recruitment of 53BP1 is a defining crossroad in channeling DSB repair to one of the two dominant pathways. 53BP1 is phosphorylated by ATM that recruits RIF1. Presence of 53BP1-RIF1 complex channels the DSBs to repair by a rapid, but somewhat error prone pathway called the Non-Homologous End Joining pathway that promotes direct ligation of the DSB ends with minimal processing. However, a cell cycle dependent influence of BRCA1 at these sites specifically in S-G2 phase antagonizes the 53BP1-RIF1 complex and promotes DNA end-resection via Mre11 and C-terminal binding protein-interacting protein (CtIP) committing to the more accurate but slower Homologous Recombination Repair pathway (Escribano-Diaz et al., 2013).

1.5 Double-strand break repair pathways

Given the harmful nature of DSBs, it is perhaps unsurprising that the cell has devoted so many resources for their repair. In mammalian cells, DSBs are most commonly repaired by two well-known pathways; Non-Homologous End Joining and Homologous Recombination repair (Davis & Chen, 2013). In the absence of these major pathways, other backup repair systems like the Alternative End Joining (A-EJ, also referred to as Microhomology-mediated end joining, PARP1-dependent end joining, Pol θ -mediated end joining in the DNA repair lexicon), single-strand annealing (SSA) and synthesis-dependent strand annealing (SDSA) are used (Ceccaldi et

al., 2016). The backup systems are relatively less understood but are considered to be more dangerous at the same time. However, it is important to note that these backup systems are really subtypes of the two main repair pathways mentioned above and can takeover in the absence of the canonical factors.

1.6 Non-Homologous End Joining (NHEJ)

NHEJ is the major pathway DSB repair pathway that is active throughout the cell cycle and is the only major pathway functioning in the G₀/G₁ phase. As the name suggests, this pathway does not need a homologous template and promotes direct end joining of two adjacent non-homologous ends across a DSB. Apart from repairing pathological DSBs induced by ionizing radiation, radiomimetic drugs or other chemotherapeutic agents, NHEJ is also critical for repairing physiological DSBs generated during the V(D)J and Class switch recombination processes during B- and T-lymphocyte maturation (Lieber, 2010). An interesting aspect of NHEJ is its ability to accept a diversity of substrates and convert them to joined products. This demands a great flexibility in mechanical interaction of involved proteins to accept a plethora of different substrates that are generally produced following exposure to free radicals. Reactive oxygen species can interact with DNA to produce multiply damaged sites with different lengths of overhangs, end termini blocked with oxidation products and several types of base damage most commonly 8-oxoguanine and thymine glycols. These variously modified overhangs are joined by NHEJ regardless of the sequence, overhang length or DNA end products. Although, the process looks deceitfully naïve and guileless, in actuality, it is an incredibly intricate, orchestrated process involving a variety of proteins performing highly specific functions in order to achieve the aim of repairing these deleterious DSBs.

NHEJ can be arbitrarily divided into 3 major steps: A) DNA end recognition, assembly and bridging; B) DNA end processing (if required) and C) DNA end ligation (Davis & Chen, 2013). Immediately upon DSB formation, the ring-shaped heterodimer Ku70/Ku80 (hereafter referred to as Ku) recognizes and rapidly binds to the DSB ends initiating the NHEJ repair pathway. Ku then recruits DNA-PKcs (DNA-dependent protein kinase catalytic subunit) and together they form the DNA-PK core complex resulting in activation of the kinase activity of DNA-PK. If the DSB ends are modified/ unligatable, an arsenal of end processing enzymes is available to the cell to process the ends and make them ligatable. These proteins include the nucleases like Artemis, Polynucleotide Kinase/ Phosphatase, Tyrosyl-DNA Phosphodiesterase 1 and 2 (TDP1/TDP2), Aprataxin and PNKP-like factor (APLF) and the polymerases μ and λ . The terminal step involves direct ligation of the broken DNA ends by DNA Ligase IV in association with XRCC4 and XLF (Sishc & Davis, 2017). Improper regulation of the end processing steps in NHEJ can potentially lead to insertions or deletions in the DNA sequence and thus, NHEJ is often termed as error-prone. The three steps are outlined in more detail below.

1.6.1 DSB recognition and complex assembly

Ku is highly abundant in cells with concentrations of $4\text{-}5 \times 10^5$ molecules of Ku per cell and it has an extraordinarily high affinity for DNA ends with equilibrium constant in the nanomolar range allowing it to immediately localize to DSBs (Lieber, Ma, Pannicke, & Schwarz, 2003). X-Ray Crystallography studies have revealed that the structure of Ku is ring-shaped which fits the DNA perfectly inside it, allowing it to slide onto the DNA strands. Recruitment of Ku also has been linked with aligning of the DNA strands, maintaining their stability and protecting them from non-specific degradation. Upon recruitment, Ku acts as a scaffolding platform and mediates recruitment of several other NHEJ proteins including DNA-PKcs, XRCC4, Ligase IV, XLF, APLF

and TDP1. Upon recruitment of DNA-PKcs, Ku translocates inwards allowing DNA-PKcs to contact the terminal ~10bp (Davis & Chen, 2013). Atomic force Microscopy studies show that DNA-PKcs molecules on each end of a DSB form a bridge between the two ends ultimately leading to the formation of a synaptic complex involving DNA ends, Ku and DNA-PKcs (Lieber et al., 2003). The kinase activity of DNA-PK is critical and a number of NHEJ proteins are substrates of DNA-PK. DNA-PK phosphorylates Artemis and activates its endonuclease function. DNA-PK also phosphorylates XRCC4 and XLF and this is thought to promote the dissociation of the complex upon ligation (Deriano & Roth, 2013).

1.6.2 DSB end-processing

Complex ends formed by ionizing radiation or reactive oxygen species possess chemical modifications and are unligatable. These incompatible termini thus, have to be processed before the ends can be rendered ligatable. Auto-phosphorylation of DNA-PKcs results in the DNA ends being accessible to the end-processing nucleases and polymerases. Most of the end processing enzymes are recruited to the DSB ends via the Ku-XRCC4 scaffold (Sishe & Davis, 2017). Artemis is a key enzyme that possesses an intrinsic 5'-3' exonuclease function but acquires an endonuclease activity upon phosphorylation by DNA-PKcs allowing it to trim many DNA substrates irrespective of the end blocking groups (Lieber, 2010). PNKP, a bifunctional enzyme recruited by an interaction with XRCC4/Ligase IV complex, processes both 3'-phosphate- and 5'-hydroxyl-ended DSBs (Weinfeld, Mani, Abdou, Aceytuno, & Glover, 2011). 3'-phosphoglycolate residues formed upon radiation or radiomimetic drug treatment can be biochemically removed by TDP1 or APE1 (Kawale & Povirk, 2018). The nature of the break also dictates whether the polymerases are needed to fill-in gaps at these DSB ends. Polymerases μ and λ function in NHEJ by interacting with Ku via their N-terminal BRCT domains. In the presence of Ku and

XRCC4/Ligase IV, Pol μ can polymerize in a template-independent manner. Although these polymerases are ubiquitous, primary cells from pol μ and λ knockout mice do not show sensitivity to IR (H. H. Y. Chang, Pannunzio, Adachi, & Lieber, 2017).

1.6.3 DNA end-ligation

The final stage in the repair of DSBs through the NHEJ pathway involves gap filling followed by ligation of the DNA ends that have been aligned, tethered and processed by making them ligatable. DNA Ligase IV is the principal ligase in NHEJ and in association with XRCC4, forms the central component of mammalian NHEJ. Cells deficient in either proteins show dramatic sensitivity to radiation. Mice deficient in XRCC4 or Ligase IV are embryonically lethal. XRCC4 stimulates Ligase IV activity by promoting adenylation of Ligase IV. XRCC4 and XLF form alternating filaments that enable synapsis and bridging of the DNA ends (Menon & Povirk, 2017). XLF is also essential for gap filling by the polymerases μ and λ and is believed to play a role in aligning the two ends prior to ligation (Akopiants et al., 2009). APLF is believed to aid in ligation in the presence of Ku (Hammel et al., 2016).

At one-ended DSBs formed upon replication, the nuclease activities of MRN complex counteract Ku and release a DNA fragment bound to Ku thereby eliminating Ku from DNA ends (Chanut, Britton, Coates, Jackson, & Calsou, 2016). However, at regular two-ended DSBs, owing to the stability of Ku on the DNA ends, it could theoretically be trapped onto DNA after ligation of DSB ends. Evidence suggests that Ku removal from DSB ends is directed via its ubiquitination. Ku80 K48 is polyubiquitylated by Skp1-Cul1-Fbx112 resulting in degradation of Ku by the proteasome (Postow & Funabiki, 2013). RNF8 was also thought to promote Ku dissociation as depletion of RNF8 prolonged retention of Ku at laser-induced DSBs (Feng & Chen, 2012).

1.7 Radiomimetic Agents

The idea of treating cancer through chemotherapy brought forth many anti-tumor antibiotics that target the DNA by inducing DNA damage (Dedon & Goldberg, 1992). These chemical agents induce free-radical based single- as well as double-strand breaks in the DNA molecule by attacking the deoxyribose moieties in the DNA phosphodiester backbone. Since their effects mimic that of ionizing radiation, these chemotherapeutic agents are termed as radiomimetic drugs. Although the action of these radiomimetic agents is highly specific, forming lesions which represent a subset of the lesions generated due to IR, the effect of IR and radiomimetic agents on cells is surprisingly similar. Significant work has been published on some radiomimetic drugs like Bleomycin, Neocarzinostatin and Calicheamicin. Bleomycins are a family of glycopeptides first isolated from *Streptomyces verticillus* by Umezawa and colleagues in 1966 (Umezawa, Maeda, Takeuchi, & Okami, 1966). Since their discovery, the bleomycins have been an important component in a number of combination chemotherapy protocols against testicular cancer (Einhorn, 2002) and certain types of lymphoma (Bayer, Gaynor, & Fisher, 1992; J. Chen & Stubbe, 2005).

Neocarzinostatin and Calicheamicin are compounds which belong to the bicyclic enediyne family of anti-tumor antibiotics and are amongst the most studied of the radiomimetic drugs. These agents have a 10-membered characteristic unsaturated core containing two acetylenic groups conjugated to a double bond. These drugs are unique for their potential to produce sequence specific double stranded lesions which transpire due to the action of carbon-centered radicals of a single drug molecule (Dedon & Goldberg, 1992). Treatment of DNA with NCS in presence of Glutathione led to formation of double strand breaks in a very high proportion with the ratio of single strand lesions: double strand lesions being around 2:1. The reaction of DNA with Calicheamicin was even more potent producing single strand lesions: double strand lesion ratio of

around 1:20 (Chaudhry, Dedon, Wilson, Demple, & Weinfeld, 1999). Both bleomycin and the enediyne neocarzinostatin (NCS) are potent clastogens, and they can also induce, in various systems, base substitutions small deletions, large-scale gene rearrangements, with reasonable efficiencies. That these mutations seem to so rarely result in carcinogenesis is certainly one of the most intriguing aspects of the genetic toxicology of these agents (Povirk, 1996).

1.7.1 Neocarzinostatin (NCS)

NCS was the first of the bicyclic enediyne antibiotics that was discovered. It was isolated from the bacterial species *Streptomyces carzinostaticus*. It was recognized as a simple antitumor antibiotic protein competent in inhibiting DNA synthesis and inducing the degradation of DNA in cells. However, only 15 years after its discovery it was realized that the true biological function of NCS was not due to the protein but rather to a previously unrecognized tightly, but non-covalently, bound labile non-protein chromophore (NCS-Chrom). The apoprotein contains a hydrophobic cleft where NCS-Chrom is believed to reside and is protected from degradation. The structure of NCS can be divided into 3 domains, the naphthoate region which serves as the DNA binding domain, the enediyne core which form the DNA-damaging machinery and cyclic carbonate structure responsible for uptake of the drug in the cells (Dedon, P., & Goldberg, I. 1992).

The interaction of NCS with DNA has been extensively characterised. The drug binds to the DNA in a two-step process involving external binding followed by the intercalation of the chromophore. Electric dichroism studies have shown that the naphthoate acts as a classic intercalator, orienting itself parallel to the DNA bases which causes a distortion of the DNA helix (Dasgupta, D & Goldberg, I. H. 1985; Povirk, L. F. 1996) This leads to the positioning of the active enediyne portion of the NCS-chromophore in the minor groove of the DNA molecule with favourable electrostatic interactions between the positively charged amino sugar in NCS and the

negatively charged Phosphodiester backbone. This binding of the drug in the minor groove is evident from 2 sources: Modification of the major groove did not alter the binding constant of NCS whereas Netropsin and distamycin, two minor groove binding agents competed with NCS for binding to DNA (Dasgupta, D., and Goldberg, I. H. 1985).

Mechanism of Action

The mechanism of action of NCS and the damage caused by it is highly complex. NCS-mediated DNA damage results in the formation of single as well as double strand breaks. Similar to all radiomimetic drugs, its mechanism of action is based on the hydrogen atom abstraction principally at the 1st, 4th and 5th carbon of the deoxyribose sugar leading to its oxidation (Povirk and Steighner. 1989). The identity of these hydrogen atoms abstracted have been verified using isotope labelling studies (Dedon, P., & Goldberg, I. 1992). Abstraction of the hydrogen from the C-5' end is the characteristic trait of the enediyne compounds resulting in the formation of a 3'-phosphate and a 5'-aldehyde molecule at the DNA terminus (Kappen et al., 1982). A small subset of breaks also involves 3'- and 5'- phosphates at the termini as well. This hydrogen abstraction from the 5th carbon of the deoxyribose sugar followed by the incorporation of oxygen into the aldehyde leads to the production of single strand breaks in the DNA strands.

In contrast to the above mechanism, hydrogen abstraction from both C-1' and C-4' leads to the formation of bi-stranded lesions. Elimination of the C-1' hydrogen by NCS mainly results in the formation of an abasic site in the form of 2'-deoxyribonolactone. This species is quite unstable in alkali and ultimately leads to the formation of a strand break with 3'- and 5'-phosphate termini. (Povirk and Houlgrave, 1988; Povirk et al. 1988). NCS mediated attack at C-4' adds oxygen at C-4' ultimately leading to the production of strand breaks with ends containing 3'-phosphoglycolates and 5'-phosphates with the formation of a base, propenal (Chaudhry, M. et al 1999).

1.7.2 Calicheamicin

The calicheamicins are produced by the fermentation of *Micromonospora echinospora ssp calichensis*, a bacterium isolated from a chalky, or caliche, soil sample collected in Texas. They were discovered in the mid- 1980s in a fermentation products screening program through the use of the biochemical induction assay (BIA), which utilized a genetically engineered strain of *Escherichia coli* to detect DNA damaging agents (Lee, M. et al 1991). Calicheamicin and Esperamicin lack intercalating moieties and thus bind to DNA by other means than NCS. The carbohydrate side chains of Calicheamicin serve as a DNA binding domain. The DNA damaging element present in Calicheamicin is similar to NCS consisting of a highly strained ring system with a pair of triply unsaturated carbon bonds surrounding a carbon-carbon double bond (Lee, M. et al 1991).

The nature of DNA damage instigated by Calicheamicin has not been as extensively studied as some of the other enediynes like NCS. However, it is known to produce both single as well as double strand lesions with an astoundingly high proportion of double strand lesions (Dedon, P., & Goldberg, I. 1992).

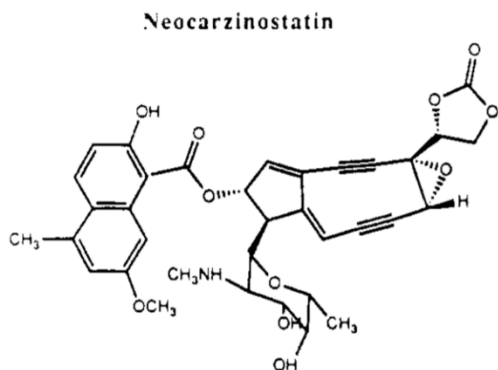
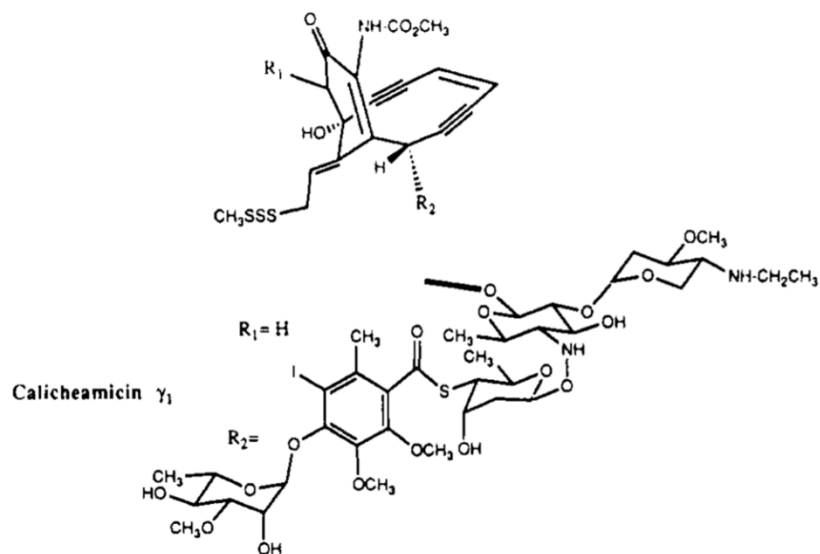


Figure 1-5: Structures of enediyne antitumor antibiotics - Calicheamicin (Top) and Neocarzinostatin (bottom)

Adapted from (Dedon & Goldberg, 1992)

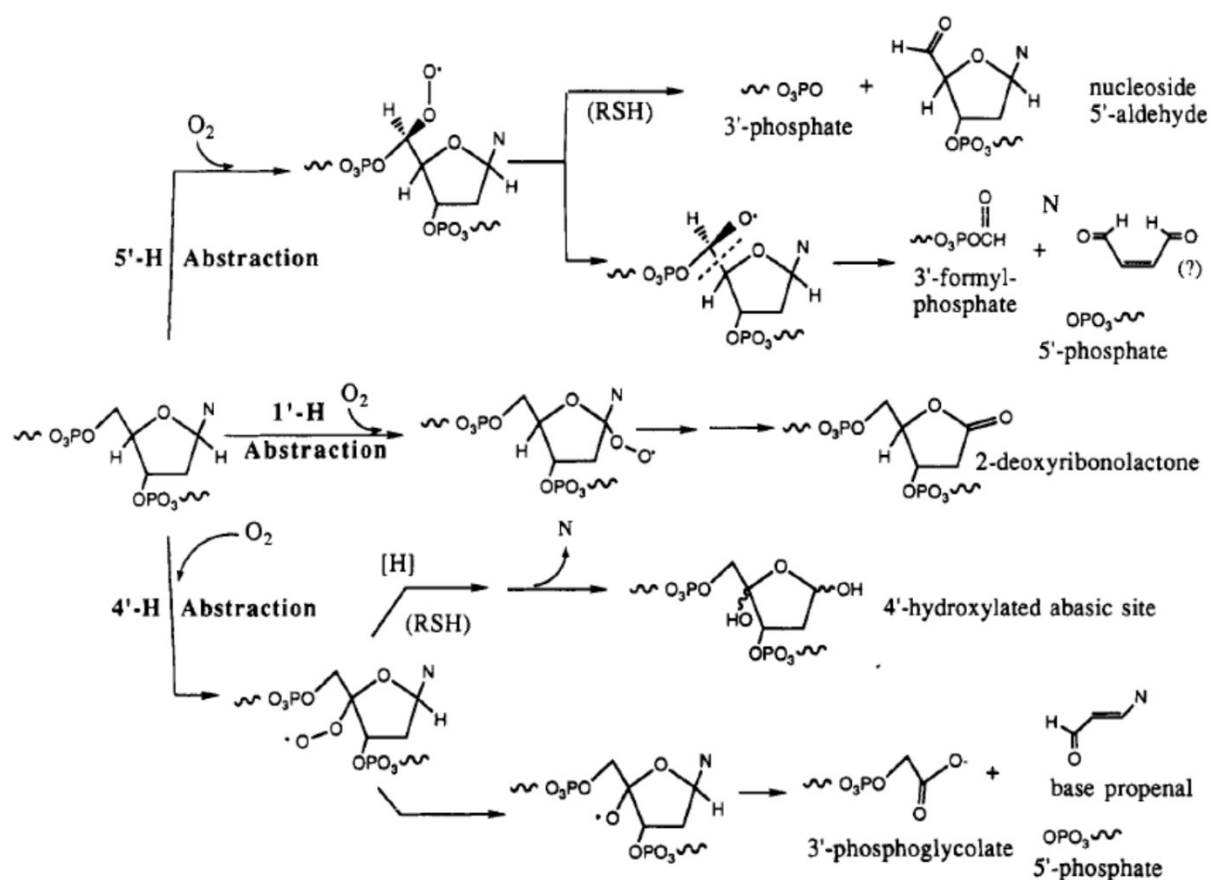


Figure 1-6: Mechanism of NCS action and typical DSB ends formed

NCS mediated hydrogen atom abstraction can take place from 1', 4' or 5' carbon of the deoxyribose sugar. 5'-H abstraction followed by oxidation leads to the production of 3'-phosphate and a nucleoside 5'-aldehyde in presence of thiols whereas in absence of thiols, 3'-formyl-phosphate and 5'-phosphate are formed. 1'-H abstraction leads to the formation of an abasic site and a 2-deoxyribonolactone. 4'-H abstraction, in presence of thiols, leads to the formation of a 4'-hydroxylated abasic site whereas in the absence of thiols, 3'-phosphoglycolate and a 5'-phosphate with the release of the base propenal. Adapted from (Dedon & Goldberg, 1992)

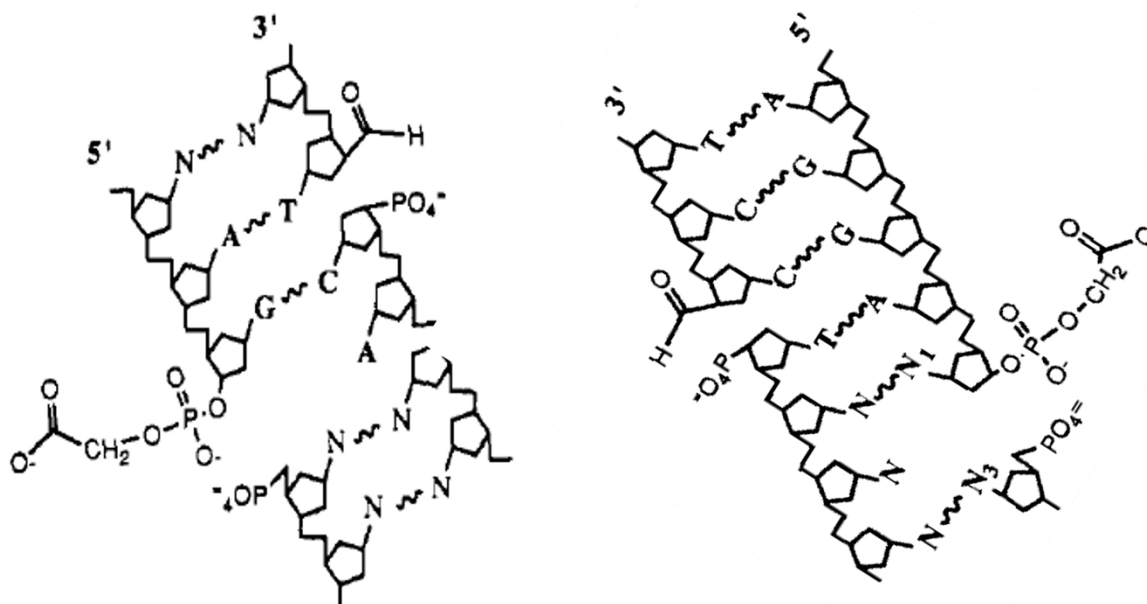


Figure 1-7: NCS and CAL induced bistranded lesions with specific modifications

NCS and CAL have been shown to produce two types of bistranded lesions: At the AGT.ACT sequence, bistranded lesions consists of mainly C4' -hydrogen abstraction at the T of AGT, as suggested by the presence of 3'-phosphoglycolate residues and 4' -hydroxylated abasic sites, and C5'-aldehyde at the T of ACT. Adapted from (Dedon & Goldberg, 1992)

2. INTRODUCTION TO THE THESIS

2.1 Tyrosyl-DNA Phosphodiesterase 1 (TDP1)

The double-helical structure of DNA is paramount for the storage of genetic information and its transmission through DNA metabolic processes such as replication, transcription, recombination and chromatin remodeling. Local unwinding of DNA induced by these DNA metabolic processes causes supercoiling of DNA leading to topological entanglements that need to be untangled in order to maintain cellular function and genomic stability. Fortunately, cells have evolved special, highly conserved biological tools called topoisomerases to resolve these genomic entanglements.

For example, Topoisomerase 1 regulates DNA topology using a cleavage-religation mechanism in which transient single-strand breaks (SSBs) induced in the DNA, link Top 1 to the 3'-DNA end via an active site tyrosine residue (Y723) (Ashour, Atteya, & El-Khamisy, 2015). This leads to the formation of a DNA-Top 1 covalent intermediate commonly referred as Top 1 cleavage-complexes (Top1cc) (Pommier, 2013). Normally, this intermediate is briskly religated, relaxing the supercoiled DNA. However, presence of modifications in the DNA such as abasic sites, nicks or gaps, mismatches, modified bases, nucleotide analogs and almost all kinds of DNA lesions as well as topoisomerase poisons like camptothecin interferes with the ligation reaction

and result in trapped covalent DNA-enzyme intermediates (D. Davies, Interthal, Champoux, & Hol, 2002). Consequently, these trapped covalent complexes pose a risk to the integrity of the genome and need to be processed.

2.1.1 Discovery

In 1996, it was serendipitously observed that an oligonucleotide bearing a phosphotyrosine residue at the 3'-end was processed in an unpredicted manner upon its incubation with extracts of several eukaryotic cells (Yang et al., 1996). Treatment of the substrate resulted in the formation of product with mobility similar to that expected from the hydrolytic loss of terminal tyrosine. The specificity of this tyrosyl-DNA phosphodiesterase activity, its conservation across a range of eukaryotic species and the fact that 3'-phosphotyrosyl (3'-pTyr) substrates mimic trapped Top 1 cleavage complexes suggested that this enzyme might be a part of the pathway for the repair of Top1cc (Yang et al., 1996). Subsequently, the *Saccharomyces cerevisiae* gene encoding TDP1 was isolated by random mutagenesis and screening of clones for loss of TDP1 activity. TDP1-defective mutants were found to be hypersensitive to camptothecin (CPT), an anticancer chemotherapeutic drug that specifically traps Top 1, further drawing attention to its role in the repair of Top1cc (Pouliot, Yao, Robertson, & Nash, 1999). The human gene for TDP1 was soon cloned and it was found by mutational and sequence analysis that TDP1 was a member of the phospholipase D (PLD) superfamily (Interthal, Pouliot, & Champoux, 2001). Subsequent work established the crystal structure of TDP1 and the mechanism of its action (D. Davies et al., 2002). Shortly after, it was determined by linkage analysis, physical mapping and a positional candidate gene approach in a Saudi Arabian family that mutation in TDP1, and thereby a deficiency in repairing the stalled Topoisomerase I complexes, caused an extremely rare genetic disease Spinocerebellar Ataxia with Axonal Neuropathy (SCAN1) (Takashima et al., 2002). With the

TDP1 gene cloned and its crystal structure solved, new avenues opened allowing researchers to investigate the biochemistry and the molecular biology of a previously-challenging niche of DNA repair.

2.1.2 Structure

Human tyrosyl-DNA phosphodiesterase 1 is a predominantly nuclear protein comprising 608 amino acids with a molecular weight of 68.5kDa. The protein can be subdivided into two domains – an N terminal regulatory domain extending up to amino acid 148 and a C-terminal catalytic domain extending from 149 to 608 (D. Davies et al., 2002). The N-terminal domain is dispensable for the catalytic function but is important for the recruitment of TDP1 to the sites of damaged chromatin. Indeed, an N-terminal deletion mutant (Δ 1-148) of human TDP1 (hTDP1) in vitro retained wild type levels of processing of the Top 1 peptide from the 3' end of an oligonucleotide substrate (Interthal et al., 2001). Sequence alignments of TDP1 orthologs from different species have demonstrated that TDP1 represents a unique subclass within the PLD superfamily of proteins. The uniqueness of TDP1 and its orthologs is attributed to the two 'HKN' catalytic motifs instead of the characteristic HKD motifs found in the other members of the PLD superfamily. Each of the sequence motifs contain a highly conserved histidine, lysine and asparagine (H263, K265 and N283 in the N-terminal motif and H493, K495 and N516 in the C-terminal motif). Site-directed mutagenesis established that both H263 and H493 are the key catalytic residues as H263A, H493A and H493N mutants were 10000X, 3000X and 15000X less active than the wild-type protein (Interthal et al., 2001). The other conserved residues in the 'HKN' motifs K265, N283, K495 and N516 are key for substrate binding and the stabilization of the transition state (D. R. Davies, Interthal, Champoux, & Hol, 2003). These two HKN motifs together

make up the active site at the bottom and near the center of the protein allowing it to function as a monomer.

2.1.3 Catalytic Mechanism

TDP1 catalyzes the removal of tyrosyl-peptide from the DNA in a two-step 'ping pong'-type phosphoryl transfer reaction via a covalent phosphoenzyme intermediate (Gottlin, Rudolph, Zhao, Matthews, & Dixon, 1998). The first step involves a nucleophilic attack on the tyrosyl-DNA 3'-phosphate by the imidazole N₂ atom of H263 of the N-terminal HKN motif. H493 of the C-terminal HKN motif acts as a general acid catalyst to protonate the tyrosyl moiety of the departing Top 1 peptide. This results in the formation of the covalent intermediate in which the cleaved substrate is temporarily linked to TDP1. In the second step, H493 acts as a general base catalyst and activates a water molecule which subsequently hydrolyzes the phosphoenzyme intermediate (Interthal et al., 2005). This leads to the release of 3'-phosphate ended DNA which is converted by polynucleotide kinase/ phosphatase (PNKP) into 3'-OH DNA. A missense mutation in the TDP1 gene (A1478G) causing a substitution of H493 with an arginine residue is the genetic basis behind the pathology of an extremely rare autosomal recessive neurodegenerative disorder, Spinocerebellar Ataxia with Axonal Neuropathy (SCAN1) characterized by ataxia, cerebellar atrophy and peripheral neuropathy. TDP1 H493R mutant manifests around 25X decreased rate of hydrolysis of the tyrosyl-containing peptide from the DNA and ironically itself becomes covalently trapped with a relatively long half-life of around 13 min (Interthal et al., 2005). The autosomal recessive nature of the disease suggests that WT TDP1 can resolve the mutant TDP1-DNA covalent complexes.

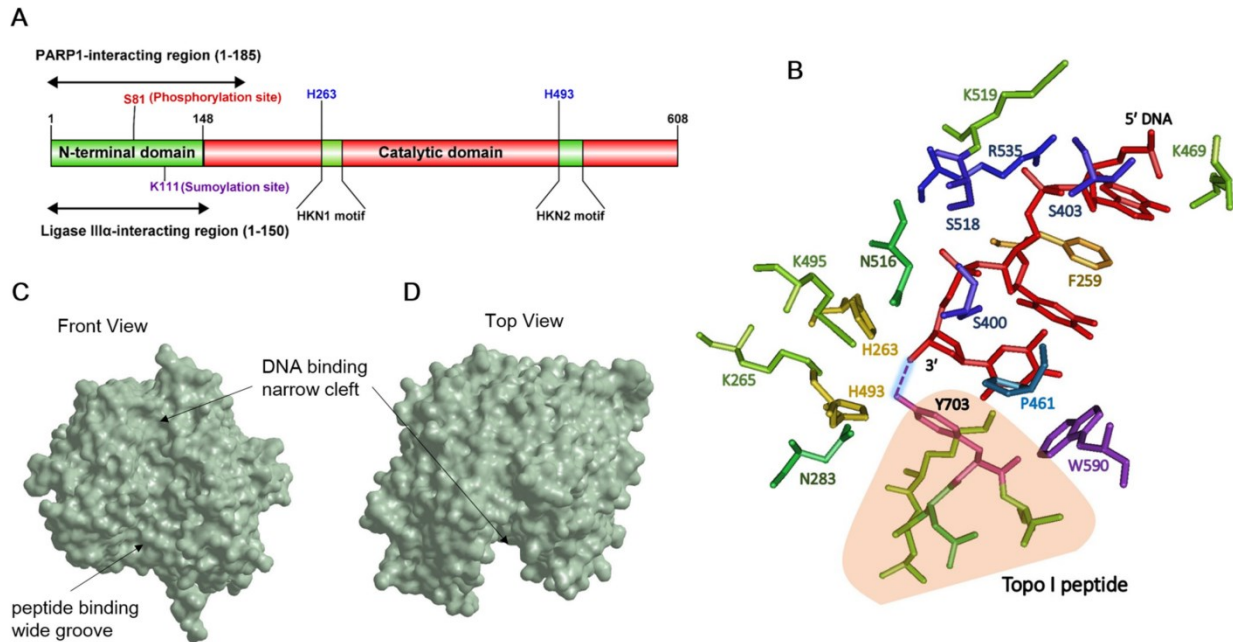


Figure 2-1: Structure of TDP1

(A) Domain structure of human TDP1. Sites shown in blue are key residues in the active site of TDP1. (B) Critical TDP1-substrate interactions in the TDP1 active site. Crystal structure of TDP1 (1NOP) obtained from Protein Data Bank (PDB) website was used to generate a model of the TDP1 active site in complex with the DNA substrate and the Topo I peptide using Cn3D. Amino acids in the active site are represented as sticks and color-coded. DNA substrate is shown in red. 3'-phosphotyrosyl bond is indicated as a dashed line between 3' end of the substrate and Y703 and highlighted. Topo I peptide is shown in light orange. (C and D) Surface representation of TDP1 substrate binding channel was generated using Chem3D on crystal structure of TDP1 (1JY1) obtained from PDB (C) Front view and (D) Top view of the substrate binding channel with the DNA and peptide binding regions highlighted (Kawale & Povirk, 2018).

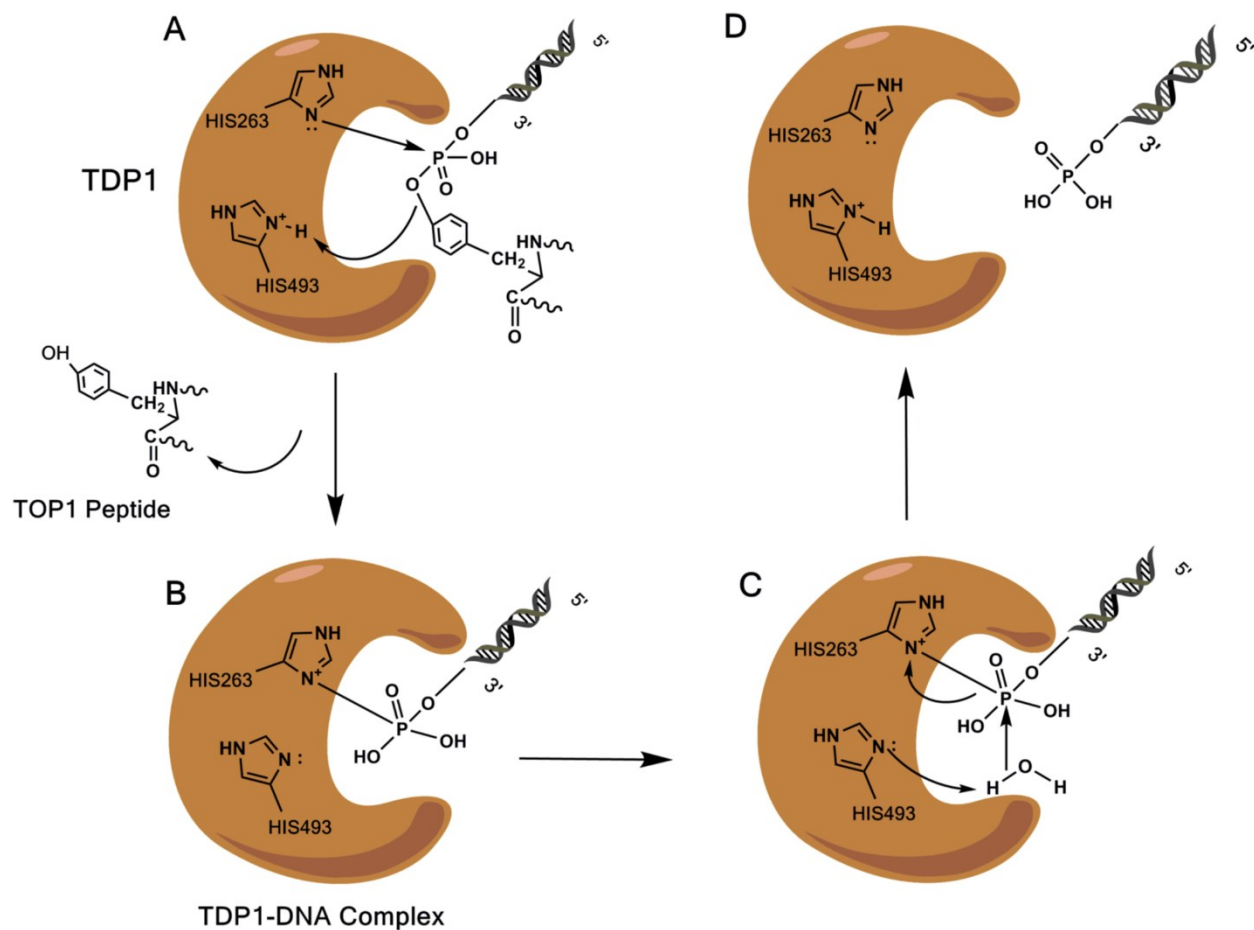


Figure 2-2: Catalytic mechanism of TDP1 in its canonical function

(A) Nucleophilic attack on the tyrosyl–DNA 3'-phosphate by the imidazole N₂ atom of H263. H493 donates a proton to the outgoing Top I peptide. (B) Formation of the TDP1-DNA covalent intermediate. (C) H493 activates a water molecule which attacks the 3'-P breaking the N-P bond and hydrolyzing the phosphoenzyme intermediate. (D) Release of DNA 3'-phosphate from TDP1 (Kawale & Povirk, 2018).

2.1.4 Role in SSB repair

TDP1 was initially described as a clean phosphodiesterase activity that explicitly removed a tyrosyl containing peptide from a DNA end leaving a 3'-phosphate and was shown to be critical for the repair of TopIcc (Pouliot et al., 1999). Consequently, TDP1 deficient cells are hypersensitive to CPT and its clinical derivative irinotecan (Meisenberg et al., 2015; Miao et al., 2006). On the other hand, as observed by single cell gel electrophoresis experiments, HEK293 cells overexpressing WT but not mutant TDP1^{H263A} exhibit significantly reduced DNA damage induced by CPT (Barthelmes et al., 2004). To date, TDP1 remains one of the very few enzymes that specifically remove a 3'-block from the DNA end without actually resecting the DNA by even a single base (Interthal, Chen, & Champoux, 2005). Although it shows a weak activity in removing a normal nucleoside from a 3' DNA end, the inability of TDP1 to act on the resulting 3'-P terminus prevents TDP1 from functioning as a general 3'-exonuclease. For this reason, activity of TDP1 in the removal of 3'-phosphotyrosyl residues in human cells is coupled with a specific DNA 3'-phosphatase, PNKP, to generate 3'-OH, which can then be readily acted upon by DNA polymerases and ligases (Weinfeld et al., 2011).

The sensitivity of TDP1-deficient cells to Top 1 poisons was initially hypothesized to be specific to cells in the DNA synthesis phase where collision of approaching replication forks with TopIcc would lead to the formation of DSBs. However, TDP1's involvement in the pathology of SCAN1, a disease of terminally differentiated post-mitotic neurons, and the fact that SCAN1 cells show hypersensitivity to Top 1 poisons led to the emergence of a new question: Why does TDP1 mutation and Top 1 poisoning kill post-mitotic neurons, cells that do not enter S-phase? An explanation to this discrepancy was provided when it was shown that sensitivity of SCAN1 cells to CPT was abrogated by DRB (5,6-dichloro-1-β-D-ribofuranosylbenzimidazole), a transcription

inhibitor, but not by aphidicolin, a replication inhibitor suggesting that SCAN1 cells are defective for the repair of transcription-induced Top1cc (Miao et al., 2006). In addition, these transcription-induced cleavage complexes cause the formation of transcription-dependent DSBs after Top 1 proteolysis prior to TDP1's action leading to the activation of the DNA damage response via ATM and DNA-PK and that these co-transcriptional DSBs kill quiescent cells (Cristini et al., 2016). Thus, the highly elevated transcription rates and increased oxygen demands in neuronal cells lacking TDP1 produce increased levels of unrepaired Top1cc and oxidative damage due to enhanced topoisomerase activity providing molecular insights in the pathogenesis of SCAN1.

TDP1 eliminates 3'-phosphoglycolate ends both in vitro and in cells formed as a result of oxidative DNA damage although the efficiency of this processing is hundred times less than that of its canonical 3'-pTyr substrate (Hawkins et al., 2009; Zhou et al., 2005). SCAN1 cells are defective in repairing IR-induced SSBs (El-Khamisy, Hartsuiker, & Caldecott, 2007). The alkylating agent methyl methane sulfonate (MMS) produces N7-methyl guanine adducts which are processed by DNA N-glycosylases/AP lyases to form abasic (AP) sites and 3'-deoxyribose phosphate (3'-dRP) ends (Murai et al., 2012). Tdp1^{-/-} DT40 chicken cells and human TDP1 knockdown (KD) cells show hypersensitivity to alkylating agent MMS and this sensitivity can be almost fully averted by complementing with human TDP1. Additional depletion of APE1 in TDP1 KD cells enhances the hypersensitivity of these cells to MMS (Alagoz, Wells, & El-Khamisy, 2014). Thus, these results suggest involvement of TDP1 in the base excision repair pathway (BER) in removing abasic sites independently of APE1.

Chain terminating nucleoside analogs (CTNAs) lack a 3'-OH group and thus block DNA synthesis after getting incorporated in DNA. These CTNAs are extensively used as anti-viral and anti-cancer agents specially in treating HIV and adult T-cell leukemia (ATL). TDP1 repairs

nuclear and mitochondrial DNA damage induced by CTNAs including acyclovir (ACV), cytarabine (Ara-C), zidovudine (AZT) and zalcitabine (ddC) (Huang et al., 2013). Tdp1^{-/-} DT40 and mouse embryonic fibroblast (MEF) cells are hypersensitive to ACV and Ara-C and show enhanced depletion of mitochondrial DNA in response to AZT and ddC. ATL cells are deficient in TDP1-dependent repair and are thus selectively killed by anti-HIV drug Abacavir (ABC) (Tada et al., 2015). Very recently, in the first published evidence of successful inactivation of the human TDP1 by genetic manipulation, it has been shown that Tdp1^{-/-} HCT116 and TSCER2 cells display enhanced sensitivity to CNDAC, an analog of Ara-C further underscoring the importance of TDP1 in the repair of CTNA-induced DNA damage (Abo et al., 2017).

2.1.5 Regulation of TDP1

The biology of TDP1 is elegantly regulated by its interactions with other DNA repair factors and post-translational modifications (PTMs) including poly ADP-ribosylation (PARylation), phosphorylation and sumoylation. The N-terminal region of TDP1, which is dispensable for catalytic function, is the target for these modifications. Thus, these PTMs do not play a role in enhancing the catalytic function of the protein but merely increase stabilization and recruitment to the sites of DNA damage.

Poly (ADP-Ribose) Polymerase 1 (PARP1) is a highly conserved multifunctional enzyme that catalyzes the polymerization of ADP-ribose moieties derived from NAD⁺ onto itself or other target proteins (Rouleau, Patel, Hendzel, Kaufmann, & Poirier, 2010). PARP1 and TDP1 are epistatic for the repair of TopIcc as TDP1^{-/-}.PARP1^{-/-} double mutant DT40 avian cells show similar sensitivity to CPT as their single mutant counterparts (Das et al., 2014). C-terminal region of PARP1 binds the N-terminal region of TDP1 and poly ADP-ribosylates (PARylates) TDP1 without inhibiting its catalytic activity and promotes its recruitment to TopIcc-induced DNA

damage sites. Micro-irradiation with live-cell microscopy and biochemical analysis show that PARylation of TDP1 promotes the recruitment of both itself and XRCC1 to the sites of Top1-induced DNA damage and leads to the stabilization of TDP1 in response to Top1cc-induced DNA damage (Das et al., 2014).

In human cells, TDP1 is phosphorylated at serine 81 by ATM and DNA-PK following ionizing radiation and CPT treatment (Das et al., 2009). As this site is located in the N-terminal region which is dispensable for enzyme activity, phosphomutants show no difference in enzymatic activity in yeast *in vitro* (Chiang, Carroll, & El-Khamisy, 2010). However, pS81-TDP1 forms nuclear foci that co-localize with γ H2AX foci which presumably are sites where Top1 induced SSBs are converted to DSBs following replication fork collision (Das et al., 2009). In addition, phosphorylation of TDP1 is important for its stabilization and promotes binding to XRCC1 and Ligase III α as seen from co-immunoprecipitation and immunofluorescence microscopy (Chiang et al., 2010). XRCC1 is a scaffolding protein that interacts with several BER factors and is also known to play a role in the repair of Top1cc presumably by recruiting TDP1 and PNKP (Plo et al., 2003). The interaction of TDP1 with Ligase III α also likely contributes to mitochondrial BER (Tomkinson & Sallmyr, 2013).

2.1.6 TDP1 in DSB repair

The biochemical competency of TDP1 in the resolution of glycolate ends first suggested the possible involvement of TDP1 in the repair of DSBs bearing terminally-occluded 3'-overhangs (Inamdar et al., 2002). Tdp1^{-/-} MEF extracts are completely inept in removing protruding 3'-phosphoglycolate termini from similar substrates suggesting that, in extracts, the processing of DSBs with protruding 3'-PG termini is entirely dependent on TDP1 (Hawkins et al., 2009). Tdp1^{-/-} mice and Tdp1^{-/-} DT40 chicken cells both show hypersensitivity to bleomycin (Murai et al.,

2012). Whole cell extracts (WCEs) from lymphoblastoid cells derived from SCAN1 patients are deficient in catalyzing the conversion of 3'-PG termini on 3'-overhanging model DSB substrates in vitro with no measurable processing for several hours (Zhou et al., 2005). In comparison, normal cells from unaffected relatives show substantial processing within a few minutes. Treatment with calicheamicin leads to increased chromosomal aberrations in SCAN1 cells, particularly dicentric chromosomes suggesting that absence of TDP1 leads to mis-joining of DSB ends (Zhou et al., 2009).

In yeast, TDP1 has been shown to be an accessory component of the Non-Homologous End Joining (NHEJ) pathway (Bahmed, Nitiss, & Nitiss, 2010). Clean DSB ends generated by linearizing plasmid substrates with restriction enzymes are mis-repaired leading to inaccurate repair joints with insertions in the absence of TDP1. Additional deletion of yeast NHEJ proteins like Ku and Ligase IV does not increase the frequency of mis-repair suggesting that yTDP1 promotes repair fidelity in the context of NHEJ (Bahmed et al., 2010). Furthermore, human TDP1 has been suggested to play a role in the early stages of mammalian NHEJ by promoting the assembly of NHEJ protein complexes on DNA (Heo et al., 2015). TDP1 associates with the NHEJ protein complexes by directly interacting with XLF and Ku70/80. This contrasts with other end-processing factors like PNKP, APLF and Aprataxin that play a role in NHEJ by interacting with XRCC4. XLF stimulates activity of TDP1 on dsDNA. Additionally, TDP1 promotes DNA binding by Ku70/80 and stimulates the kinase activity of DNA-PK (Heo et al., 2015). Furthermore, it was recently reported that TDP1 was required for efficient NHEJ in human cells as HEK293 cells deficient in TDP1 showed an increase in insertions at I-SceI-induced DSB repair joints (J. Li, Summerlin, Nitiss, Nitiss, & Hanakahi, 2017). Finally, TDP1 has also been shown to play a role in the repair of etoposide-generated DSBs (Borda, Palmitelli, Veron, Gonzalez-Cid, & de Campos

Nebel, 2015). Human TDP1-knockdown (Tdp1kd) cells are hypersensitive to etoposide and show increased number of chromosomal breaks and mis-joining events which are further enhanced by DNA-PK depletion. However, equal number of Rad51 foci and sister-chromatid exchanges in WT and Tdp1kd cells suggest that depletion of TDP1 disrupts classical as well as the alternative end joining pathways but not HR for the repair of TopIIcc (Borda et al., 2015). Thus, taken together, these results present persuasive evidence for the involvement of TDP1 in DSB repair (Kawale & Povirk, 2018).

2.2 Artemis

2.2.1 Discovery

Immunoglobulins produced by lymphocytes are important molecules of the humoral immune system for the neutralization of foreign antigens. The antigen-binding region of these immunoglobulins is encoded by the variable (V), diversity (D) and joining (J) gene segments that recombine through a mechanism known as V(D)J recombination (Roth, 2014). The V, D and J segments are each flanked by recombination signal sequences (RSS). The process of V(D)J recombination begins with the introduction of a double-strand break by specialized nucleases known as RAG1 and RAG2 upon recognition of the RSS. Induction of a DSB is accompanied by hairpin sealed coding ends that need to be opened. This leads to the activation of the NHEJ repair pathway requiring the Ku70/80-DNA-PKcs complex. DNA-PK activity is essential for opening of the hairpin ends (S. H. Lee & Kim, 2002). Along these lines, a defect in the V(D)J recombination process was observed in patients suffering from severe combined immunodeficiency (SCID) owing to an early arrest of both B and T cell maturation. Mutations in RAG1 or RAG2 genes were observed in a subset of patients with SCID (Schwarz et al., 1996).

However, in other patients, a V(D)J recombination defect was often accompanied by an increased sensitivity to ionizing radiation (RS-SCID) and was not caused by mutations RAG1 or RAG2, DNA-PKcs or other V(D)J proteins mentioned above (Cavazzana-Calvo et al., 1993; Nicolas et al., 1998). This suggested that the defect in V(D)J recombination in these patients was characterized by a defective gene encoding a novel undescribed factor. Moshous and colleagues, first identified and cloned this novel factor defective in human radiosensitive - severe combined immunodeficiency (RS-SCID) (Moshous et al., 2001). In classical Greek mythology, Artemis was the goddess of protecting young children and as this condition was lethal within the first year of life of young children, the protein was named Artemis.

The gene encoding Artemis is DNA Cross-Link Repair 1C (DCLRE1C). Athabascan SCID or RS-SCID is a highly rare, autosomal recessive inherited disease which is characterized by early onset of severe opportunistic infections with severe oral and genital ulcers. Affected children generally die from these infections within six months without a bone-marrow transplant (L. Li et al., 2002). A unique, autosomal recessive non-sense mutation in exon 8 of DCLRE1C gene leading to the truncation of the protein product at the 192nd amino acid was also shown to cause SCID in Athabascan-speaking Native Americans (L. Li et al., 2002).

2.2.2 Structure

Artemis is a 78 kDa protein, encoded on p arm of chromosome 10, belonging to the metallo- β -lactamase family consisting of 692 amino acids. Two domains in its N-terminus, a metallo- β -lactamase domain, spanning amino acids 1-155 and a β -CASP domain spanning amino acids 156-385, have been shown to be important for the catalytic activity of Artemis (Callebaut, Moshous, Moron, & de Villartay, 2002). The β -CASP domain is highly conserved in other proteins belonging to the same family that specifically act on nucleic acids. Like all proteins

belonging to metallo- β -lactamase superfamily, Artemis also needs divalent cations, specifically Mg^{+2} , to be catalytically active (Pannicke et al., 2004). The active site of Artemis contains 4 Histidine residues and 4 Aspartic acid residues which are highly conserved between Artemis and other metallo- β -lactamase proteins. These active site histidines and aspartates are thought to coordinate metal ions for a nucleolytic attack onto the DNA (Pannicke et al., 2004). Thus, the N-terminal region of Artemis is the catalytic region for the Artemis protein. The regulatory C-terminal region of Artemis is predicted to be unstructured and has been shown to be important for the interaction with DNA-PKcs and Ligase IV. Specifically, residues 399-403 which are adjacent to the nuclease domain interact with DNA-PKcs whereas residues 485-495 interact with Ligase IV (Niewolik et al., 2006). DNA-PKcs phosphorylates Artemis in its C-terminal region and causes a conformational change resulting in its activation.

2.2.3 Biochemical properties

Artemis possesses a single-strand DNA (ssDNA)-specific 5'-3' exonuclease activity but acquires an endonuclease activity upon phosphorylation by and association with DNA-PK (Ma, Schwarz, & Lieber, 2005). The endonuclease function is important during the process of V(D)J recombination for the opening of hairpin DNA ends as well as for the trimming of 3'- and 5'-overhangs on DSB ends during the NHEJ repair pathway (Ma, Pannicke, Schwarz, & Lieber, 2002). This endonucleolytic trimming completely eliminates 5'-overhangs whereas the 3'-overhangs are only shortened to 2-3 nts upon prolonged incubation. Artemis is biochemically competent in processing 3'-phosphoglycolate overhangs into 3'-hydroxyl ends in an ATP- and DNA-PK-dependent manner, suggesting its involvement in repairing unligatable modified DSB via NHEJ (Povirk, Zhou, Zhou, Cowan, & Yannone, 2007). The 5'-3' exonuclease function of

Artemis is unlikely to play a role during NHEJ as this activity is suppressed by DNA-PK at DSB ends.

Although WT Artemis demonstrates 5'-3' exonuclease activity, its endonucleolytic function is absent *in vitro*. In contrast to WT Artemis however, C-terminal deletion mutants of Artemis (Artemis without the C-terminal region) exhibit endonucleolytic hairpin opening activity *in vitro*. This suggested that the C-terminal domain of Artemis performs a regulatory role (Niewolik et al., 2006). Studies performed to elucidate this function indeed showed that a physical interaction between the N-terminal catalytic domain and the C-terminal region mediates autoinhibition of Artemis (Niewolik, Peter, Butscher, & Schwarz, 2017).

Initially, Artemis was shown to be catalytically active on hairpin- and overhanging substrates. However, it is now known that Artemis is effective on a wide range of DNA structures albeit weakly, including blunt ends and ssDNA-dsDNA transitions. Artemis resects AT-rich, but not GC-rich blunt ends via a DNA end-breathing step in a manner dependent on both Ku and DNA-PKcs (H. H. Chang, Watanabe, & Lieber, 2015). Recently, a physical model describing the key contact points of Artemis•DNA-PKcs with their known DNA substrates was developed (H. Chang H.Y. & Lieber, 2016). According to this model, Artemis•DNA-PKcs contacts the DNA substrate at 3 positions; 2 contact points are located right at the dsDNA-ssDNA boundary one on each strand and the third point (which is the catalytic site) is located one nucleotide on the 5'-end of point B. This model proposed that without these contact points, the activity of Artemis•DNA-PKcs was negligible. This model also explains the differential function of Artemis on 3'- and 5'-overhangs.

2.2.4 Function in DSB repair

Cells deficient in NHEJ proteins including DNA-PK show intensive radiosensitivity as do Artemis-defective cells, thus giving evidence to the requirement of Artemis in the NHEJ pathway for the repair of DSBs. Ionizing radiation, and radiomimetic drugs like Neocarzinostatin (NCS) create chemically modified, unligatable DSB ends like 3'-phosphates and 3'-phosphoglycolates. As Artemis deficient cells are sensitive to IR, it was postulated that Artemis could mediate the end-processing of these chemically modified termini. Indeed, biochemical analysis have shown that Artemis in association with DNA-PKcs can convert such unligatable ends to a form that is appropriate for ligation with a minimal loss of the terminal nucleotides. ATM hyperphosphorylates Artemis in response to IR treatment and thus ATM is required for Artemis-dependent processing of damaged DNA ends. ATM, however, is not required for V(D)J recombination activity of Artemis as A-T cells deficient in ATM are proficient in V(D)J recombination (Jeggo & Lobrich, 2005).

Moreover, Artemis-deficient CJ179 fibroblasts from SCID patients show increased sensitivity to radiation, NCS and bleomycin compared to normal cells (Mohapatra, Kawahara, Khan, Yannone, & Povirk, 2011). Artemis is required for the repair of a subset of IR-induced DSBs as observed from an increased persistence of γ -H2AX foci in cells deficient in Artemis and for this function, Artemis and ATM are epistatic (Riballo et al., 2004). Interestingly, Artemis and ATM were also shown to promote homologous recombination of IR-induced DSBs in the G2 phase of the cell cycle. The endonuclease function of Artemis was shown to be important for resecting DSBs leading to the formation of ssDNA and Rad51 foci at these DSBs in G2 (Beucher et al., 2009). In contrast, only ATM and not Artemis is required for HR-mediated repair of IR-induced DSBs in S-phase (Kocher et al., 2012).

More recently, novel roles of Artemis have come to light. Artemis associates with PTIP in mediating repair pathway choice by acting as a major downstream effector of 53BP1 limiting end resection and promoting NHEJ (J. Wang et al., 2014). Quite surprisingly, Artemis mediates DNA double-strand break resection in G1 phase via a slow repair component involving classical NHEJ. This process requires CtIP interacting with BRCA1 to initiate resection, Mre11 exonuclease activity, EXD2 and Exo1 execute the process and the endonuclease function of Artemis completes the process (Biehs et al., 2017).

Apart from its end-processing function, Artemis also plays a role in the DNA damage signaling. (Kurosawa & Adachi, 2010). Artemis is phosphorylated by ATM and in response to ionizing radiation, is needed for recovery from the G2/M cell cycle checkpoint by regulation of Cdk1-Cyclin B (Geng, Zhang, Zheng, & Legerski, 2007). Artemis was shown to be phosphorylated by ATR at Ser516 and Ser645 in response to replication stress leading to ubiquitination and degradation of cyclin E, thus promoting recovery from S-phase checkpoint (H. Wang, Zhang, Geng, Teng, & Legerski, 2009).

2.3 Polynucleotide Kinase/ Phosphatase

Eukaryotic polynucleotide kinases (PNK) were identified in the early 1960s and were observed to function similar to the T4 phage counterparts in specifically phosphorylating 5'-hydroxyl termini on DNA and RNA oligonucleotides. Subsequently, this enzyme was also shown to possess a 3'-phosphatase activity in addition to the 5'-kinase function (Pheiffer & Zimmerman, 1982). Several years later, the human PNKP gene was cloned and was identified as one of the two known mammalian DNA 3'-phosphatase along with the previously described weak 3'-phosphatase APE/HAP1 (Jilani et al., 1999). Since then, extensive research has been carried out on this bifunctional enzyme and has been shown to play a critical role in DNA SSB as well as DSB repair.

2.3.1 Structure

Based on amino acid sequence conservation and secondary structure predictions, the PNKP protein can be divided into 2 distinct domains; an N-terminal forkhead associated (FHA) domain and a C-terminal catalytic domain comprising of the phosphatase and kinase sub-domains fused to each other. The FHA domain is important for the interaction of PNKP with other DNA repair factors such as XRCC1 (in SSB repair) and XRCC4 (in NHEJ). Although a crystal structure of a full length human PNKP is not available, that of the murine PNKP has revealed several key aspects of the protein.

The phosphatase sub-domain (136 – 337 amino acids) belongs to haloacid dehalogenase (HAD) superfamily of proteins whose activity is dependent on Mg²⁺ and a catalytic aspartate residue. Unlike the TDP1-mediated reaction, which proceeds via a phosphohistidine intermediate, PNKP reactions proceed via a phosphoacyl intermediate. The phosphatase active site is narrow and cannot accommodate a double-stranded DNA suggesting of a DNA end-breathing step prior to phosphatase activity on blunt- or recessed-end DNA substrates. The kinase sub-domain (340 – 521 amino acids) belongs to the P-loop kinase family and has separate ATP and DNA-binding sites. Unlike the phosphatase domain cleft, the active site cleft in the kinase domain is able to accommodate SSB as well as DSB substrates owing to a wide recognition groove composed of 2 positively charged surfaces (Weinfeld et al., 2011).

2.3.2 Function

Owing to its bifunctional nature, the promiscuity of PNKP in several DNA repair pathways is perhaps unsurprising. In response to single-strand breaks formed upon IR treatment, PNKP is required to hydrolyze the 3'-phosphate groups formed either directly or upon enzymatic treatment of 3'-phosphoglycolates by TDP1/ APE1 and also phosphorylate 5'-hydroxyl ends (Weinfeld et

al., 2011). XRCC1-deficiency sensitizes cells to H₂O₂-induced SSBs, but this sensitization can be completely rescued by overexpression of a WT, but not a phosphatase-defective PNKP protein (Breslin et al., 2017). XRCC1 is phosphorylated by casein kinase 2 (CK2) and this phosphorylation promotes interaction of p-XRCC1 with the PNKP-FHA domain. Along these lines, p-XRCC1 enhances the kinase as well as the phosphatase function of PNKP and is required for the recruitment of XRCC1 and PNKP to nuclear foci for SSB repair (Hanzlikova, Gittens, Krejčíková, Zeng, & Caldecott, 2017). PNKP depletion renders human cells sensitive to camptothecin and other topoisomerase 1 poisons suggesting that, similar to 3'-PG repair, PNKP functions downstream of TDP1 for repairing Top1-associated SSBs (Kawale & Povirk, 2018).

Similar to SSB repair, PNKP plays a critical role in DSB repair and is a part of the elite cast of end processing enzymes during NHEJ. Experiments in extracts have shown that PNKP is critical for ligation of a 5'-hydroxyl ended linearized plasmid substrate. A549 cells depleted of PNKP show sensitivity to ionizing radiation. Similarly, inhibition of PNKP with a small molecule inhibitor confers radiosensitivity in these cells (Freschauf et al., 2009). As for SSB repair, PNKP interacts with XRCC4 phosphorylated by CK2 and this interaction enhances the 5'-kinase activity of PNKP (Weinfeld et al., 2011). Mutations in PNKP gene lead to neurological conditions including microcephaly with seizures (MCSZ), an autosomal recessive disorder characterized by a delay in development and Ataxia with Oculomotor Apraxia 4 (AOA4) characterized by ataxia and peripheral neuropathy (Dumitrache & McKinnon, 2017). The pathogenic mutations in MCSZ are associated with both the kinase and the phosphatase sub-domains of PNKP, whereas those in AOA4 are observed only in the kinase domains.

2. 4 Specific Aims

Compared to normal cells, whole cell extracts (WCEs) from SCAN1 cells are deficient in processing the 3'-PG termini on overhanging DSB substrates. Strangely, however, SCAN1 cells show neither hypersensitivity nor any deficit in the repair of DSBs induced by ionizing radiation. Moreover, HeLa cells with TDP1-knockdown show only marginal sensitivity to calicheamicin, expected to produce 3'-PG ended DSBs. This argues for the presence of other enzymes functioning in parallel to TDP1 for the processing of 3'-PG DSBs.

A few candidate enzymes including apurinic/apyrimidinic endonuclease 1 (APE1) and the Artemis nuclease have been implicated in 3'-PG removal. However, although APE1 can process 3'-PG on blunt or recessed DSB ends, overhanging 3'-PGs are completely refractory to removal by APE1. In contrast, Artemis can effectively remove 3'-PG on overhanging DSB ends by endonucleolytic trimming. Moreover, Artemis-deficient cells show increased sensitivity to IR as well as to neocarzinostatin (NCS) and bleomycin, radiomimetic agents that produce 3'-PG DSBs, and this sensitivity can be rescued by expressing wild-type, but not endonuclease-deficient (D165N) Artemis. Thus, Artemis, via its endonuclease function, is a likely candidate enzyme functioning in parallel to TDP1 for the repair of 3'-PG on DSB overhangs.

In this dissertation, we proposed:

- 1. To determine the biological significance of the function of TDP1 in repairing 3'-phosphoglycolate-ended DSBs.**
- 2. To investigate the interplay between Artemis and TDP1 in response to radiomimetic 3'-phosphoglycolate-terminated DSBs.**

Polynucleotide Kinase Phosphatase is a critical enzyme for the processing of 3'-phosphate- and 5'-hydroxyl-modifications on DNA DSBs. PNKP also participates in the base-excision repair pathway for repairing SSBs as well as in the PARP1-dependent alternative end joining pathway for DSB repair. Knockdown of PNKP conferred increased sensitivity to ionizing radiation in A549 lung cancer cells. However, several limitations, including the heterogeneity of damage and a high ratio of SSBs to DSBs induced by IR, along with the persistence of residual PNKP upon its knockdown, complicate the interpretation of these results. To further clarify the role of PNKP, we proposed:

- 3. To investigate the importance and biological significance of PNKP specifically in the repair of NCS-induced 3'-phosphate-terminated DSBs.**

3. MATERIALS AND METHODS

3.1 Cell lines and reagents

HCT116 TDP1^{-/-} cells, constructed in the laboratory of Dr. Yves Pommier, NIH, have been described (Abo et al., 2017). HCT116 Artemis^{-/-} cells were obtained from the lab of Dr. Eric Hendrickson, University of Minnesota. Human Embryonic Kidney (HEK) 293 cells were obtained from American Type Culture Collection (ATCC). HCT116, HEK293 and HEK293T cells were maintained in Roswell Park Memorial Institute (RPMI) 1640 medium (GIBCO) supplemented with 10% fetal bovine serum (Atlanta Biologicals) and antibiotics (GIBCO) at 37°C in 5% CO₂ atmosphere. 48BR WT and CJ179 Artemis deficient fibroblasts were maintained in Minimal Essential Medium Alpha (MEM- α) with 10% Serum (HyClone Fetal Clone II Bovine Serum), 1X Glutamax and antibiotics. NU-7441 (aka KU-57788), KU-60019, AZD-2287 and ABT-888 were obtained from Selleckchem. Neocarzinostatin (NCS) was from Sigma or Nippon-Kayaku and Calicheamicin (CAL) was a gift of Wyeth Pharmaceuticals (now Pfizer).

3.1.1 HCT116 cells.

Artemis^{-/-}•*TDP1*^{-/-} : TDP1 was knocked out in HCT116 *Artemis*^{-/-} cells using CRISPR editing technique as described (Abo et al., 2017). Briefly, *Artemis*^{-/-} cells were transfected CRISPR editing reagents along with a vector harboring a cloned sequence targeting TDP1 exon 5 (GTTTAACTACTGCTTTGACGTGG) and a puromycin resistance gene flanked by homology arms upstream and downstream of the target site. Transfected cells were selected in 0.8 µg/mL puromycin for 4 days. Single cell clones were subsequently screened for TDP1 activity to obtain clones without any detectable TDP1 activity.

shTDP1 and Artemis^{-/-}•*shTDP1* : For the expression of a TDP1 shRNA, the pLSLP lentiviral vector, a distant relative of the pLV vector containing an RNA polymerase III-driven H1 RNA promoter controlling the expression of a small hairpin RNA (shRNA) transcript and harboring the puromycin N-acetyl transferase (pac) gene conferring resistance to puromycin was used (Budanov, Sablina, Feinstein, Koonin, & Chumakov, 2004). Phosphorylated oligonucleotides with sequences 5'-GATCCGGTGATAAGCGAGAGGCTAACTTCGTGTCATTAGCCTCTCGCTTATCACTTTTG-3' and 3'-GCCAGTATTCGCTCTCCGATTGAAGGACAGTAATCGGAGAGCGAATAGTGAAAAAC TTAA-5' were annealed at a 1:1 ratio in annealing buffer (10 mM Tris, pH 7.5, 50 mM NaCl, 1 mM EDTA) by heating the mixture at 95°C for 5 min followed by cooling of the mixture at a rate of 1°C/ min and stored at 4°C. The lentiviral pLSLPw backbone construct was restriction enzyme digested using BamHI and EcoRI, dephosphorylated and gel purified. The annealed oligomers were ligated in the digested lentiviral construct. This vector expresses a hairpin that targets the sequence GUGAUAAGCGAGAGGCUA (bases 20300-20319 in exon 6 of the TDP1 gene,

GenBank #NG009164). shTDP1 lentiviral constructs were transfected into HEK293T cells along with packaging plasmid psPAX2 and envelope plasmid pMD2.G using calcium chloride. Supernatant containing packaged lentiviral particles was collected, centrifuged at 4000 RPM at 4°C. The viral supernatant was then collected and filtered through a 0.25 µm filter, aliquoted in 1 mL vials and flash frozen and stored at -80°C. HCT116 WT and HCT116 Art^{-/-} cells were seeded at 75% confluency in 6-well plates and incubated for 24 hr. The medium was aspirated, cells washed with PBS, incubated with 1 mL of the lentiviral stock in the presence of 4 µg/mL polybrene overnight on a rocker at 37°C in 5% CO₂. The viral supernatant was removed and cells were fed with fresh medium containing 0.8 µg/mL puromycin and selected for 4 days. Cells from each genotype were expanded under selection and cryogenic stocks were stored. Genomic DNA was extracted from a fraction of selected cells using QIAGEN DNeasy Blood and Tissue kit and DNA concentration was measured. 100 ng genomic DNA was used as a template in a 50 µL PCR reaction for the amplification of the puromycin resistance gene using forward primer: 5'-CGAGTACAAGCCCACGGT-3' and reverse primer: 5'-AGACCCTTGCCCTGGTG-3' (synthesised by IDT) with initial denaturation at 94°C for 6 min followed by cycles of denaturation at 94°C for 10 sec, annealing at 58°C for 20 sec and extension at 72°C for 30 sec for 35 cycles, followed by a final extension step at 72°C for 7 min and analyzed on a 1% Agarose gel. Single cell clones were obtained and screened for maximum knockdown efficiency by TDP1 activity assay.

3.1.2 HEK293 and HEK293T cells.

***TDPI*^{-/-}** : HEK293 or HEK293T cells were triply transfected with hCAS9, pMaxGFP and a pUC19 vector expressing a gRNA targeting bp 24880-24899 in exon 7 of the TDP1 genomic sequence (GCAAAGTTGGATATTGCGTT) from a U6 promoter. Cells were grown on a 10 cm

dish to 70% confluence and then medium was replaced with 1.5 mL OptiMem (GIBCO). A DNA mixture consisting of 12 µg hCAS9 (Mali et al., 2013), 2.4 µg pMaxGFP and 9.6 µg targeting vector was prepared in 50 µL OptiMem, combined with a transfectant solution consisting of 60 µL Lipofectamine 2000 (ThermoFisher) and 50 µL OptiMem, incubated for 40 min at 22°C and then added to the medium in the dish. Cells were bathed in the transfection mixture for 4 hr at 37°C on a rocker. The mixture was then replaced with 10 mL complete medium and the cells incubated for 16 hr. Cells were harvested and single GFP+ cells were sorted into individual wells and expanded. DNA was isolated as above and clones with deletions/insertions at the target site in both alleles were identified by amplifying a 141-bp fragment encompassing the target using one Cy5-labeled (Cy5-AAATGACAATGCTTGAGGG) and one unlabeled primer (CCAGTAGATATGGATATTAGTGAG), and analyzing the products on a denaturing sequencing gel, with detection on a Typhoon imager. Extracts were prepared and screened for phosphodiesterase activity and a clone with no detectable activity (<0.1% of parental) was selected.

shArtemis and shArtemis.TDP1-/- : shArtemis vector in the w16-1 backbone (pLenti X2 Puro DEST) was obtained from the lab of Dr. Steven Yannone (Campeau et al., 2009). The sequence used to express double-stranded oligonucleotides encoding Artemis shRNA were: 5'-GATCCCCTGAAGAGAGCTAGAACAGGTGTGCTGTCCCTGTTCTAGCTCTCTTCAGTTTTGGAAA-3'. This vector expresses a hairpin that targets the sequence CTGAAGAGAGCTAGAACAG (bases 34662-34680) in exon 13 of the Artemis (DCLRE1C) gene, GenBank #NG_007276.1. Lentiviral stocks were generated as mentioned above. HEK293 WT and TDP1-/- cells were seeded in 6-well plates and infected with the 1 mL of the lentiviral

stock. Cells were cultured in 1 $\mu\text{g}/\text{mL}$ Puromycin for 5 days. Selected cells were further expanded to 10 cm flasks and genotyped by PCR amplification of the *pac* gene as mentioned above.

3.1.3 48BR WT and CJ179 Artemis deficient fibroblasts

TDP1 was knocked-down in 48BR normal and CJ179 Artemis-deficient fibroblasts in a way similar to described before for HCT116 cells. However, since these cells were already resistant to puromycin, the lentiviral vector was modified by inserting a Turbo-GFP gene fragment from the pGIPZ vector and cells were selected based on their GFP expression. pGIPZ vector was digested using XbaI and XhoI enzymes that releases a 2684bp fragment with the Turbo GFP and puromycin resistance gene under the control of a CMV promoter. pLSLPw was sequentially digested by XbaI and Sall to remove the puro resistance gene. Sticky ends created by digestion using Sall are compatible with XhoI. The vector and the insert were gel-purified and 50 ng of total DNA mixture was ligated overnight at 16°C in the presence using T4 DNA Ligase. Competent cells were then transformed with this ligated vector and allowed to form colonies overnight. Plasmids isolated from these colonies were ~9 kb in size. The presence of insert was confirmed by digesting the vector with an insert specific enzyme.

In addition, TDP1 was also knocked out in these fibroblasts in a similar manner as mentioned above for HEK293 cells. Cells were bathed in the transfection mixture for 24 hours followed by single cell sorting using FACS. Single-cell clones were screened for absence of TDP1 activity by TDP1 activity assay.

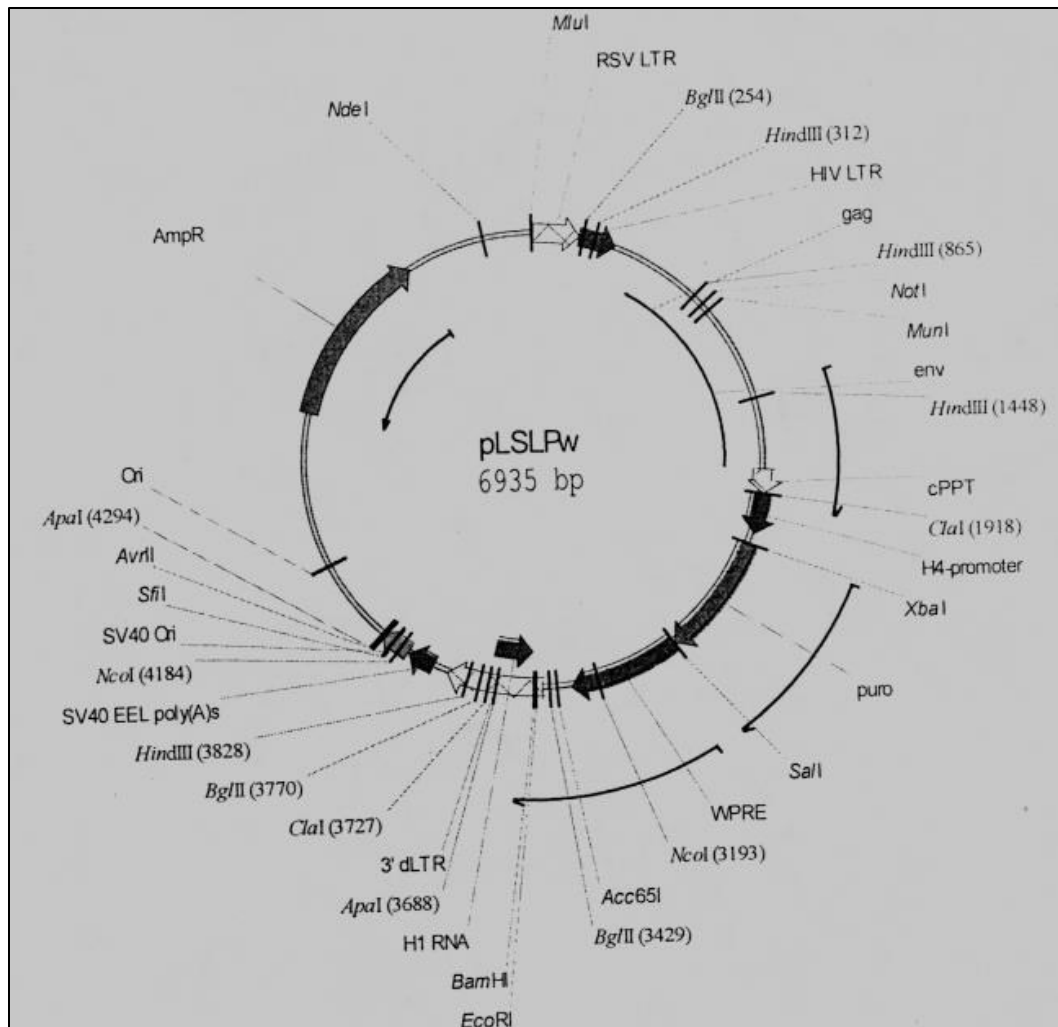


Figure 3-1: Lentiviral transfer vector pLSLPw harboring the shRNA against TDPI

The shTDPI construct was cloned into the BamHI and EcoRI sites seen at the bottom. The vector carries a puromycin N-acetyl transferase (pac) gene seen here as puro on the right in between XbaI and SalI sites which confers resistance to the antibiotic puromycin.

3.2 Dilution cloning for selection of clones.

From the puromycin-selected cells, 5 cells were seeded in 15mL complete medium in 15 cm dishes and the cells were made to form colonies over a period of 14 days. Following colony formation, the medium was removed and the colonies were washed with 5mL of PBS. A sterile cloning cylinder was placed on top of the colonies and 70 μ L trypsin was added in each ring to dissociate the cells. The trypsinized cells were sub-cultured into individual 10 cm dishes to obtain individual clones.

3.3 Growth curve assay

Cells (1×10^5) were seeded in 6-well plates in duplicates in 3 mL complete medium. At the appropriate time points, cells were washed with 1X PBS, trypsinized and counted using a hemocytometer.

3.4 TDP1 activity assay

Cells (2×10^6) from each derivative cell line were collected using trypsinization and centrifuged at 1200 RPM for 5 min at room temperature (RT). The cell pellet was washed once in 1X PBS and treated with lysis buffer (10 mM HEPES at pH 7.8, 60 mM KCl, 1 mM EDTA, 0.5% NP-40) in the presence of 2 mM serine protease inhibitor phenylmethanesulfonyl fluoride (PMSF), 1 mM NaVO₄, 1 μ g/mL leupeptin, 1 μ g/mL aprotinin and 1 μ g/mL pepstatin, vortexed until the pellet was disrupted, incubated on ice for 10 min and centrifuged at 13000 RPM for 5 min at 4°C. The supernatant ("cell extract") was collected and serially diluted in dilution buffer (50 mM Tris at pH 8.0, 5 nM DTT, 100 mM NaCl, 5 mM EDTA, 10% glycerol, 500 μ g/mL BSA). Serial dilutions of 1 μ L of the extract was incubated with 100 attomoles of an 18-base 5'-Cy5 labelled 3'-phosphotyrosyl oligonucleotide with sequence TCCGTTGAAGCCTGCTTT (18Y) (Midland Certified Reagents Midland, TX) in 1X reaction buffer (60 mM KOAc, 10 mM MgOAc, 50 mM

triethanolamine-HAc pH 7.5, 2 mM ATP, 1 mM DTT) in total 5 μ L reaction volume and incubated at 37°C for 1 hr, denatured at 95°C for 5 min and separated on 20% denaturing polyacrylamide sequencing gels by electrophoresis for around 4 hr at 42 V/cm. Gels were then imaged on a Typhoon 9410 Variable Mode Imager (GE Healthcare) in Fluorescence Acquisition mode with a Cy5 Emission filter using a Red (633 nm) laser at PMT of 800 V and analyzed on ImageQuant 5.1 software.

3.5 Sequencing polyacrylamide gel electrophoresis

Denaturing polyacrylamide gels with acrylamide: bisacrylamide ratio of 20:1 and Urea at a final concentration of 8M were used for separation of the oligonucleotide substrate with and without the Tyrosyl attached to its 3'-end. The gel dimensions were 33cm X 38cm X 0.1cm. Urea was dissolved into the mixture before adding 0.075% ammonium persulfate and 0.0625% TEMED (N, N, N', N'-tetramethylethylene diamine). The gel was allowed to set for around 1 hour, following which the samples were loaded into the wells of the gel and electrophoresed at constant power of 60 W for around 4 hours in 1X TBE buffer (10X stock solution: 108 g of Tris base, 55 g of boric acid, 9.3 g of disodium EDTA in 1L Distilled water). The gel was wrapped in saran wrap following electrophoresis and scanned on a Typhoon 9410 Variable Mode Imager in Fluorescence Acquisition mode with 670BP 30 Cy5 Emission filter using a Red (633) laser at PMT of 800 V.

3.6 Cytosol-Nuclear Fractionation

For detection of TDP1, two million cells were fractionated using a nuclear/cytosol fractionation kit (BioVision #K266-25). Briefly, cells were collected by trypsinization and centrifuged at 600 X g for 5 min at 4°C. Cell pellets were mixed with a proprietary cytosol extraction buffer (CEB-A) mix containing 1mM DTT and 2X protease inhibitor cocktail. Cells were vortexed and incubated on ice for 10 min followed by addition of 11 μ L cytosol extraction

buffer B (CEB-B) and incubating on ice for 1 min. Cells were centrifuged at 16000 X g and the supernatant was collected as the cytosolic fraction. The pellet was washed once with PBS to remove any contaminating cytosolic material. 100 μ L of nuclear extraction buffer was added and the samples were vortexed for 15 sec every 10 min at 4°C. The samples were then centrifuged at 16,000 X g for 10 min at 4°C and the supernatant was collected as the nuclear fraction. Protein concentration estimation was performed using a BCA assay (Pierce).

3.7 Western blot analyses

Laemmli buffer (2% SDS, 10% glycerol, 5% 2-mercaptoethanol, 0.004% bromophenol blue, 0.125 M Tris-HCl pH 6.8) was added to the cytosolic and nuclear lysates and heated for 10 min at 95°C. 25 μ g of the nuclear and 50 μ g of the cytoplasmic lysates were separated on a 10% polyacrylamide gel at 120V for around 2 hr. Proteins were transferred onto nitrocellulose membrane in 1X transfer buffer (10X - 500 mM Tris, 400mM glycine, 3.7 g SDS) containing 20% methanol at a constant current of 350 mA for 2 hr. Membranes were blocked using 1% casein in PBS for 1 hr and then probed with either a mouse polyclonal anti-TDP1 primary antibody (Abnova) at a 1:1000 dilution or rabbit anti-Lamin (nuclear fractionation control) primary antibody at 1:3500 for 16 hr at 4°C. Membrane was washed thrice with 1X TBST for 10 min each and incubated in peroxidase-conjugated secondary goat anti-mouse at 1:2500 or goat anti-rabbit at 1:5000 for 1 hr at 22°C. Membrane was then washed thrice with 1X TBST for 10 min each and developed with ECL Super Signaling substrate. Lamin was used as a nuclear control.

3.8 Clonogenic survival assays

Cells were seeded at densities ranging from 300 to 10,000 in 6 cm dishes and incubated for 12 hr to allow attachment. Cells were then treated either with NCS (stock concentration 37 μ M diluted to 2 μ M in 20 mM sodium citrate buffer, pH 4.0) at concentrations ranging from 0.25 nM

to 2 nM for 6 hr or they were treated with CAL (stock concentration 20 μ M diluted to 1 μ M in 50% ethanol, further diluted in PBS to obtain a final working concentration of 1.2 nM) at concentrations ranging from 0.3 pM to 2.4 pM for 24 hr. Following treatment, cells were incubated in fresh medium for 9 to 12 days to form colonies. Colonies were fixed with 100% methanol for 10 min (for HEK293 and HEK293T cells, colonies were fixed with formaldehyde solution, Sigma - #25249), stained with 0.5% crystal violet in 20% methanol for 10 min, washed under tap water, air dried and counted manually. Plating efficiency (PE) was calculated as the number of colonies formed/number of cells seeded *100 for each dose. Surviving fraction (SF) was calculated as PE of treated/PE of control *100. Dose enhancement factor (DEF) was calculated as IC_{90} of control/ IC_{90} of the mutant cell line. For experiments using IR, cells were irradiated using a MDS Nordion Gammacell 40 research irradiator (ON, Canada), with a ^{137}Cs source. For experiments with KU-60019, NU-7441, AZD-2287 and ABT-888, the respective inhibitor was added 1 hr prior to NCS treatment and left in the medium during and 24 hr after NCS treatment.

3.9 Mitotic shake-off for G1-phase synchronization

Cells were synchronized in the G1-phase by mitotic shake-off. Briefly, cells were seeded in 15 cm dishes and allowed to reach around 60-70% confluency. The dishes were kept for 1 min on the thermomixer set at 1000 RPM and agitated. The medium from the dish (with suspended mitotic cells) was collected and kept on ice. This procedure was repeated twice. The medium was centrifuged, the cell pellet resuspended in 1 mL media and counted. Cells were then seeded in individual wells of 6 well plates, harvested after 1-6 hr and then processed for cell cycle analysis. For survival assays, cells were counted and directly seeded in 6cm dishes and then treated after 2 – 6hr with NCS as described above.

3.10 Immunofluorescence

Twenty-five thousand cells were seeded in 4-well chamber slides (Nunc Lab Tek) and incubated overnight. Cells were then serum starved by incubating in 0.5% FBS/RPMI for 72 hr. Cells were then treated with 4 nM NCS for 1 hr and fixed at different time points using ice-cold 4% paraformaldehyde (PFA) in 1X PBS for 10 min. Cells were permeabilized in 0.5% Triton X-100/PBS for 10 min and blocked in 1X PBS 1% Casein blocker (Bio-Rad, 1610783) for 1 hr at 22°C. Primary antibodies (mouse monoclonal anti 53BP1 at 1:1000 (BD Pharmingen) and mouse anti-TDP1 (Abnova) at 1:100) were added and incubated overnight at 4°C. Slides were washed 4 times with PBS for 15 min each and incubated with secondary goat anti-mouse CFL594 antibody at 1:1000 (sc-362277) for 2 hr at 22°C. Slides were washed 4 times with PBS for 15 min each and post-fixed using ice-cold 4% PFA for 10 min. Nuclei were counterstained with Vectashield mounting medium containing 1.5 µg/mL 4',6-diamidino-2-phenylindole (DAPI) (Vector Laboratories, H-1200). Confocal images were obtained with the Zeiss LSM700 Confocal Laser Scanning Microscope equipped with a 63X, 1.4 NA oil immersion objective, located in the Virginia Commonwealth University Microscopy Core Facility using a 405 nm laser (DAPI) and a 555 nm laser (CFL594).

3.11 Cell cycle analysis by flow cytometry

All the four cell lines were seeded at a density of 5×10^5 cells/ dish in 10 cm dishes and cultured in complete medium. After 24 hours, the medium was removed and cells were washed thrice with 1X PBS and were synchronised by serum starving them in medium containing 0.5% FBS for 96 hours. Cells were then treated with 4 nM NCS for 1 hr following which, the medium was changed. Cells were washed with PBS and released in serum and harvested after 12 hr and 18 hr. At the prescribed time points, the medium was removed, cells were washed with PBS twice

and trypsinized. 1.5×10^6 cells were then counted using a hemocytometer, centrifuged at 800 RPM for 5 min and fixed in ice-cold 70% ethanol for minimum 1 hr. Ethanol-treated cells are more buoyant and thus were centrifuged at 2000 RPM for 5 min. The pellets were resuspended in 1 mL Propidium Iodide (PI) solution (3.8 mM Sodium Citrate, 0.05 mg/mL PI, 0.1% Triton X-100) in the presence of 10 μ g/mL RNase A (Sigma) and stored in dark for 30 min in 5 mL Polystyrene Round-Bottom Tube with Cell-Strainer Cap (Fisher Scientific). Cell Cycle Analysis was performed using a Becton Dickinson (San Jose, CA) FACS Canto II flow cytometer. The argon ion laser set at 488 nm was used as an excitation source. Cells having DNA content 2N were designated as being in the G1 phase of the cell cycle, those having 4N were designated as being in the G2 phase while the cells showing intermediate DNA content between 2N and 4N were designated as S-phase cells. Minimum ten thousand events were acquired for each sample and the data obtained was analysed using the Modfit LT software.

3.12 Centromere-fluorescence in situ hybridization

One million cells were seeded in 6-cm dishes and incubated overnight. Cells were treated with 1 mM caffeine to abrogate the G2/M block 10 min before treating with 2 nM NCS for 6 hr. 4 hours into NCS treatment, cells were treated with 1 μ g/mL colchicine for 2 hr. After 6 hr NCS treatment, cells were collected by trypsinization, washed with PBS and swollen in 75 mM KCl for 10 min at 37°C, then centrifuged and fixed with ice-cold Carnoy's fixative (3:1 methanol:glacial acetic acid) for 10 min. Samples were centrifuged and washed twice with methanol/acetic acid. Cells were dropped onto ethanol-cleaned, ice-cold slides and dried overnight. Slides were dehydrated by immersing for 2 min each in 70%, 90% and 100% ethanol followed by baking at 65°C for 10 min, washing in acetone for 10 min and air drying. Slides were treated with 100 μ g/mL RNase A in 2X SSC under a parafilm coverslip for 30 min at 37°C then washed for 5 min in

2XSSC and for 10 min in PBS, dehydrated in an ethanol series and allowed to dry. Chromosomes were denatured by immersing in 70% formamide / 2XSSC (pH =7) for 2 min at 75°C and then in ice-cold 70% ethanol for 2 min. Slides were again dehydrated in an ethanol series and air-dried. 25 μ L of 200 nM Cy3-labeled PNA CENP-B probe (PNA Bio – F3002) in hybridization buffer (20 mM Tris, pH 7.4, 60% formamide, 0.1 μ g/mL salmon sperm DNA) was added, covered with a 24 mm X 50 mm coverslip and allowed to hybridize for 2 hr at 37°C in dark. Slides were then washed in 2X SSC for 5 min at 37°C, three changes of 0.5X SSC / 0.3% NP-40 for 10 min at 55°C, two changes of 2X SSC / 0.1% NP-40 for 5 min at 22°C, and finally in 2X SSC for 5 min at 22°C. The washed slides were dried and counterstained with Vectashield mounting medium containing DAPI (Vector Laboratories) under a coverslip and was sealed with nailpolish. Metaphases were then imaged using a Zeiss LSM700 Confocal Microscope as described. For experiments using NU-7441, the inhibitor was added 1 hr prior to NCS treatment. All washes were performed in 50-mL glass Coplin jars.

3.13 Transformation

Transformation reactions were performed using the NEB Turbo or Alpha-Gold Select competent cells. 25 μ L aliquots of cells were thawed on ice and incubated with 50 ng (2 μ L) of the plasmids on ice for 30 min, then subjected to a heat shock for 30 sec at 42°C followed by 2 min incubation on ice. Pre-warmed SOC medium (1 mL) was added and the reactions were incubated at 37°C with shaking at 1000 RPM for 1 hour. Culture was spread on LB Carbenicillin plates at 3 dilutions and incubated overnight at 37°C.

3.13 Statistics

Graphical analysis was performed using SigmaPlot 13 statistical software. Statistical significance values were obtained by performing a Two-way Anova followed by Holm-Sidak post-

hoc test for all clonogenic survival assays whereas unpaired two-tailed students t-test was used for 53BP1 repair kinetics analysis and FISH experiments.

4. RESULTS

4.1 Generation of TDP1-mutant (shTDP1 and TDP1^{-/-}) cell lines

It has been previously shown that TDP1 is critical for the repair of overhanging 3'-phosphoglycolates on model DSB substrates in whole cell extracts (Hawkins et al., 2009). However, experiments performed to understand the role of TDP1 in DSB repair in cells have shown otherwise (El-Khamisy et al., 2005; Hawkins et al., 2009; Zhou et al., 2009). In order to clearly demonstrate the role of TDP1 in DSB repair, TDP1 was knocked-down in WT HCT116 human colorectal adenocarcinoma cell line using a lentiviral vector carrying a small hairpin RNA for TDP1 (Budanov et al., 2004; Chumakov, Kravchenko, Prassolov, Frolova, & Chumakov, 2010) (Fig 3-1). Cells were selected in medium containing 0.8 µg/mL puromycin for four days. Single cell clones were obtained by dilution cloning using cloning towers. Stable single cell clones were then scaled up and cultured in 6-well plates. Stable single-cell clones were screened for maximum knockdown efficiency using a biochemical gel-based TDP1 activity assay, capable of detecting as little as 0.1% TDP1 activity. Due to the high specificity of TDP1 towards 3'-phosphotyrosyl oligonucleotides, TDP1 catalytic activity was measured in cell extracts by the extent of the conversion of a 5'-Cy5-labelled 18-base oligonucleotide substrate bearing a

3'-phosphotyrosine (18pY) to a 3'-phosphate (18p) product migrating with an increased electrophoretic mobility in a polyacrylamide gel (Gao et al., 2014). Clone #18 (shTDP1#18) showed maximum (94%) knockdown efficiency with 6% residual TDP1 expression (Fig. XX). Similarly, HCT116 TDP1^{-/-} cells, screened for TDP1 activity, demonstrated a complete lack of conversion of 18Y to 18P (Fig. 4-1).

In addition to HCT116 cells, TDP1 was also knocked out in HEK293 and HEK293T cells. Initial attempts at CRISPR/Cas9-mediated knockout of TDP1 targeting the initiation codon resulted in several clones with homozygous deletions that nevertheless harbored a low (1 to 2% of parental) level of tyrosyl-DNA phosphodiesterase activity, suggesting a possible alternatively spliced or translated enzyme. Therefore, the TDP1 active site in exon 7 was targeted instead.

Clones with deletions/insertions in both alleles were identified and whole-cell extracts were screened for phosphodiesterase activity. One TDP1^{-/-} clone produced extracts that completely failed to hydrolyze the 18pY substrate to 18p product (<0.1% of WT activity, Fig. 4-2A). In addition, TDP1 was immuno-labelled and cells were analyzed for TDP1 expression by confocal microscopy. HEK293 WT but not TDP1^{-/-} cells, showed robust TDP1 expression observed as red fluorescence in the nuclei of these cells (Fig 4-2B). Some cytoplasmic red fluorescence was observed in TDP1^{-/-} cells as well although this was presumably non-specific. TDP1 expression was also analyzed by performing a western blotting experiment to further confirm the above results. The antibody against TDP1 was not sensitive and specific enough to detect TDP1 in whole cells extracts. Hence, cyto-nuclear fractionation was performed to enrich TDP1 in the nuclear extracts of these cells as done previously (Zhou et al., 2009). Western blotting performed in these fractions showed an absence of a band corresponding to TDP1 protein in nuclear extracts of TDP1^{-/-} compared to TDP1^{+/+} WT cells (Fig 4-2C).

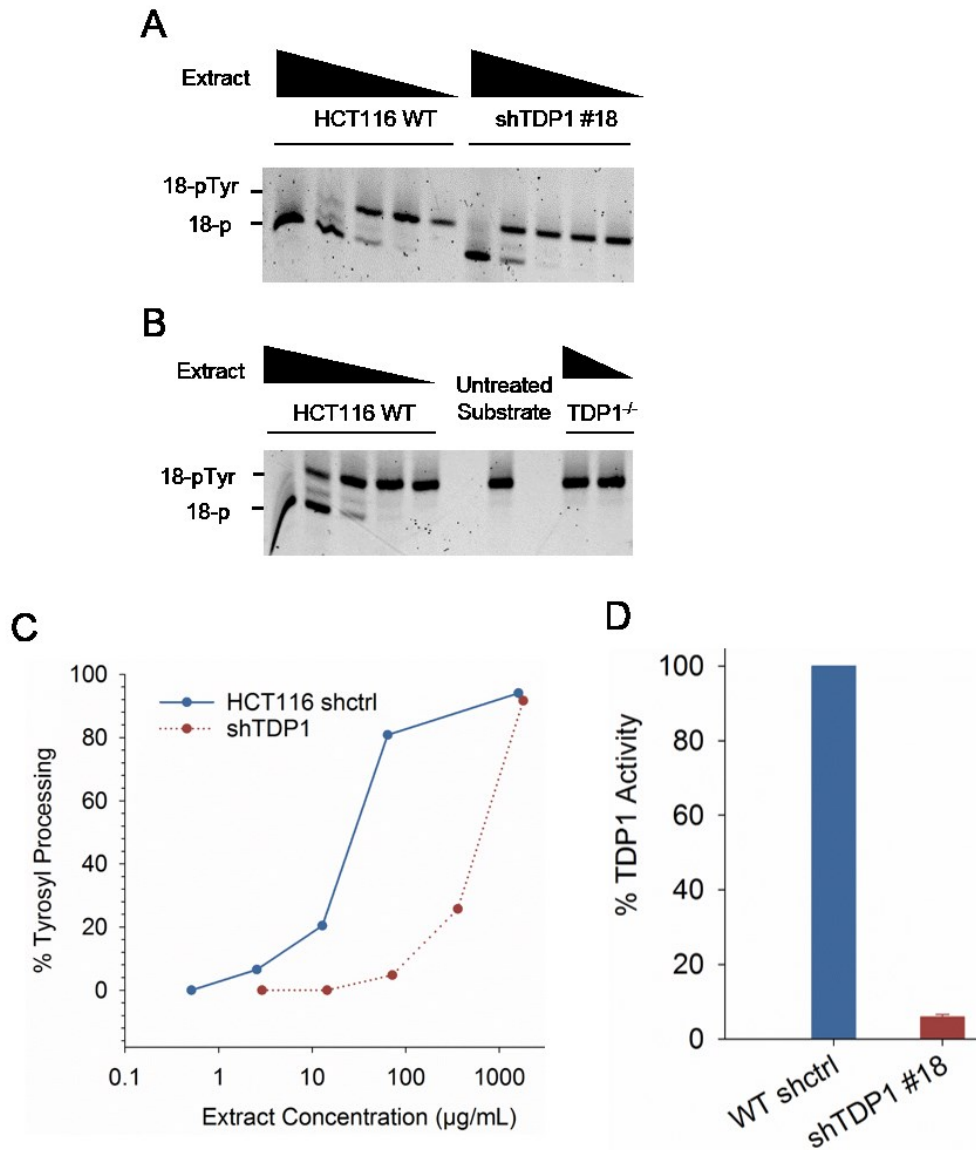


Figure 4-1- TDP1 expression in HCT116 cells.

(A, B) 18-base oligonucleotide substrate with a phosphotyrosine attached to the 3'-end was incubated with serially-diluted whole cell extracts of HCT116 WT and shTDP1#18 in (A) and TDP1^{-/-} in (B) for 1 hour and separated on a 20% polyacrylamide gel. Processed (18-P) and unprocessed (18-pTyr) forms of the substrate and serial dilutions of the extracts are indicated. Substrate incubated in reaction buffer instead of cellular extract is represented as untreated substrate in (B). (C and D) Percentage of TDP1 Activity remaining in whole cell extracts as observed in B.

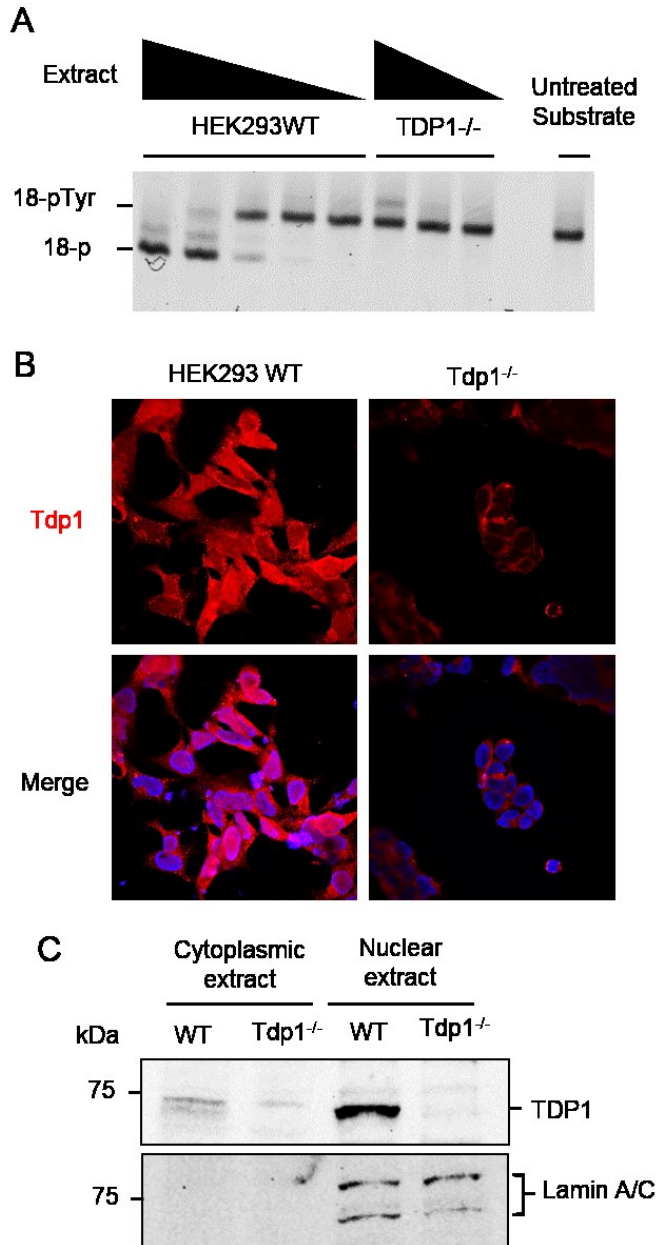


Figure 4-2: TDP1 expression in HEK293 cells.

(A) 18-base oligonucleotide substrate with a phosphotyrosine attached to the 3'-end was incubated with serially-diluted whole cell extracts of HEK293 WT and TDP1^{-/-} cell lines for 1 hour and separated on a 20% polyacrylamide gel. Processed (18-P) and unprocessed (18-pTyr) forms of the substrate and serial dilutions of the extracts are indicated. Substrate incubated in reaction buffer instead of cellular extract is represented as untreated substrate. (B) Loss of TDP1 in HEK293 TDP1^{-/-} cells as observed from immunolabelling for TDP1 followed by confocal microscopy. Red fluorescence: TDP1 (1:1000, 1° anti-TDP1 Abnova, 2° anti-mouse CFL594, SCBT). (C) Western blot depicting loss of TDP1 protein from the nuclear extracts of HEK293 TDP1^{-/-} cells.

4.2 TDP1 deficient cells are hypersensitive to ionizing radiation and radiomimetic agents.

Previously, *in vitro* studies performed using whole cell extracts from TDP1-mutant SCAN1 cells showed that TDP1 is critical for processing the 3'-PG termini from DSB overhangs (Hawkins et al., 2009; Inamdar et al., 2002; Zhou et al., 2009). To further investigate the biological significance of TDP1's function, clonogenic survival assays were performed in HCT116 WT, TDP1-knockdown and TDP1-knockout cells using Neocarzinostatin (NCS) and Calicheamicin (CAL), enediyne antitumor antibiotics that produce bi-stranded lesions, a substantial portion of which bear 3'-PG termini. TDP1-deficient (shTDP1 and TDP1^{-/-}) cells showed significant hypersensitivity to both NCS (Fig. 4-3A) and CAL (Fig. 4-3B) with a DEF of 1.6 X and 2 X respectively, as compared to the parental cells.

HCT116 cells show reduced Mre11 expression (Takemura et al., 2006). Mre11 functions in an alternative, TDP1-independent pathway for the repair of Top I-induced breaks (Sacho & Maizels, 2011). Thus, to investigate whether the hypersensitivity seen in TDP1-deficient HCT116 cells was specifically a function of TDP1 deficiency and not due to parallel TDP1-dependent and Mre11-dependent pathways being disrupted, TDP1 was knocked out in HEK293 and HEK293T cells which express normal levels of Mre11 (Staples et al., 2016), and clonogenic survival assays were performed in these cells. Importantly, TDP1^{-/-} derivatives of both HEK293 and HEK293T cells showed significant hypersensitivity to NCS compared to parental TDP1^{+/+} cells (Fig. 4-4A,B). TDP1-deficient cells were complemented with a human recombinant TDP1 protein. Surprisingly, the recombinant TDP1 only partially rescued the sensitivity of TDP1^{-/-} cells to NCS but almost fully to radiation (Fig 4-4C). In summary, these experiments demonstrated that TDP1 is not an essential gene, but that its absence results in significant cellular sensitivities consistent with observations from other laboratories (Abo et al., 2017; J. Li et al., 2017).

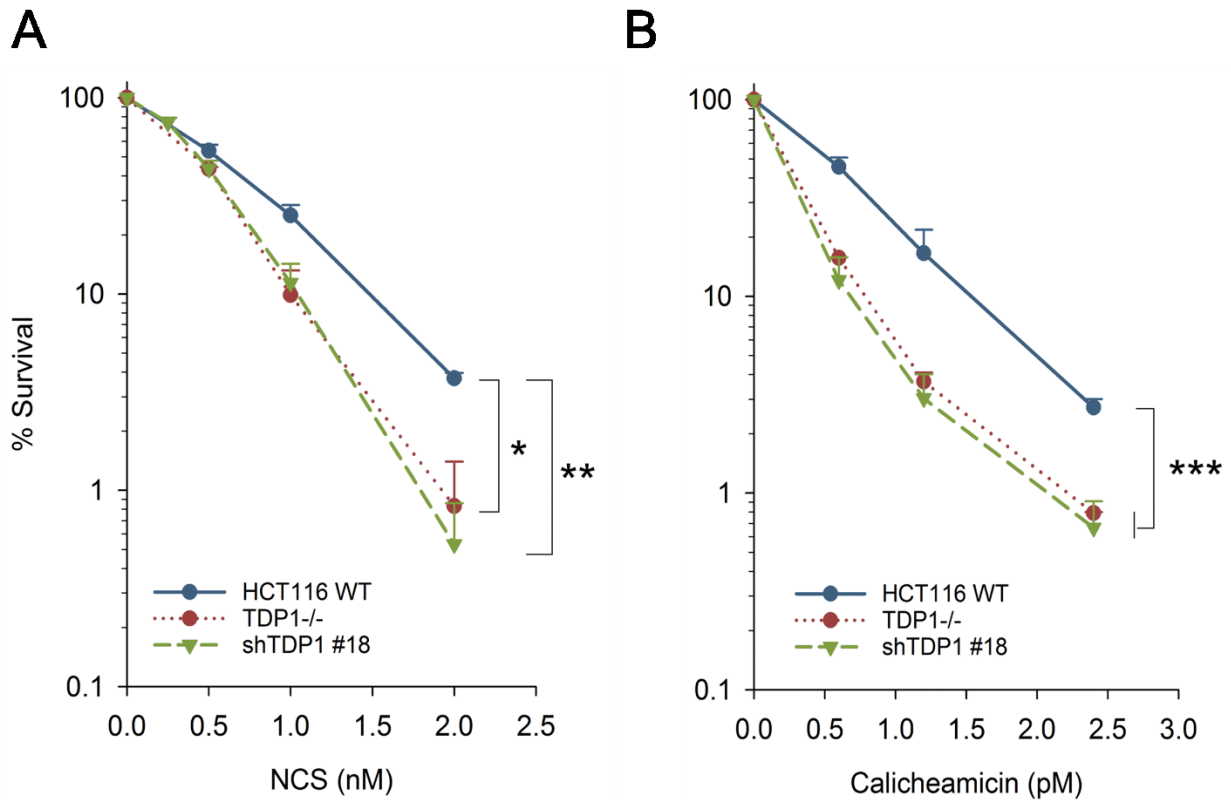


Figure 4-3: Loss of TDP1 enhances the cytotoxicity of radiomimetic agents in HCT116 cells.

Clonogenic survival assays were performed on HCT116 cells treated with NCS (A) and Calicheamicin (B). Error bars represent SEM over at least three independent experiments for all except TDP1^{-/-} HCT116 where n=2. Data were analyzed using Two-way Anova. . * - $p < 0.05$, ** - $p < 0.005$, *** - $p < 0.001$

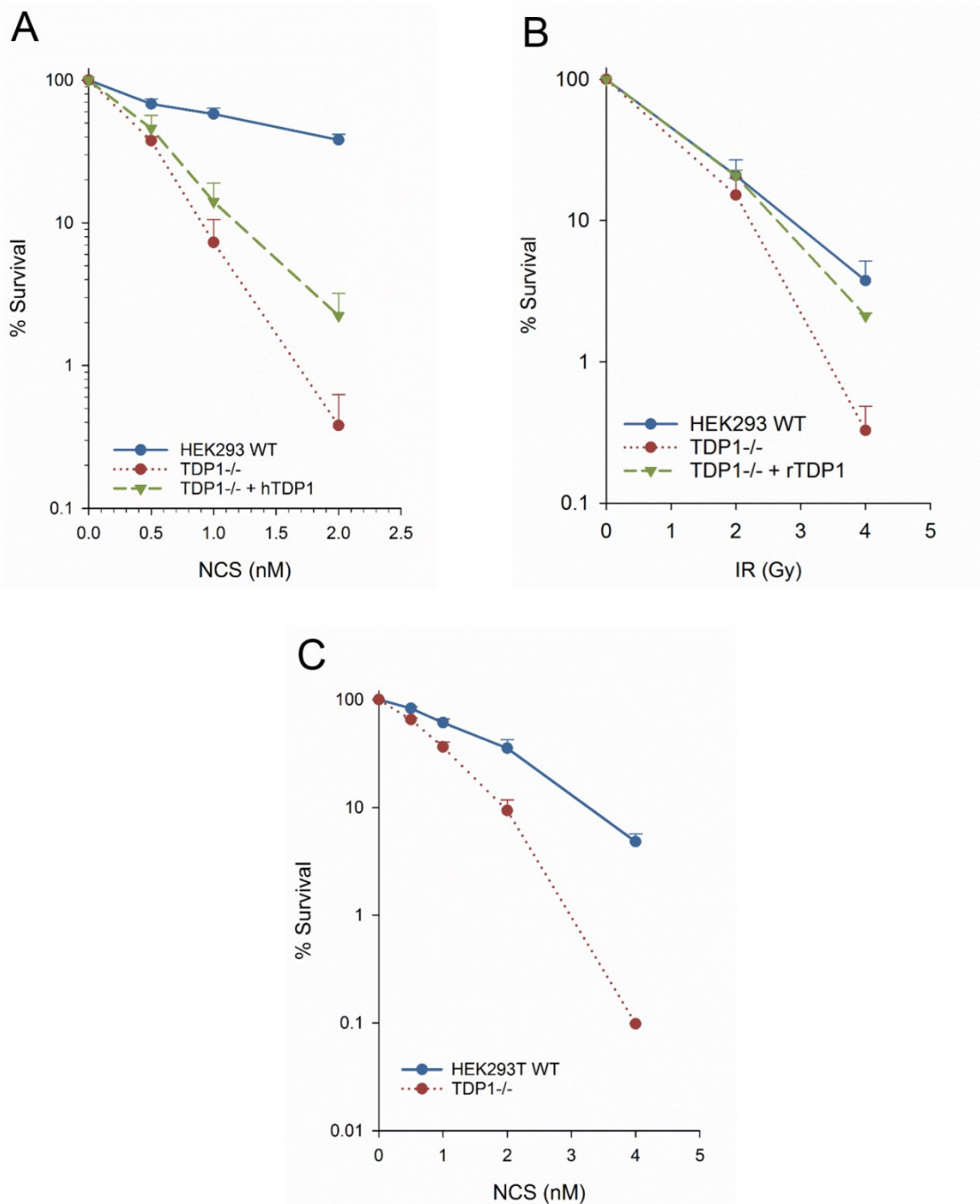


Figure 4-4: Loss of TDP1 enhances the cytotoxicity of radiomimetic agents in HEK293 and HEK293T cells.

(A, B, C) Clonogenic survival assays were performed on HEK293 (A, B) and HEK293T cells (C) treated with NCS or radiation. Error bars represent SEM over at least three independent experiments for all except TDP1^{-/-} HCT116 where n=2.

4.3 Generation of TDP1 and Artemis double knockouts

The Artemis nuclease functions in the NHEJ pathway of DSB repair and is biochemically competent in resolving 3'-PG termini by end trimming (H. Chang H.Y. & Lieber, 2016; Lieber, 2010; Povirk et al., 2007). Thus, to investigate whether Artemis and TDP1 are alternative end processing enzymes functioning in the same pathway for the resolution of 3'-PG termini, HCT116 Artemis-knockout cells were obtained from the lab of Dr. Eric A. Hendrickson. To augment these cells, TDP1 was subsequently knocked out in Artemis^{-/-} cells to generate Artemis^{-/-}•TDP1^{-/-} double knockout (DKO) mutants. In addition, TDP1 was also knocked down in Artemis^{-/-} cells to create a double-mutant Artemis^{-/-}•shTDP1 cell line. Stable integration of the lentiviral vector in pooled cells was analyzed by extracting genomic DNA and PCR amplification of the *pac* gene (Fig. 4-5A). Moreover, genotypic confirmation of Artemis^{-/-} single as well double mutants was performed by PCR amplification of the Exon 2 of Artemis gene (Fig. 4-7A). Upon genotypic confirmation of the selected pool, single cell clones were isolated and a TDP1 activity assay performed on these clones identified clone #2 as displaying maximum knockdown efficiency with a loss of around 92% activity (Fig. 4-5B, C & D). Consistent with a role for TDP1 in the repair of Top 1-mediated DNA lesions (Kawale & Povirk, 2018; Pommier et al., 2014), Artemis^{-/-}•shTDP1#2 double mutant cells were more sensitive to the Top 1 poison, camptothecin (CPT) than Artemis^{-/-} cells (Fig. 4-5E). All the mutant cell lines showed slower growth rates compared to WT cells with the double mutants showing the longest delay (Fig. 4.6)

Similarly, Artemis was also knocked-down in HEK293 WT and HEK293 TDP1^{-/-} cells using a lentivirus carrying an shRNA against Artemis. Cells were selected in 1 µg/mL puromycin and single cell clones were isolated. RT-PCR was performed to screen clones showing the highest knockdown efficiency.

Moreover, to compare the cellular response in normal and cancer cell lines, TDP1 was also knocked down in 48BR-hTert WT and CJ179-hTert Artemis-deficient fibroblasts. Since these cells were already resistant to puromycin (hTert vector had Puromycin resistance gene, used to select immortalized cells carrying hTert), the pLSLP-shTDP1 lentiviral vector was modified by replacing the endogenous puromycin resistance gene by a fragment carrying a Turbo-GFP and a puromycin resistance gene under the control of a CMV promoter. An internal ribosomal entry site (IRES) sequence after the GFP gene allows the puromycin resistance gene to be expressed from a polycistronic mRNA carrying the GFP and *pac* gene CDS. Lentiviral stocks were made and 48BR and CJ179 fibroblasts were infected with the lentiviral stocks and selected based on high GFP expression by FACS.

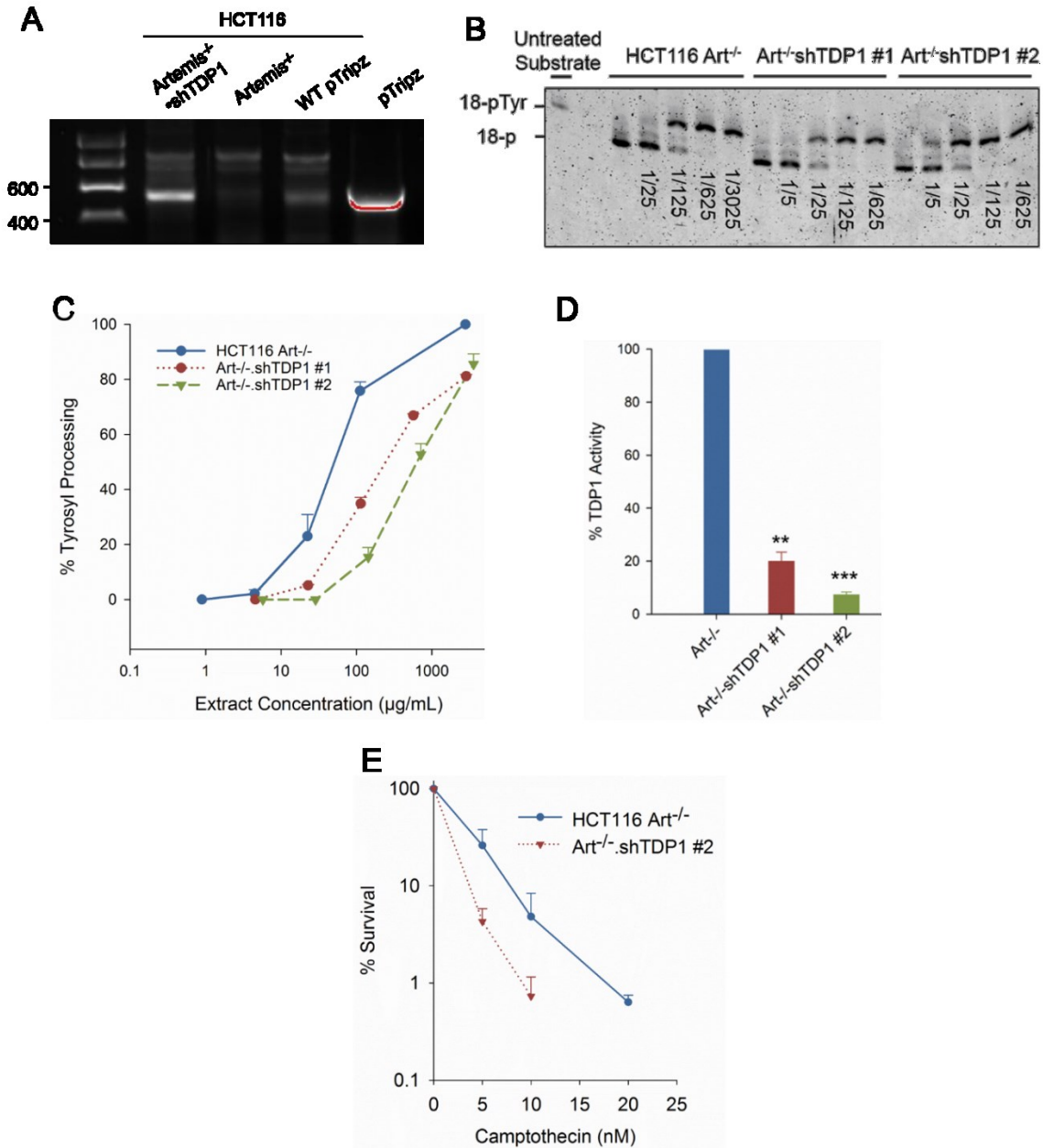


Figure 4-5: Characterization of Artemis^{-/-}shTDP1 cell line

(A) Genotypic confirmation of the lentiviral integration in the genomic DNA of cells infected with the shTDP1 lentivirus as observed from the amplification of the puromycin resistance gene. WT pTripz and pTripz are positive controls whereas uninfected Artemis^{-/-} was negative control. (B) TDP1 Activity assay (as in Fig 2, 3) in HCT116 Artemis^{-/-} and 2 clones with an additional TDP1 knockdown. Values below the lane indicate the dilution factors of the extract. Lanes where values are not mentioned represent undiluted extracts. (C and D) Percentage of TDP1 Activity remaining in whole cell extracts as observed in B. (E) Clonogenic survival assays performed upon treatment with Top 1 poison, camptothecin for 24 hours. Error bars represent SEM, n = 2. ** - $p < 0.005$, *** - $p < 0.001$.

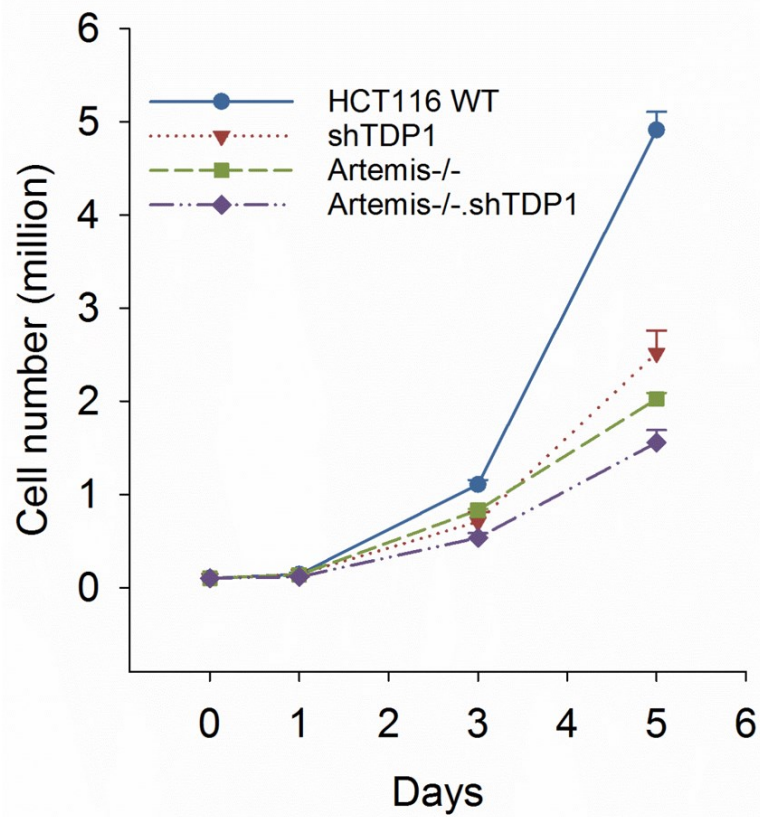


Figure 4-6: Growth curve

Cells (1×10^5) were seeded in 6-well plates in 3mL complete medium and were counted using a hemocytometer on days 1, 3 and 5. The above graph shows the number of cells in million versus number of days. $n=2$.

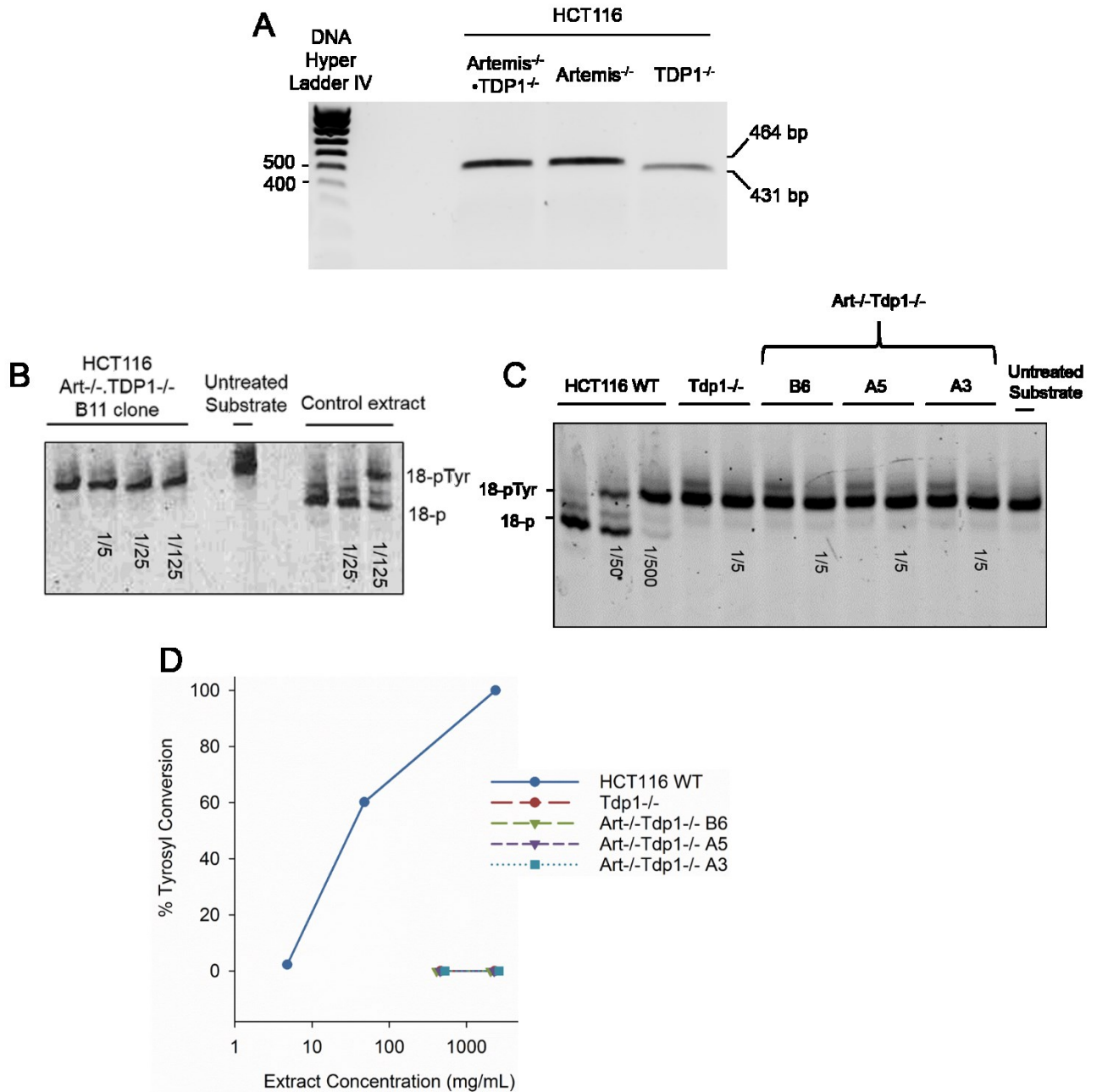


Figure 4-7: Characterization of HCT116 Artemis^{-/-}.TDP1^{-/-} mutant cells

(A) Artemis Exon 2 was amplified by PCR and the samples run on a 1% agarose gel. TDP1^{-/-} is negative control. Artemis^{-/-} is positive control. (B and C) TDP1 activity assay in various clones of Artemis^{-/-}.TDP1^{-/-}. Values below the lane indicate the dilution factors of the extract. Lanes where values are not mentioned represent undiluted extracts. (D) Quantification of processing of the tyrosyl moiety from the substrate as a function of the concentration of the extract.

4.4 TDP1 and Artemis are epistatic for the repair of 3'-PG DSBs via NHEJ

In order to determine whether TDP1 and Artemis are alternative end-processing enzymes in the repair of 3'-PGs, clonogenic survival assays were performed using NCS, CAL and IR in the WT and the mutant cells. Artemis^{-/-} cells were, as expected, hypersensitive to NCS and CAL with a DEF of 1.5 (NCS) and 2 (CAL). Surprisingly, however, an additional TDP1 deficiency in Artemis^{-/-} cells (Artemis^{-/-}.TDP1^{-/-} or Artemis^{-/-}.shTDP1#2 #2) did not enhance the hypersensitivity to NCS and to CAL, indicating that TDP1 and Artemis are epistatic and function in the same pathway for the repair of NCS/CAL-induced 3'-PG DSBs (Fig 4-8). In all cases, shTDP1 knockdown was as effective as TDP1 knockout in conferring NCS sensitivity, indicating that knockdown was sufficient to fully express the deficiency in repair of NCS-induced damage. In contrast, the double mutants were more sensitive to IR compared to the single mutants (Fig. 4-8) suggesting that TDP1 and Artemis function in parallel for the repair of IR-induced DSBs.

NHEJ is the pathway of choice for DSB repair in G1 phase (S. E. Lee, Mitchell, Cheng, & Hendrickson, 1997; Lobrich & Jeggo, 2017; Valerie & Povirk, 2003). Thus, if DSBs are induced in cells in G1 phase, cell cycle checkpoints will be activated and further progression of the cell cycle will be halted until the damage is repaired by NHEJ. Thus, to investigate whether TDP1 and Artemis are also epistatic in the G1 phase for the repair of 3'-PG DSBs via NHEJ, clonogenic survival assays were performed using NCS on cells synchronized in G1 by mitotic shake-off (Schorl & Sedivy, 2007). Cells undergoing mitosis round-up and are loosely attached to the tissue culture dish. Agitation of the dish allows these M-phase cells to detach and float in the supernatant. The supernatant can then be centrifuged and the M-phase cells collected, seeded in a new dish and harvested at different time points to obtain a synchronized population of cells. This experiment was performed in HCT116 cells by harvesting up to 6 hours after shake-off and analyzing their

cell cycle profile by FACS. Approximately 80% cells were synchronized in G1 phase as determined by cell cycle analysis using PI staining (Fig. 4-9). Similar to the observation in exponentially growing cells, the hypersensitivity to NCS observed in G1-synchronized *Artemis*^{-/-}•shTDP1#2 double-mutants was similar to the *Artemis*^{-/-} and shTDP1#18 single-mutants (Fig. 4-10), suggesting that Artemis and TDP1 are epistatic for the repair of NCS-induced 3'-PG DSBs in G1 phase.

Since TDP1 and Artemis function in the same pathway for the repair of NCS-induced DSBs in the G1-phase, the next logical line of investigation was whether they are epistatic with NHEJ factors. DNA-PKcs is critical for the repair of DSBs via NHEJ (Davis & Chen, 2013). DNA-PKcs interacts with Ku70/80 heterodimer to form the DNA-PK core complex and recruits several DNA repair factors to the DSB ends by phosphorylation (Davis, Chen, & Chen, 2014). Interestingly, DNA-PK can phosphorylate itself and this autophosphorylation activity is important for movement of the DNA-PK complex inward from the DSB ends and thereby regulate access to DNA end-processing enzymes (Uematsu et al., 2007). An inhibitor of kinase activity of DNA-PK can block this autophosphorylation and thereby stall NHEJ causing persistent DSBs (Dong et al., 2017; Dong et al., 2018). Therefore, in order to investigate whether Artemis and TDP1 repair 3'-PG DSBs via NHEJ, clonogenic survival assays were performed using NCS in the presence of a DNA-PK inhibitor, NU-7441. WT cells showed an increased hypersensitivity to NCS upon DNA-PK inhibition whereas additional depletion of TDP1 (shTDP1#18), deficiency of Artemis (*Artemis*^{-/-}) or both combined (*Art*^{-/-}•shTDP1#2) did not further enhance this sensitivity (Fig. 4-11). This result strongly suggests that Artemis and TDP1 are epistatic with DNA-PK and contribute to the repair of 3'-PG DSBs via the NHEJ pathway.

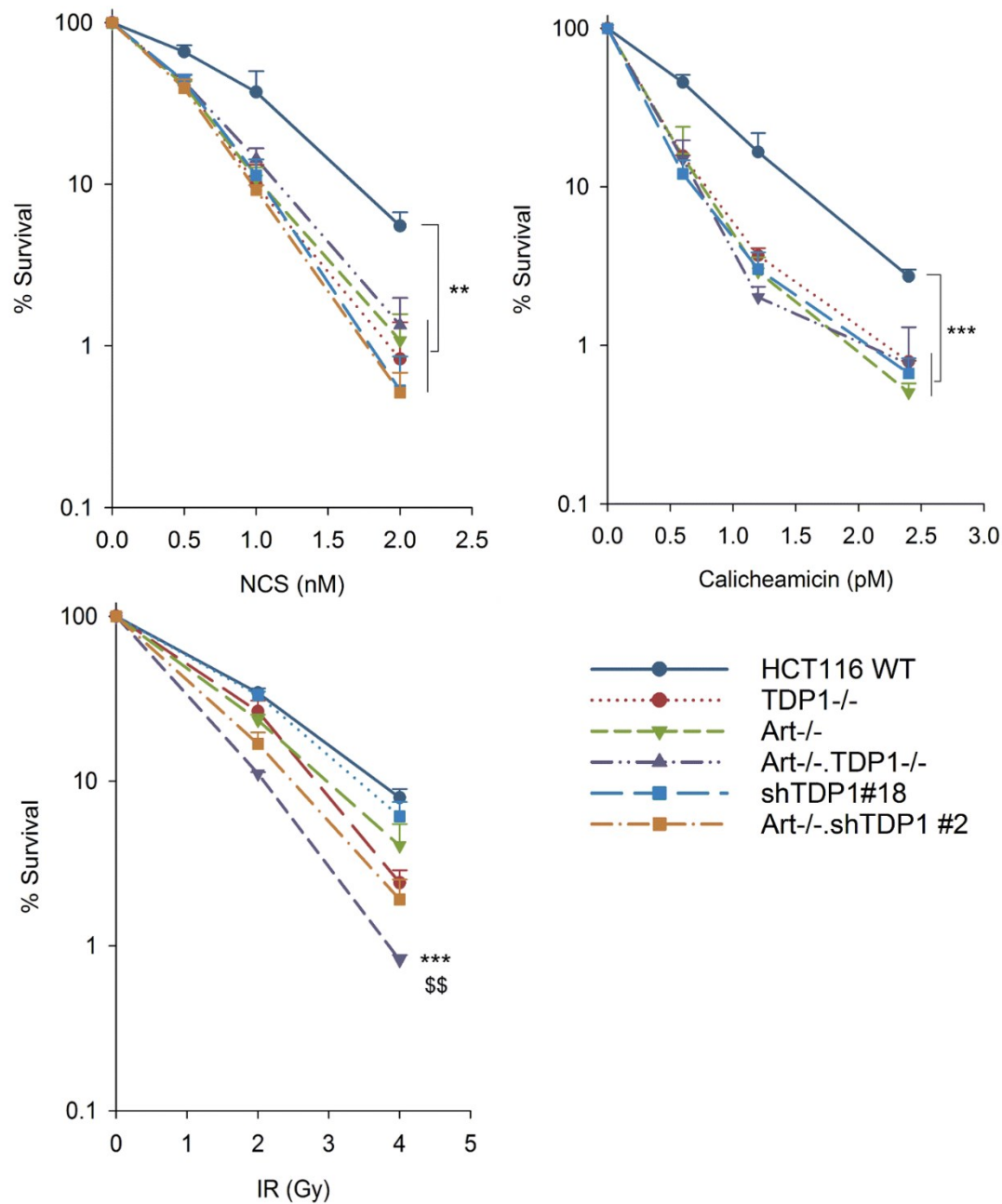


Figure 4-8: TDP1 and Artemis are epistatic for the repair of 3'-PG-ended DSBs

Clonogenic survival assays were performed on isogenic HCT116 WT, TDP1-deficient, Artemis-deficient, and TDP1/Artemis double-deficient cells treated with NCS (A), Calicheamicin (B) and ionizing radiation (C). Error bars represent SEM. $n=2$ for TDP1^{-/-} and Art^{-/-}.TDP1^{-/-} cells whereas $n=3$ for WT, shTDP1, Art^{-/-}, Art^{-/-}.shTDP1. For (A), $n=5$ for WT, shTDP1, Art^{-/-}, Art^{-/-}.shTDP1. Data were analyzed using Two-way ANOVA. ** - $p < 0.005$, *** - $p < 0.001$. In (C), *** indicates Art^{-/-}.TDP1^{-/-} comparison with WT, \$\$ indicates Art^{-/-}.TDP1^{-/-} comparison with Art^{-/-} and TDP1^{-/-} single mutants implying that the double mutants are more sensitive than the single mutants and WT.

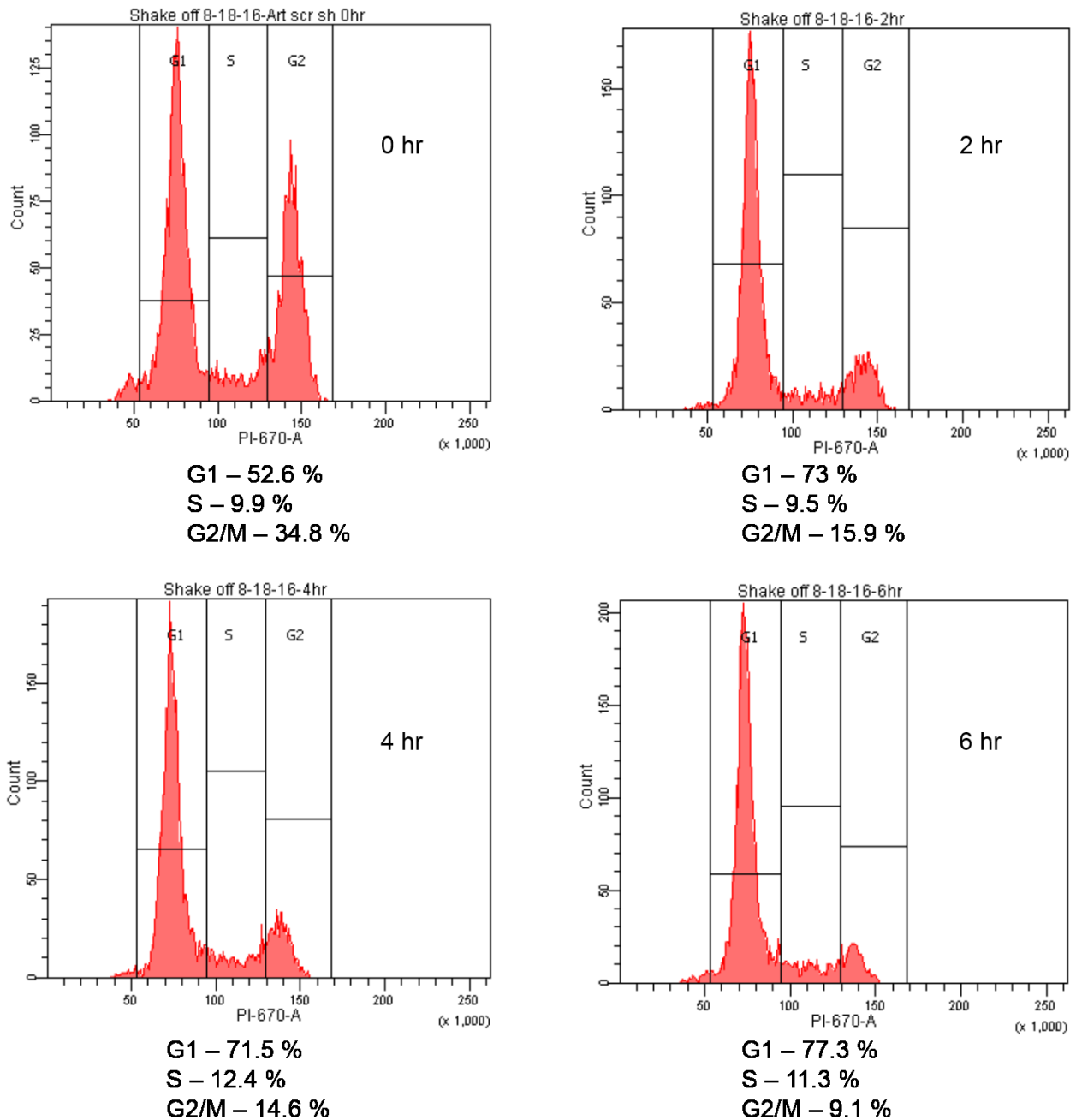


Figure 4-9: Cell Cycle Synchronization by Mitotic shakeoff

Cells were fixed and processed at the indicated time points after mitotic shake-off for cell cycle analysis 0 hr represents samples processed immediately after shakeoff without re-seeding them. Representative FACS histogram plot showing the percentage of cells in each phase of the cell cycle. Horizontal axis depicts the DNA-content. A minimum of 10,000 events were collected for each sample.

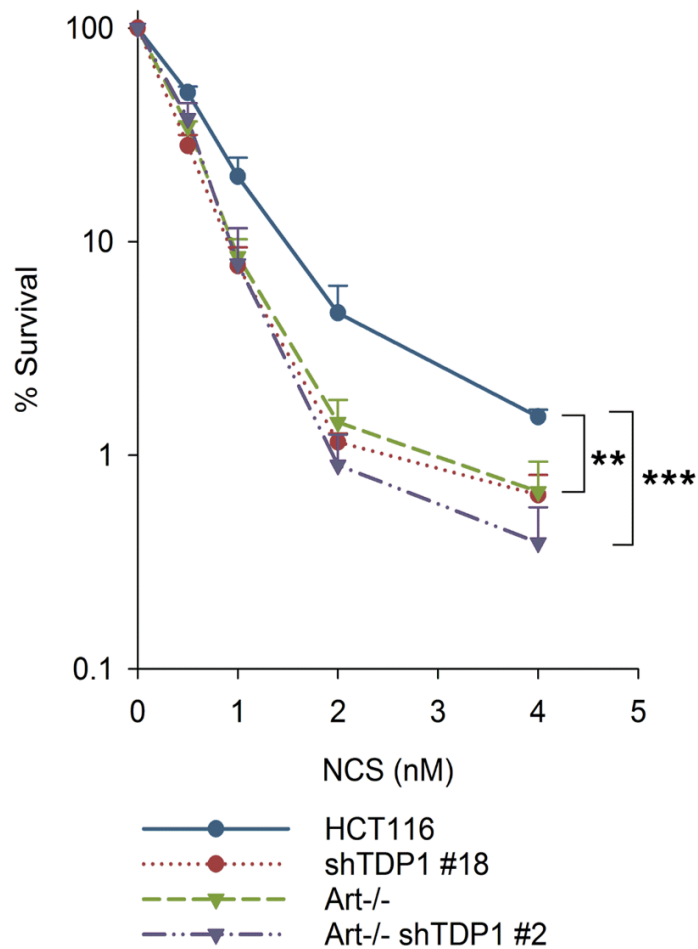


Figure 4-10: TDP1 and Artemis are epistatic in the G1-phase for the repair of 3'-PG-ended DSBs

Clonogenic survival assays were performed on G1 -synchronized cells treated with NCS. Error bars represent SEM for n=4. Data were analyzed using Two-way ANOVA, *** - $p < 0.001$, ** - $p < 0.005$.

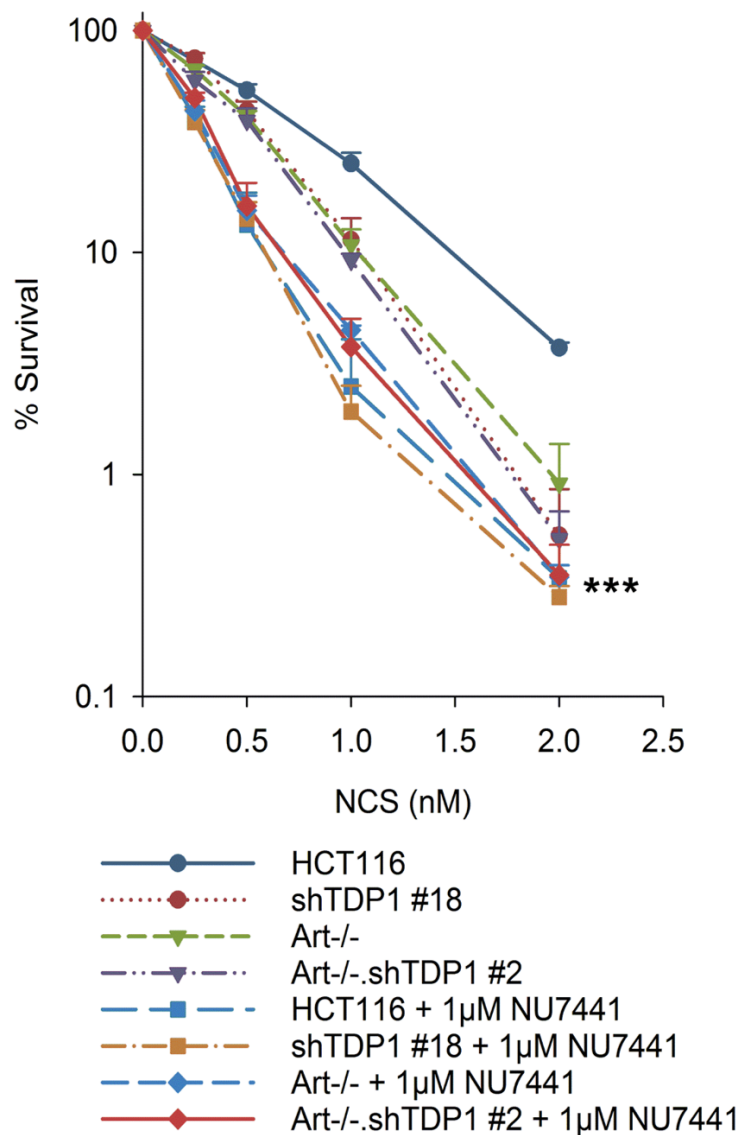


Figure 4-11: TDP1 and Artemis are epistatic with DNA-PK for the repair of NCS-induced DSBs.

Clonogenic survival assays were performed in cells treated with NCS in the presence of 1 μ M DNA-PK inhibitor, NU-7441. NU-7441 was added 1 hr prior to NCS treatment and left in the medium during and 24 hr after NCS treatment. . shTDP1, Art-/- and Artemis-/-•shTDP1#2 curves are the same as in Fig. XX. Error bars represent SEM for n=4. Data were analyzed using Two-way ANOVA, *** - $p < 0.001$, *** represents significant statistical difference between all DNA-PK inhibitor treated cells vs all cells without DNA-PK inhibitor treatment.

4.5 Absence of Artemis but not TDP1 confers a defect in DSB rejoining

Upon DSB formation, several proteins localize to the sites of DSBs to elicit a DNA damage response, that helps repair the DSBs (Ashley & Kemp, 2018; Blackford & Jackson, 2017). ATM kinase is one of the early responders and phosphorylates the histone variant H2AX at the S139 position, referred to as γ -H2AX (Burma, Chen, Murphy, Kurimasa, & Chen, 2001; Rogakou et al., 1998). This post-translational modification serves as a signal for the recruitment of various proteins including ring finger proteins, RNF168 and RNF8 that ubiquitinate histone H2A at K13/K15 (Panier & Boulton, 2014). This ubiquitination signals the recruitment of another repair factor, 53BP1 (p53-binding protein 1) which binds to ubiquitinated and methylated histones and channels DSB repair towards the NHEJ pathway by acting as a barrier to DNA end-resection (Escribano-Diaz et al., 2013).

To directly assess whether the hypersensitivity shown by the mutants to NCS and CAL was due to a deficiency in repairing 3'-PG-ended DSBs, an initial attempt was made to quantify γ -H2AX foci as DSB markers. However, the staining pattern of the γ -H2AX antibody was pan-nuclear in addition to labelling chromatin foci representing DSBs making it very difficult to quantify these foci. Hence, 53BP1 foci (which colocalize with γ -H2AX foci and represent surrogate markers of unrejoined DSBs) were quantified as representative markers of DSBs in these cells following NCS treatment.

This assay was performed on serum-deprived G0/G1-phase cells to specifically analyze DSB repair in the context of NHEJ and to avoid including spontaneous focus formation at stalled replication forks. As expected, all cells showed a robust but similar increase in 53BP1 foci immediately upon treatment with both 2 nM as well as 4 nM NCS. WT cells showed a typical biphasic kinetic curve with an initial fast component repairing almost 70% of the breaks within

the first 4 hours followed by a slow component that repaired the next 20% breaks over 16 hours (Fig. 4-12, 4-16). Surprisingly, TDP1-depleted cells showed a similar phenotype to WT cells and did not show a DSB rejoining defect as expected from their sensitivity to NCS seen in survival assays indicating that TDP1-depletion does not confer a defect in DSB rejoining (Fig. 4-13, 4-16). Artemis-deficient cells (*Artemis*^{-/-} and *Artemis*^{-/-} •shTDP1) showed an increased persistence and a delayed disappearance of 53BP1 foci, with a significant fraction of foci persisting even at 8 and 16 hr after NCS treatment compared to Artemis-proficient cells (Fig. 4-14, 4-15, 4-16). This result was consistent at both 2 nM and 4 nM concentration of NCS as shown in Fig. 4-17. Overall, these results demonstrate a defect in DSB rejoining only in the absence of Artemis but not TDP1.

HCT116 WT

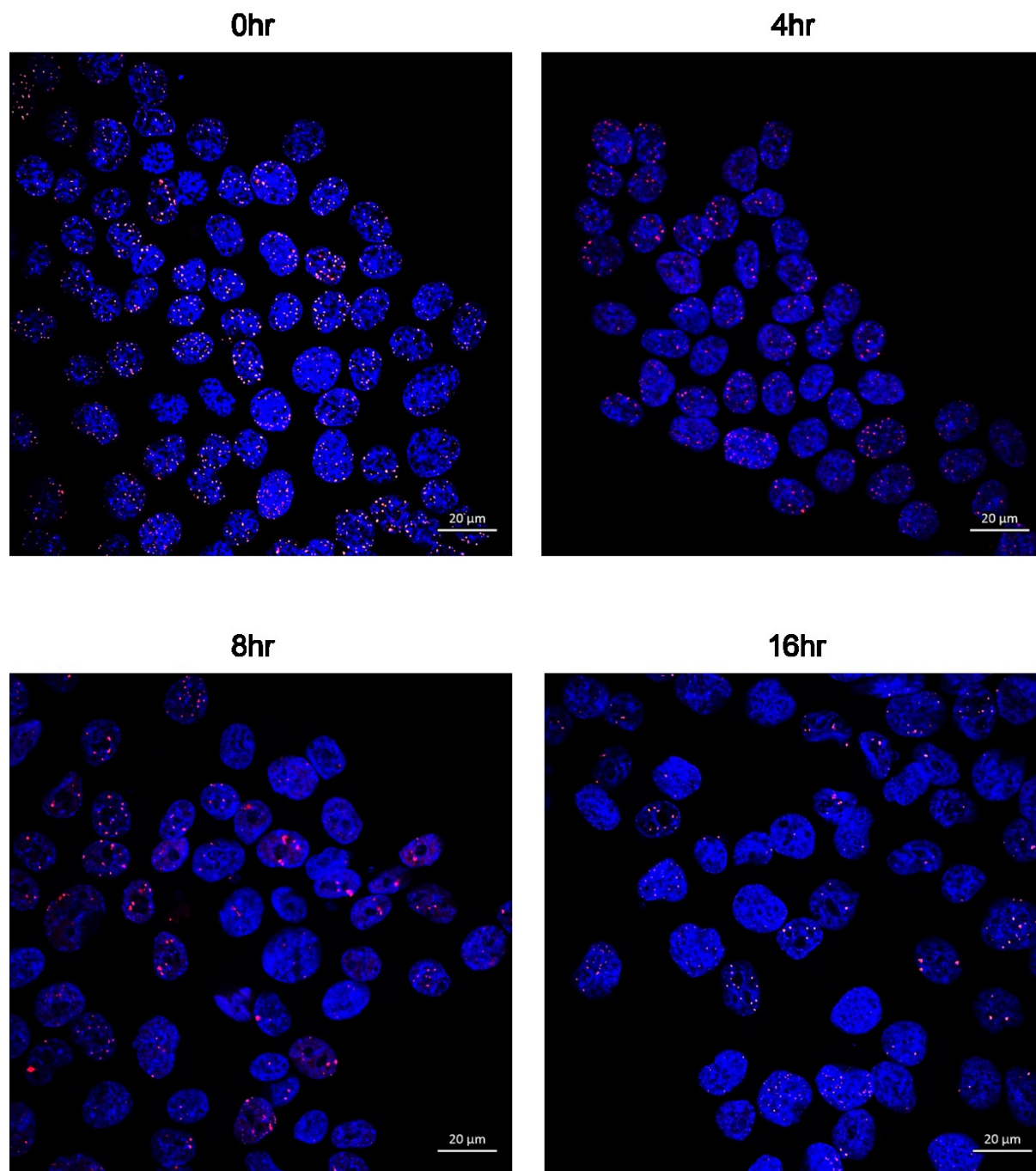


Figure 4-12: Representative confocal images of 53BP1 repair foci in HCT116 WT cells.

Immunostaining was performed to detect formation and disappearance of 53BP1 foci upto 16 hr after 4nM NCS treatment for 1 hr. 0 hr represents samples processed immediately upon NCS treatment. Red fluorescence: 53BP1 (BD Transduction Laboratories), Blue fluorescence: DAPI staining the DNA – nucleus (Vectashield).

HCT116
shTDP1 #18

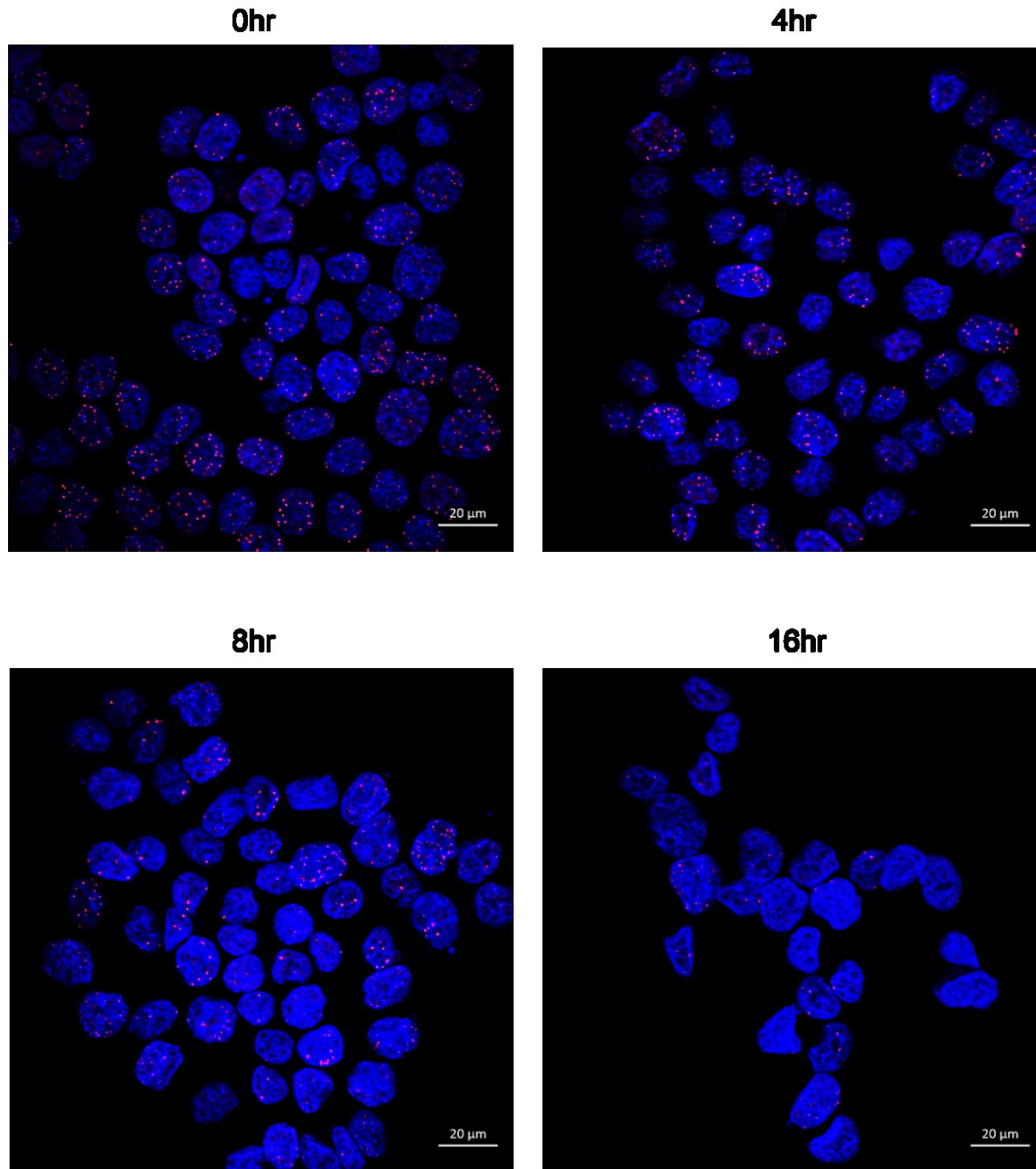
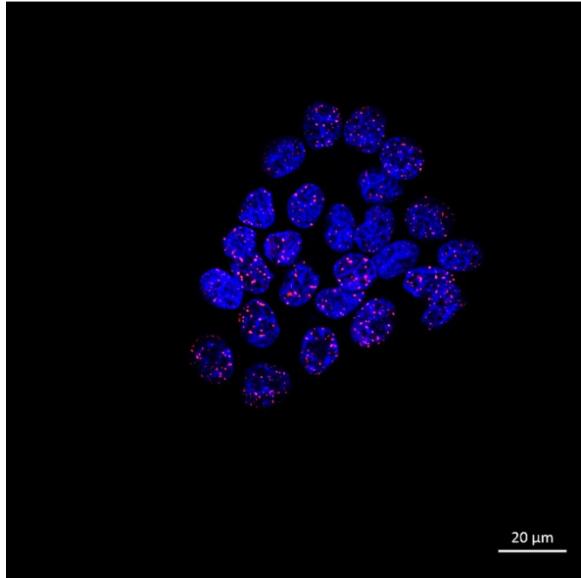


Figure 4-13: Representative confocal images of 53BP1 repair foci in HCT116 shTDP1#18 cells.

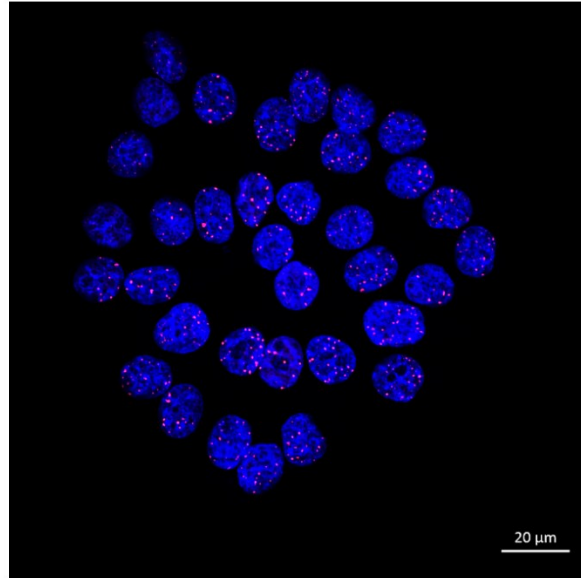
Immunostaining was performed to detect formation and disappearance of 53BP1 foci upto 16 hr after 4nM NCS treatment for 1 hr. 0 hr represents samples processed immediately upon NCS treatment. Red fluorescence: 53BP1 (BD Transduction Laboratories), Blue fluorescence: DAPI staining the DNA – nucleus (Vectashield).

HCT116
Artemis^{-/-}

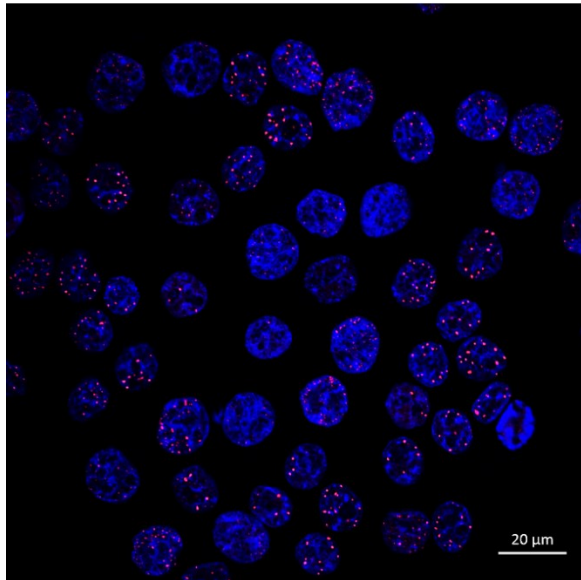
0hr



4hr



8hr



16hr

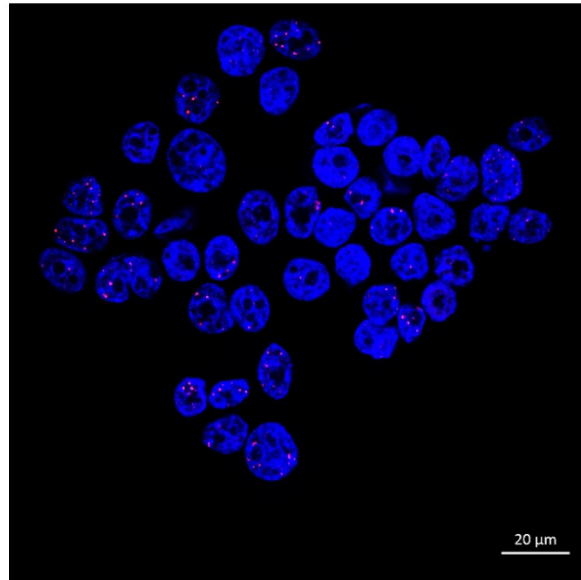


Figure 4-14: Representative confocal images of 53BP1 repair foci in HCT116 Artemis^{-/-} cells.

Immunostaining was performed to detect formation and disappearance of 53BP1 foci upto 16 hr after 4nM NCS treatment for 1 hr. 0 hr represents samples processed immediately upon NCS treatment. Red fluorescence: 53BP1 (BD Transduction Laboratories), Blue fluorescence: DAPI staining the DNA – nucleus (Vectashield).

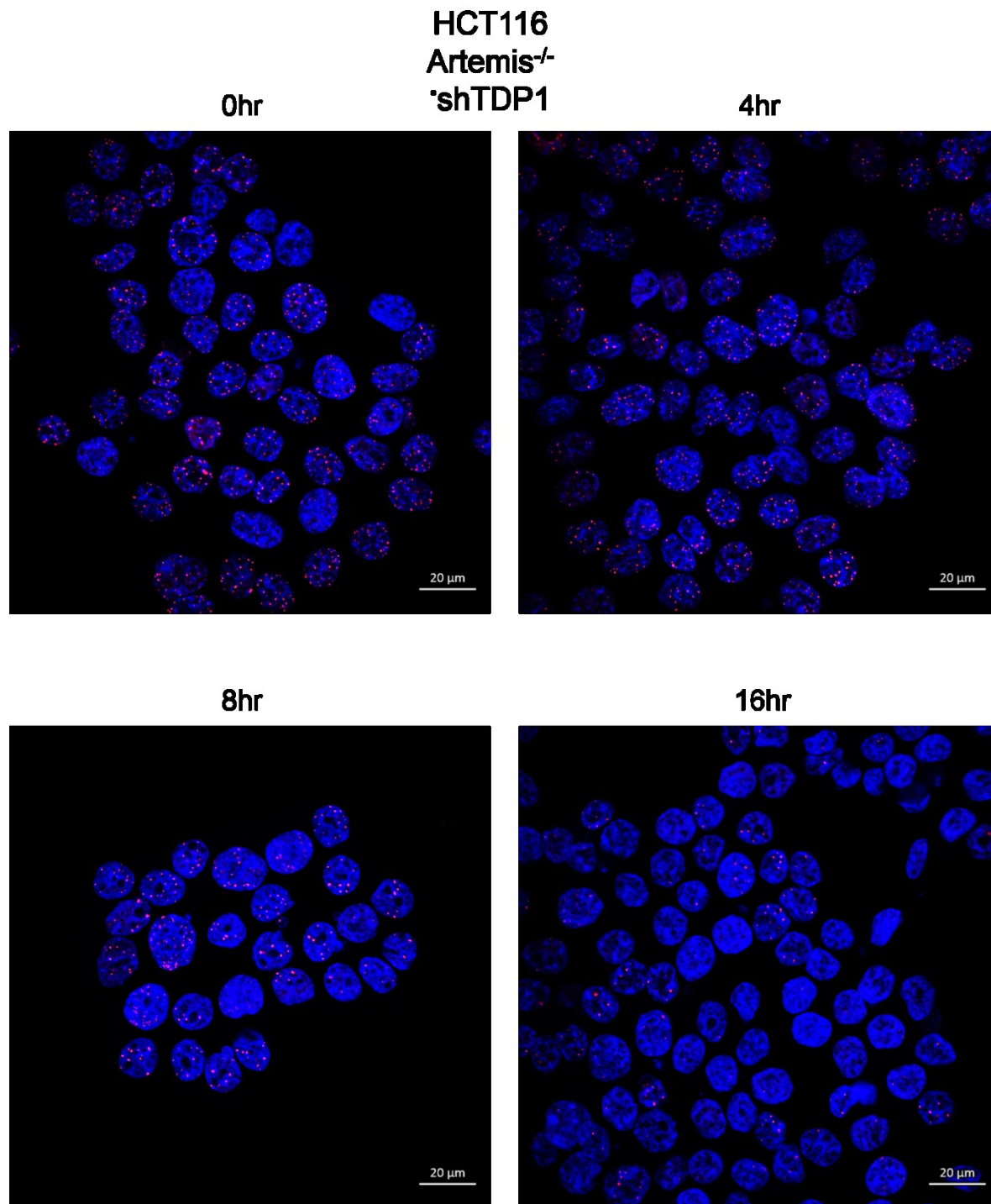


Figure 4-15: Representative confocal images of 53BP1 repair foci in HCT116 Artemis^{-/-} shTDP1#2 #2 cells.

Immunostaining was performed to detect formation and disappearance of 53BP1 foci upto 16 hr after 4nM NCS treatment for 1 hr. 0 hr represents samples processed immediately upon NCS treatment. Red fluorescence: 53BP1 (BD Transduction Laboratories), Blue fluorescence: DAPI staining the DNA – nucleus (Vectashield).

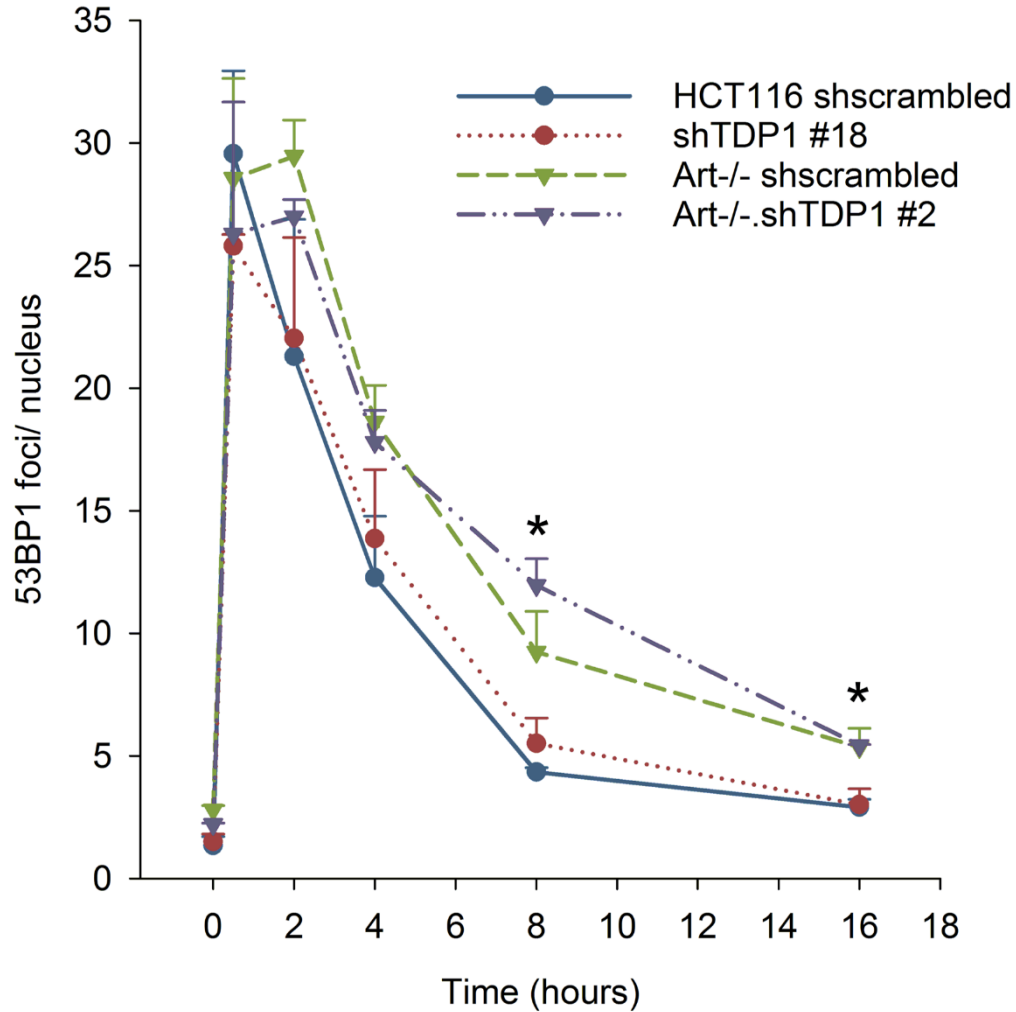


Figure 4-16: Artemis-deficient but not TDP1-depleted cells show a DSB rejoining defect

53BP1 foci were scored in serum-starved cells treated with 4 nM NCS for 1 hr and results plotted as number of 53BP1 foci per nucleus. Foci were counted using ImageJ whereas the counting of nuclei was done manually. Error bars represent SEM for n=3. Data were analyzed using unpaired two-tailed Student's t-test, * - $p < 0.05$, indicates comparison between Artemis-proficient (HCT116 WT and shTDP1) and Artemis-deficient (Art-/- and Artemis-/-•shTDP1#2) cells.

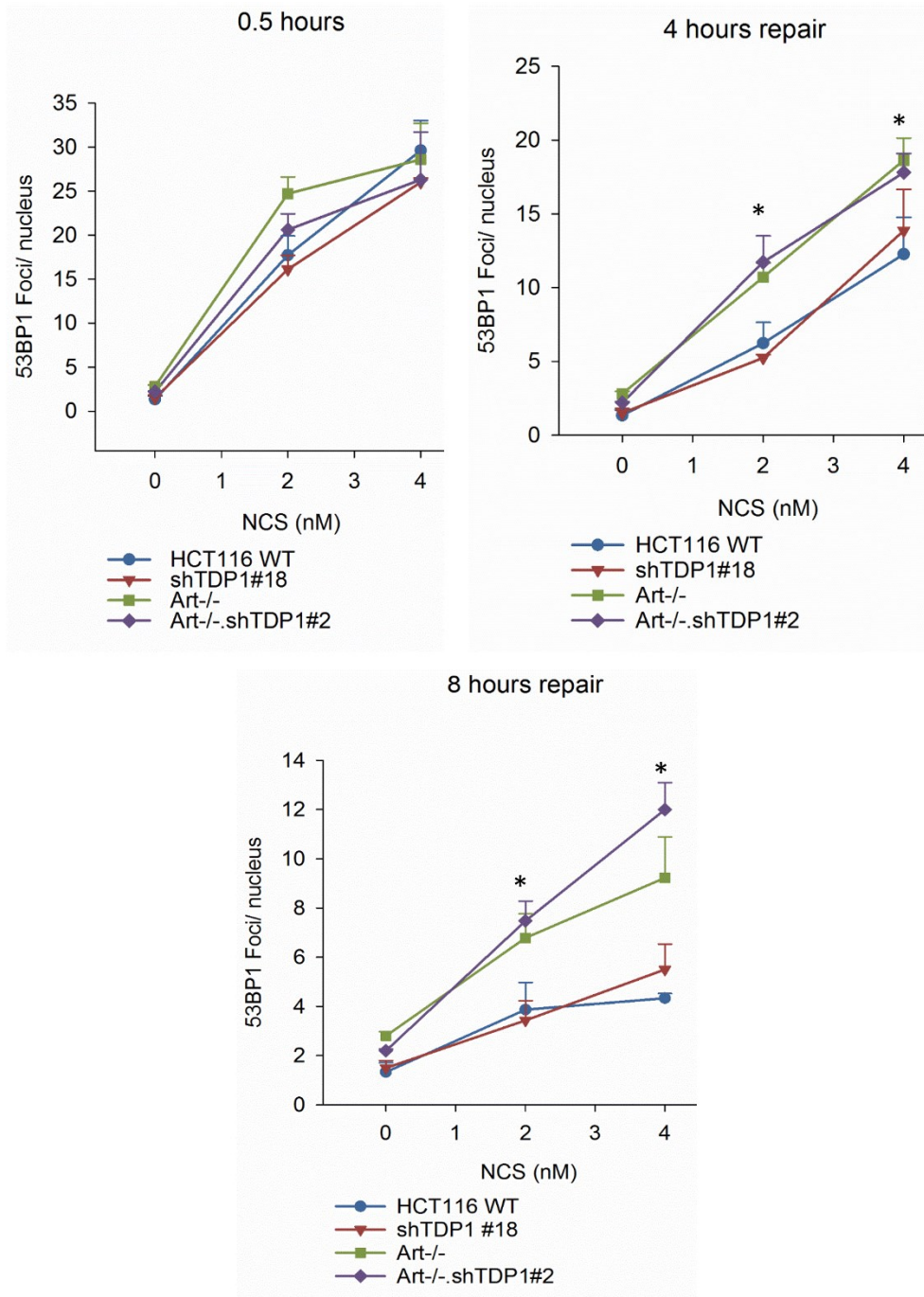


Figure 4-17: Dose-dependent increase in 53BP1 foci

53BP1 foci were scored in serum-starved cells treated with 2 nM and 4 nM NCS for 1 hr and results plotted as number of 53BP1 foci per nucleus. 0 nM samples represent untreated samples. Error bars represent SEM for n=3. Data were analyzed using unpaired two-tailed Student's *t*-test, * - $p < 0.05$, indicates comparison between Artemis-proficient (HCT116 WT and shTDP1) and Artemis-deficient (Art-/- and Artemis-/-•shTDP1#2) cells.

4.6 Loss of TDP1 but not Artemis leads to misjoining of 3'-PG DSBs

Why are 3'-PG-terminated DSBs cytotoxic in the absence of TDP1 despite being rejoined with kinetics similar to cells proficient in TDP1? An explanation to this discrepancy can be provided by understanding the fate of a DSB in cells and the limitation of the 53BP1 repair assay to detect all these fates. Theoretically, a DSB can be potentially channeled to accurate repair in the presence of the canonical repair factors, remain un-rejoined due to dysfunctional repair pathways or can be misjoined due to error-prone backup proteins in the absence of canonical factors. Although the 53BP1 repair kinetics assay is a standard for measuring the fraction of DSBs that remain unrejoined, it is limited by its inability to differentiate between DSB ends that are correctly rejoined, and DSB ends that are misjoined to ends of other DSBs in the cell.

Previously, it has been reported that TDP1-mutant SCAN1 cells show increased chromosomal sensitivity to CAL and a significant increase in the number of CAL-induced dicentric chromosomes compared to normal cells implying that more DSBs were misjoined and repaired inaccurately in the absence of functional TDP1 (Zhou et al., 2009). Thus, the toxicity of 3'-PG-ended DSBs in TDP1-depleted cells (shTDP1#18 and Artemis^{-/-}•shTDP1#2) could be because of inaccurate and mis-joined DSBs due to repair being shunted to a more error-prone pathway. To test this hypothesis, centromere-fluorescence in situ hybridization (C-FISH) was performed using 2 nM NCS. As with CAL-treated SCAN1 cells, shTDP1#18 single and Artemis^{-/-}•shTDP1#2 double mutants showed a significant increase in the levels of NCS-induced dicentric chromosomes compared to WT and Artemis^{-/-} cells, as measured on metaphase spreads with Cy3-labelled centromeres (Fig. 4-18, 4-19). Furthermore, all mutants showed an increase in the number of acentric chromosomal fragments (Fig. 4-19), as would be expected since both unjoined fragments and fragments misjoined to each other would be scored as acentrics. In addition, the

Artemis^{-/-}•shTDP1#2 showed a statistically higher number of total aberrations than either WT or either single mutant alone (Fig. 4-19). Thus, although Artemis and TDP1 appear epistatic for promoting survival against these breaks, their loss results in disparate phenotypes. Absence of Artemis is cytotoxic as it hampers rejoining in a fraction of DSBs whereas the cytotoxicity in the absence of TDP1 is as a result of erroneous misjoining of DSBs. Similarly, even in HEK293 TDP1^{-/-} cells, there was an increase in the number of mis-joined chromosomes and overall increased chromosomal abnormalities as compared to HEK293 WT cells upon 2 nM NCS treatment (Fig. 4-20, 4-21).

In order to examine the contribution of NHEJ towards the mis-joining of DSB ends in the absence of TDP1, C-FISH was performed on cells treated with NCS in the presence of the DNA-PK inhibitor, NU-7441. Treatment with NU-7441 prevents the inward translocation of DNA-PK from DSB ends, thereby limiting access to the nucleases and phosphodiesterases required for the processing of modified ends (Davis et al., 2014). DNA-PK inhibition had no effect on DSB mis-joining in WT and Artemis^{-/-} cells but led to a decrease in DSB mis-joining in TDP1-depleted shTDP1#18 and Artemis^{-/-}•shTDP1#2 cells down to the level of TDP1-proficient WT and Artemis^{-/-} cells, as all four cell lines showed similar levels of dicentric chromosomes per metaphase (Fig. 4-19). Overall, the DNA-PK inhibitor data suggest that while there is a component of mis-joining in both WT and TDP1-deficient cells that is independent of C-NHEJ, the additional mis-joining in TDP1-deficient cells is C-NHEJ-dependent.

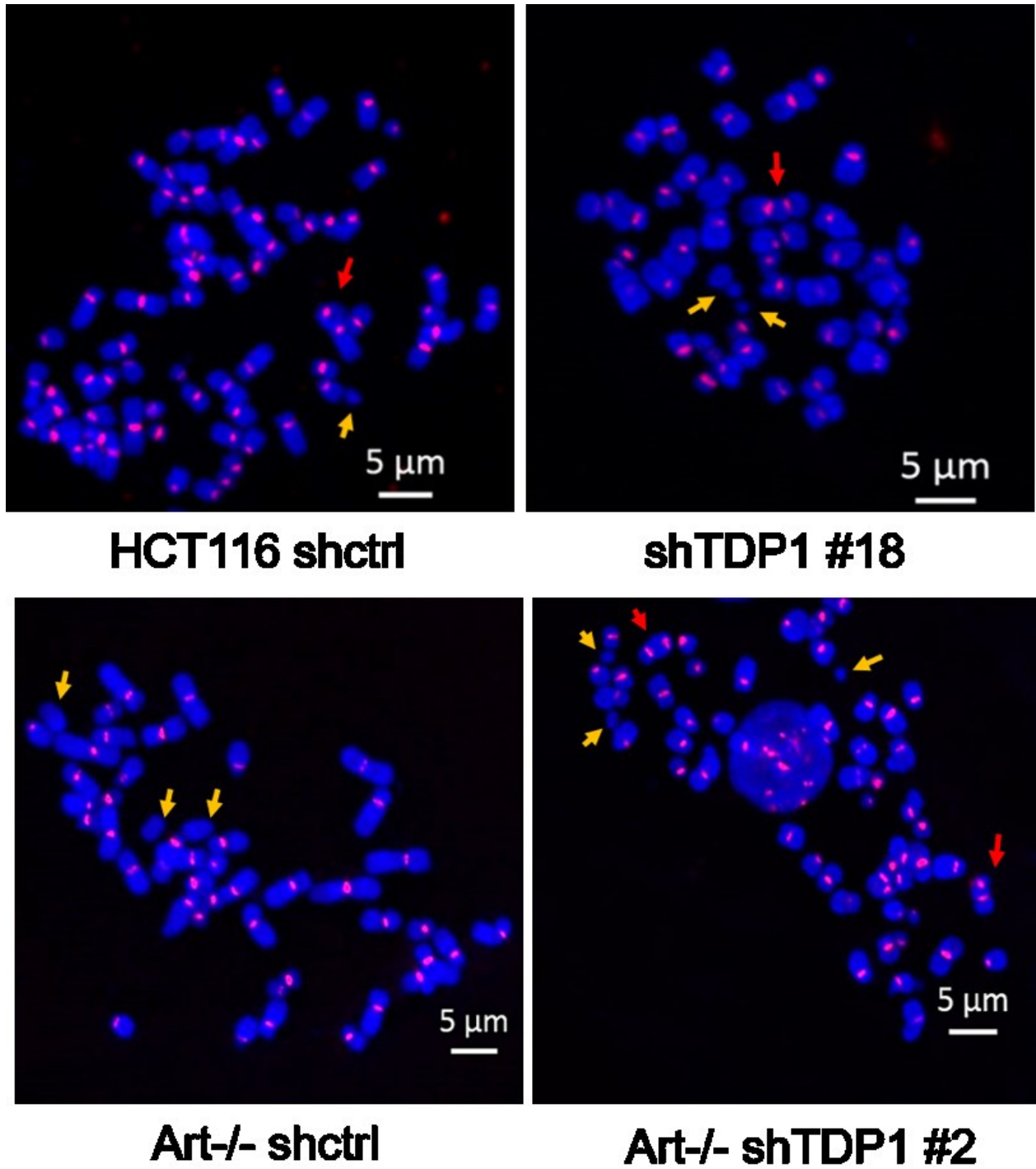


Figure 4-18: TDP1 depletion leads to misjoining of DSBs.

Metaphase spreads of HCT116, shTDP1#18, Art-/- and Artemis-/-•shTDP1#2 #2 cells. Cells were treated with 2nM NCS for 6 hours. Centromeres were labelled with a Cy3-conjugated fluorescent probe (PNA Bio Inc.). Red arrows represent dicentric chromosomes, yellow arrows represent acentric fragments.

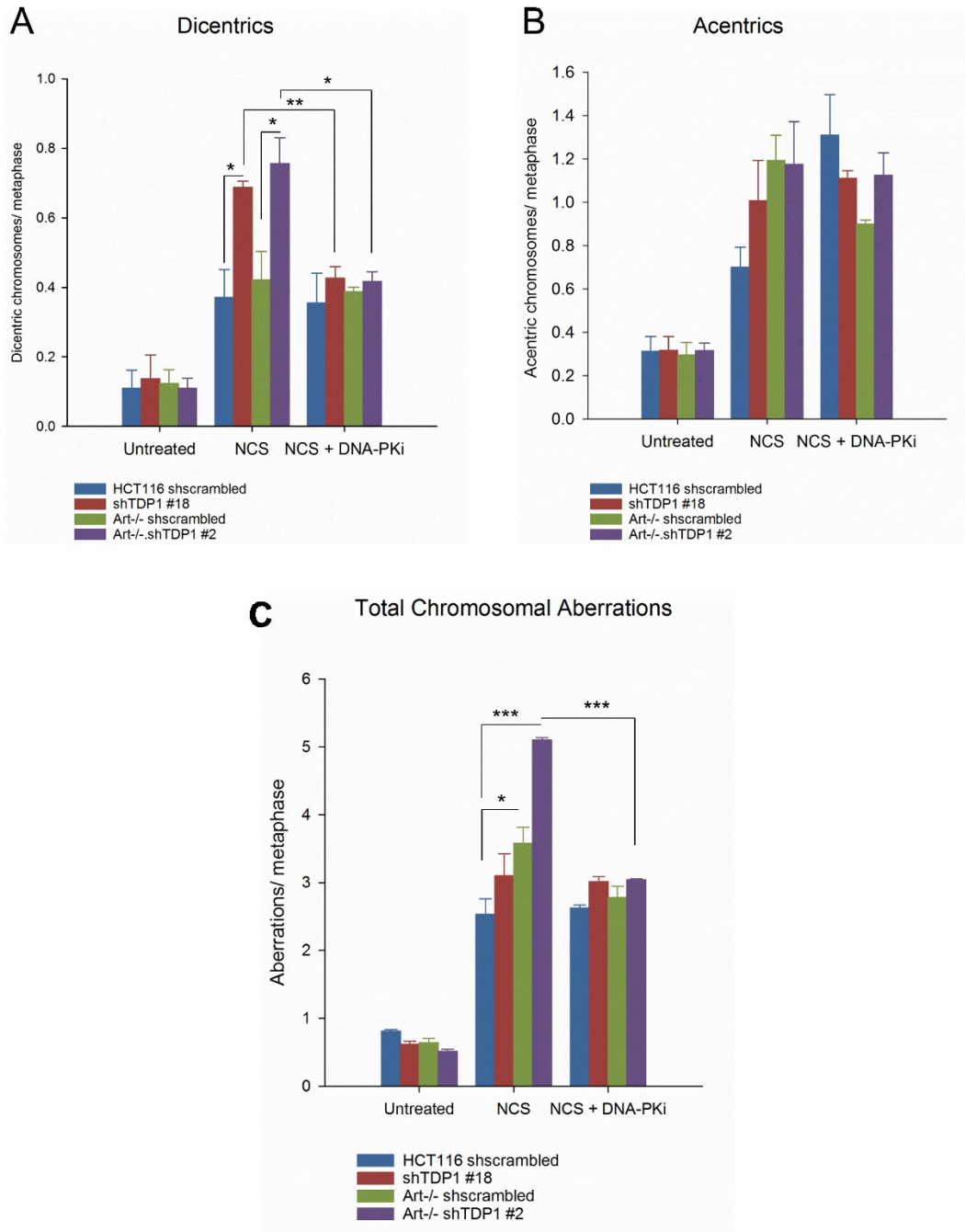


Figure 4-19: Chromosomal Aberrations in HCT116 cells upon NCS treatment

A total of approximately 40-45 metaphases from 3 independent experiments were imaged, scored for the presence of dicentric chromosomes (A), acentric fragments (B) and total aberrations (C) and results plotted as number of aberrations (dicentrics, acentrics or overall aberrations) per metaphase. Total aberrations include acentrics, dicentrics, breaks, gaps, radials, unstructured chromosomal regions. Error bars represent SEM. $n=2$ for DNA-PKi samples, $n=3$ for others. * - $p < 0.05$, *** - $p < 0.0005$

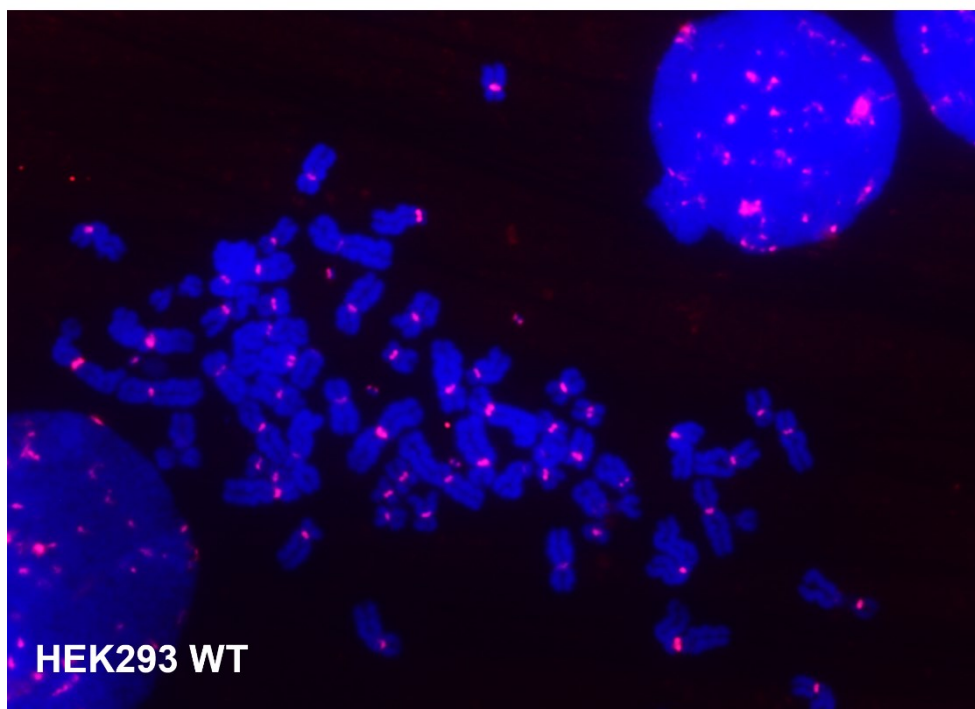
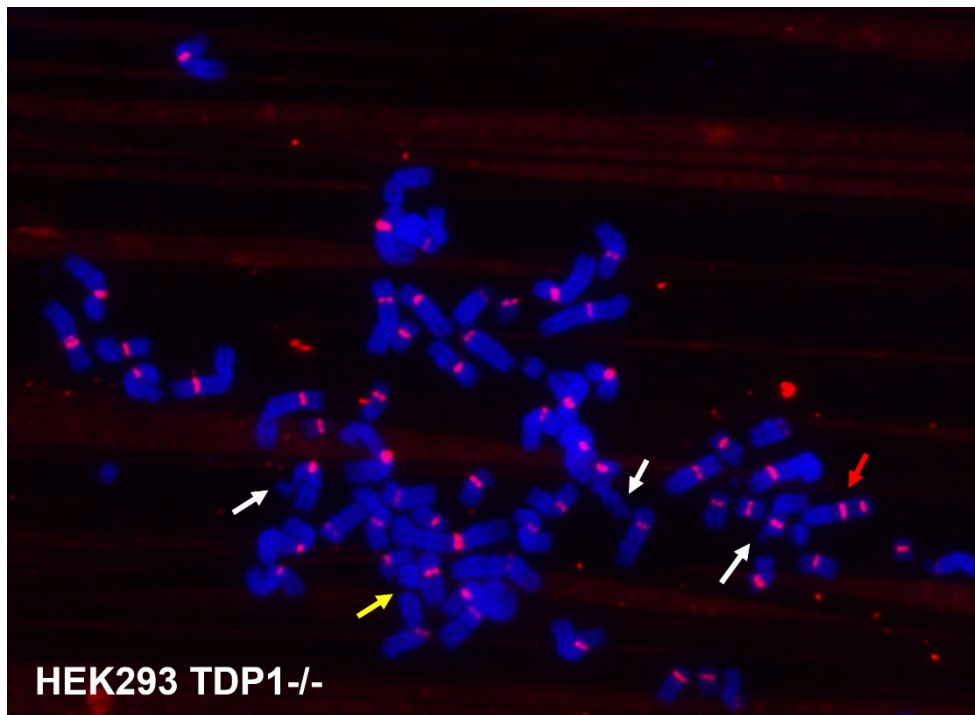


Figure 4-20: TDP1 deficiency leads to increased chromosomal aberrations in HEK293 cells upon NCS treatment

Cells were treated with 2nM NCS for 6 hours. Centromeres were labelled with a Cy3-conjugated fluorescent probe (PNA Bio Inc.). Red arrows represent dicentric chromosomes, yellow arrows represent acentric fragments. White arrows represent other aberrations.

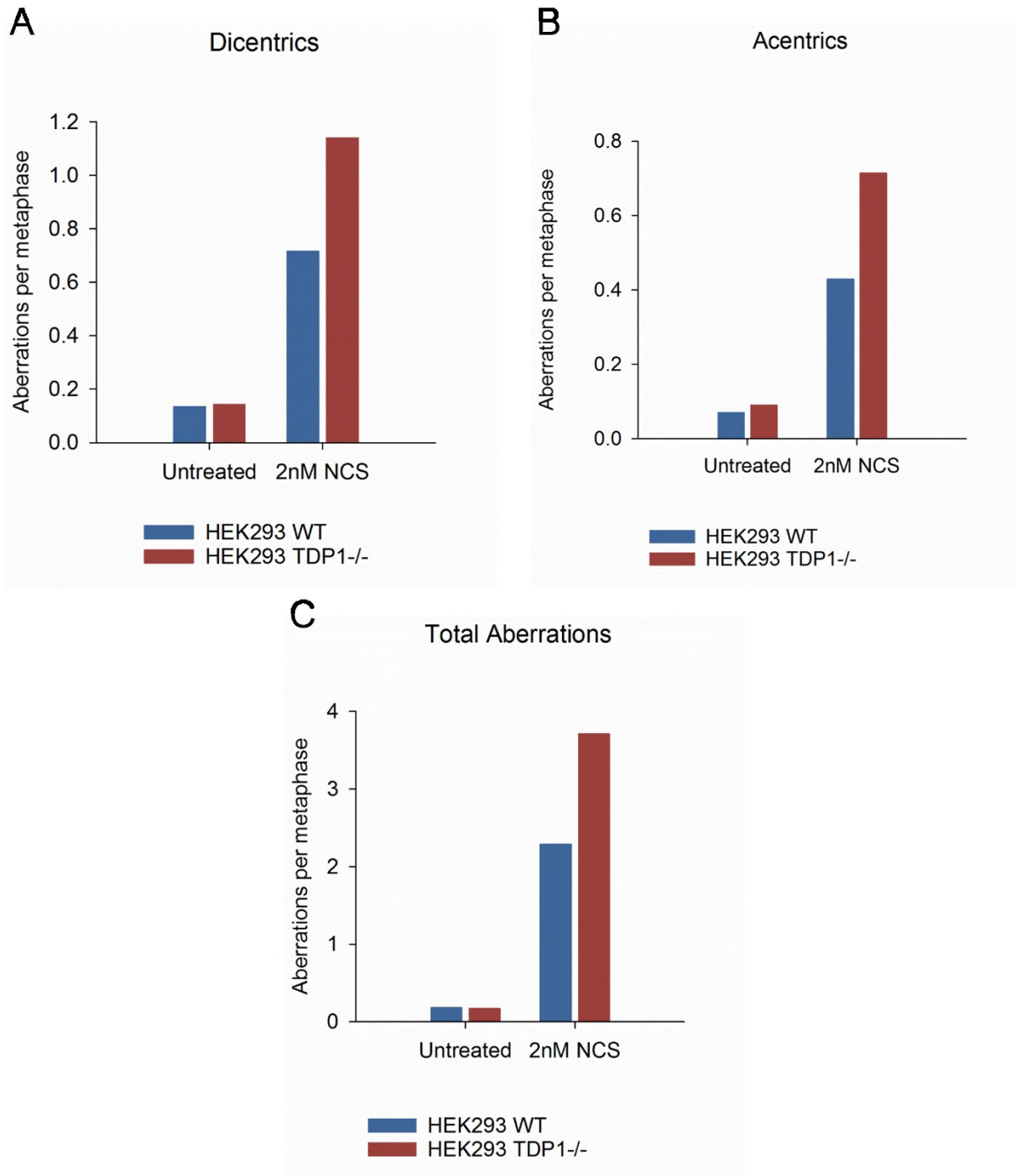


Figure 4-21: Chromosomal Aberrations in HEK293 cells upon NCS treatment

A total of approximately 40-45 metaphases from 3 independent experiments were imaged, scored for the presence of dicentric chromosomes (A), acentric fragments (B) and total aberrations (C) and results plotted as number of aberrations (dicentrics, acentrics or overall aberrations) per metaphase. Total aberrations include acentrics, dicentrics, breaks, gaps, radials, unstructured chromosomal regions.

4.7 Absence of Artemis delays G1-S progression upon DSB induction; this delay is rescued in an additional absence of TDP1

An important facet of DSB repair involves activation of cell cycle checkpoints that arrest progression of cells through the cell cycle, providing enough time for the cells to repair the induced damage. This arrest is critical as it prevents the dissemination of damaged chromosomes to daughter cells upon mitosis. HCT116 cells used in the current study are p53-positive and show an efficient ATM-mediated G1-block in response to DSBs. Thus, in order to investigate whether TDP1 and Artemis play a role in regulating cell cycle progression from G1 to S phase in response to NCS-induced DSBs, cell cycle analysis was performed.

An initial mapping experiment was performed to determine the basic cell cycle profiles of HCT116 WT cells and their isogenic mutant derivatives. Cells were synchronized in the G0/G1 phase by serum starvation for 96 hours and then released in serum containing medium for up to 18 hours. All cells showed a similar progression from G1 to S-phase. At 12 hr, Artemis^{-/-}•shTDP1#2 cells showed a slight delay in progression as compared to the WT and the single mutants. However, this difference was abolished at 18 hr (Fig. 4-22). Since a considerable fraction of cells were still in G1-phase 18hr after release in serum, it was hypothesized that these cells possibly reflect a fraction that re-enter cell cycle following mitosis. Indeed, when cells were released in serum with 100 ng/mL nocodazole, the fraction of cells in G1-phase decreased significantly (Fig. 4-23). Nocodazole is a microtubule inhibitor that arrests cells in the M-phase and prevents them from dividing and subsequently re-entering into G1-phase.

Next, cells were treated with 2 nM NCS for 6 hours after serum starvation and then released into serum containing medium to analyse the effects of 3'-PG-ended DSBs in the absence of TDP1, Artemis or both. WT and TDP1-depleted cells showed a similar progression phenotype with only

a minor fraction of cells persisting in G1-phase upon damage. Surprisingly, Artemis-deficient cells showed a considerable delay in cell-cycle progression such that a significant fraction of cells still remained arrested in G1-phase. However, an additional depletion of TDP1 in these cells rescued this delay such that the Artemis^{-/-}•shTDP1#2 #2 cells progressed much faster than the Artemis^{-/-} single mutants (Fig. 4-24). These results suggest that loss of Artemis delays progression of cells from G1 to S phase presumably due to residual un-rejoined breaks. Moreover, loss of TDP1 does not cause a delay in progression from G1-S and in fact, rescues the delay observed in Artemis-deficient cells, TDP1 may play a critical role in the G1-S checkpoint in the presence of 3'-phosphoglycolate-ended DSBs.

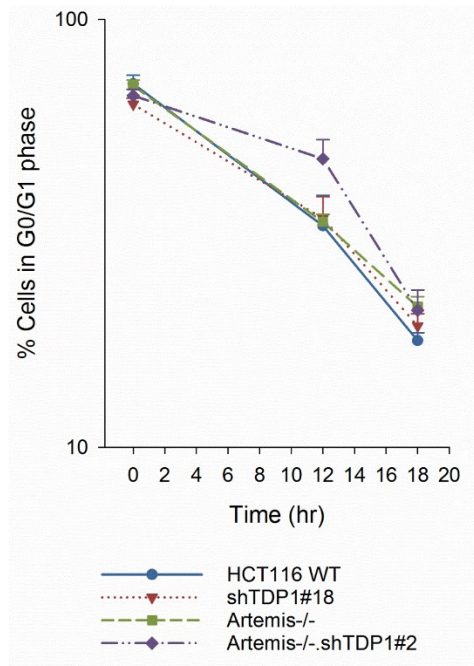
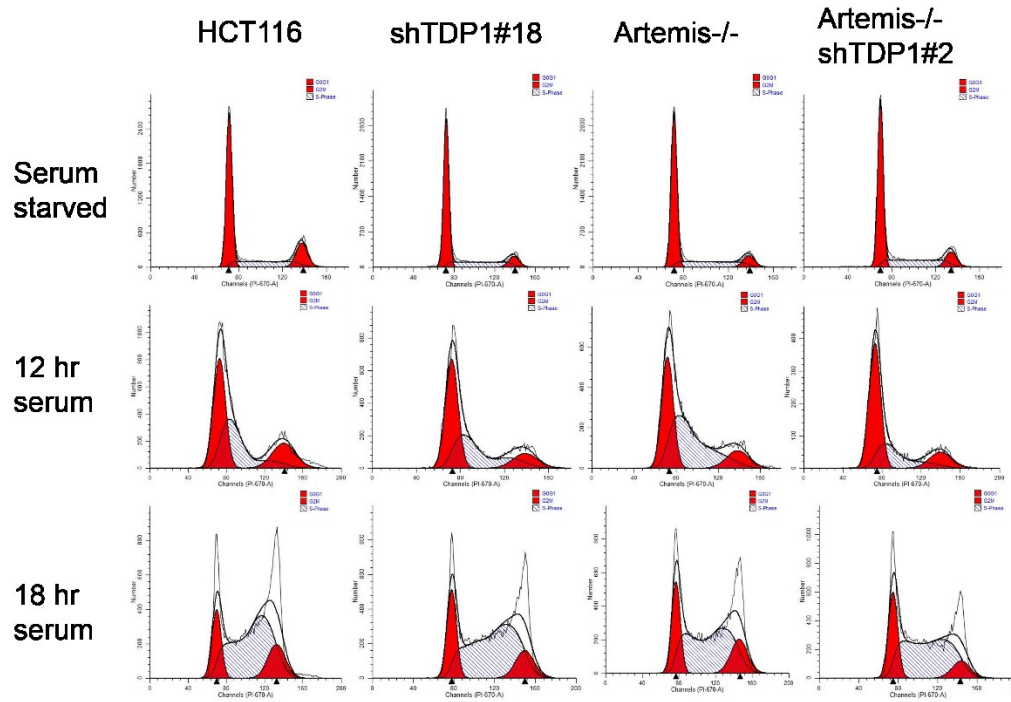


Figure 4-22: G1-S Cell Cycle Progression in HCT116 cells

Cells were synchronized in G0/G1 phase by serum starving for 96 hours. Following serum-starvation cells were released in serum and cell cycle profiles were analyzed at the indicated time points by FACS. Representative FACS histogram plots showing the percentage of cells in each phase of the cell cycle were prepared using ModFit LT software. Horizontal axis depicts the DNA-content. A minimum of 30,000 events were collected for each sample.

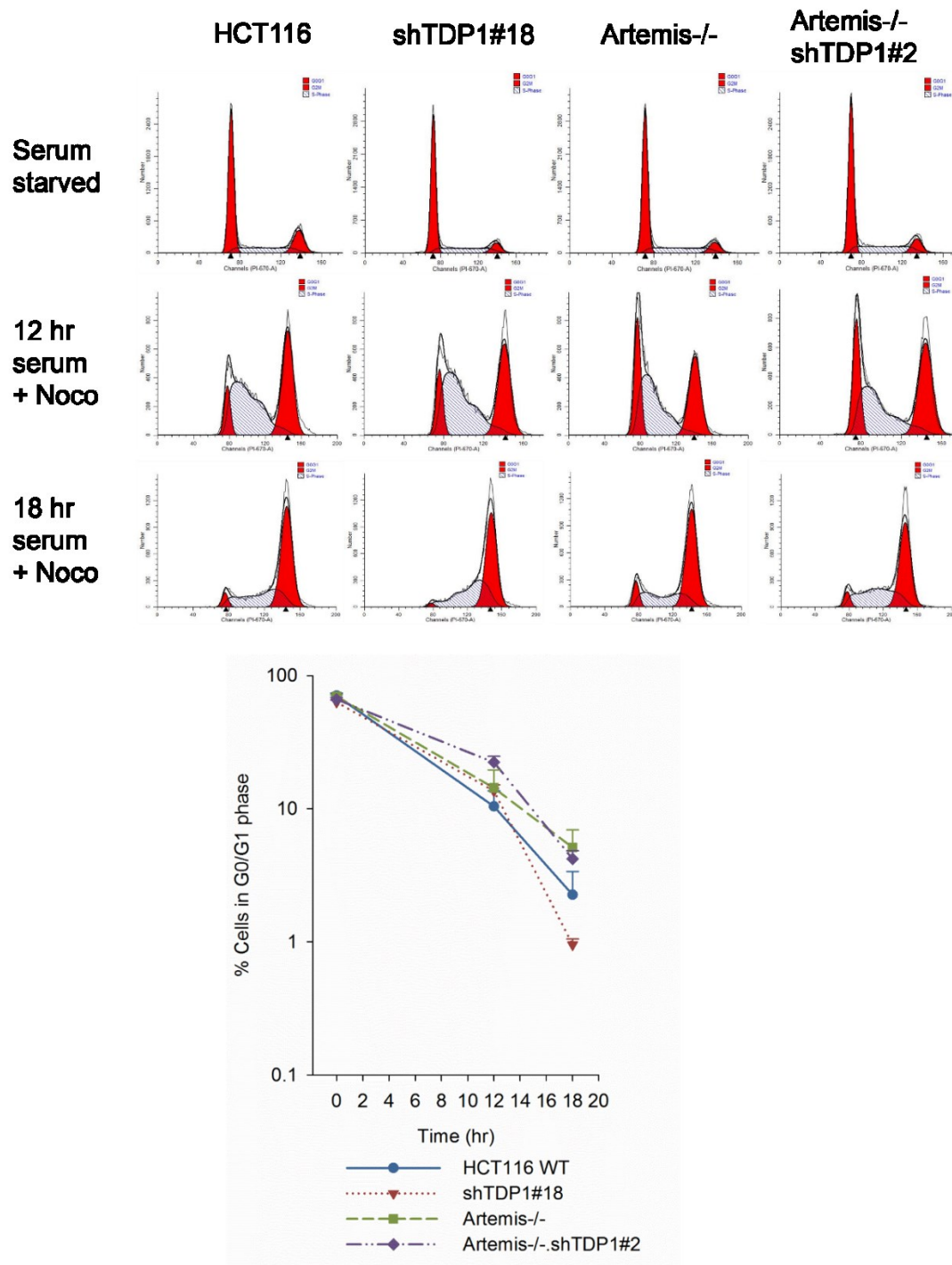


Figure 4-23: G1-S cell cycle progression followed by G2/M arrest in HCT116 cells in the presence of Nocodazole

Following serum-starvation cells were released in serum containing 100 ng/mL nocodazole and cell cycle profiles were analyzed at the indicated time points by FACS. plots showing the percentage of cells in each phase of the cell cycle were prepared using ModFit LT software. A minimum of 30,000 events were collected for each sample.

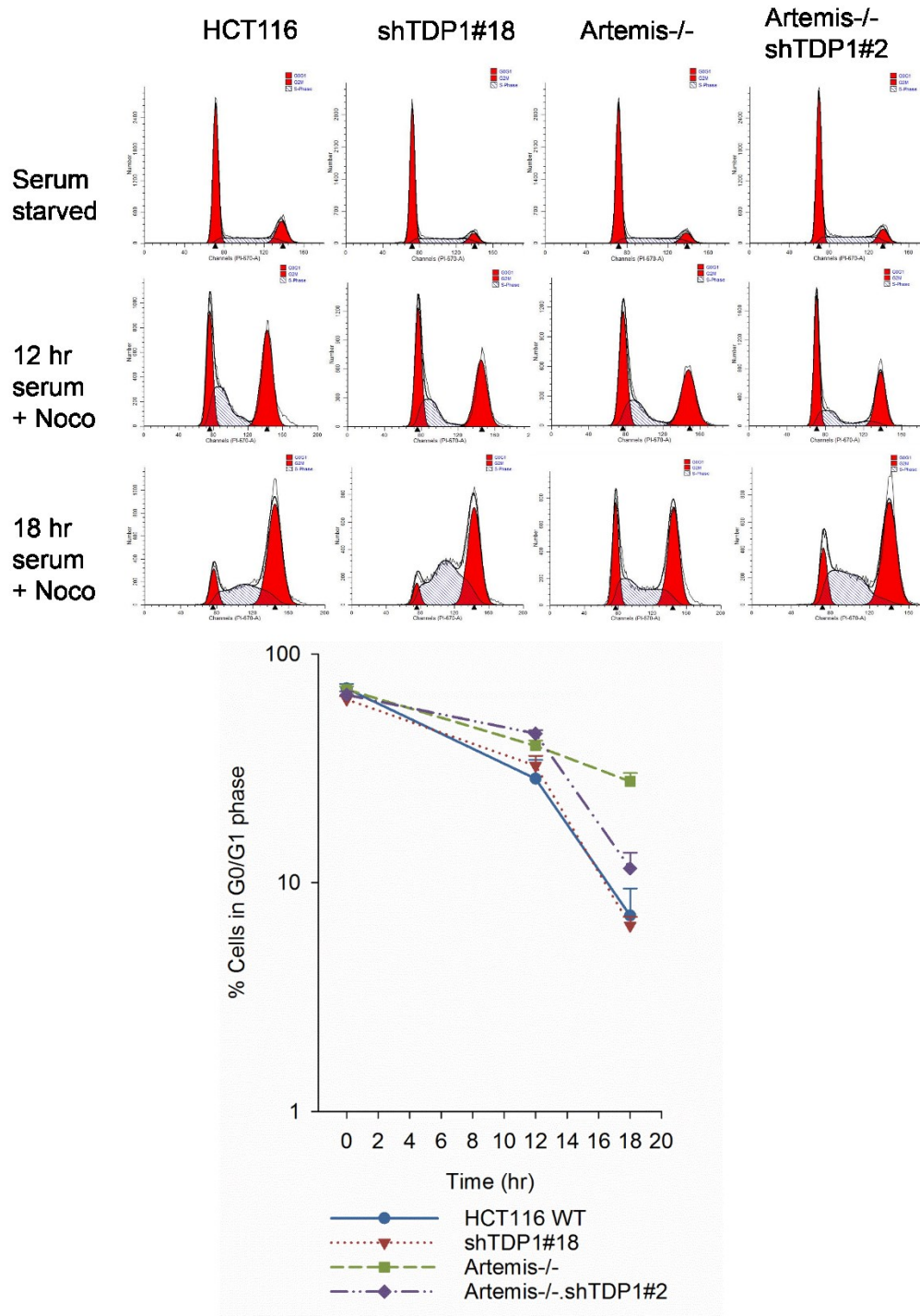


Figure 4-24: G1-S cell cycle progression upon DSB induction by NCS in HCT116 cells.

Cells were synchronized in G0/G1 phase by serum starving for 96 hours. Following serum-starvation cells were treated with 2 nM NCS for 6 hours, then released in serum and cell cycle profiles were analyzed at the indicated time points by FACS. Plots showing the percentage of cells in each phase of the cell cycle were prepared using ModFit LT software. A minimum of 30,000 events were collected for each sample.

4.8 Interplay between TDP1/Artemis with the DNA damage response proteins PARP1 and ATM.

Poly (ADP)-Ribose Polymerase (PARP) family of proteins are key early responders to DNA damage (Liu, Vyas, Kassab, Singh, & Yu, 2017). Upon DSB induction (and SSBs or base damage), PARP1 poly (ADP)-ribosylates chromatin and facilitates its opening up that enables access to critical DNA repair proteins (O'Connor, 2015). In addition, PARP1 also PARylates several other DNA repair factors, though to be necessary for their recruitment at damaged sites (Morales et al., 2014). In one such example, TDP1 and PARP1 have been shown to be epistatic for the repair of CPT-induced TopI-DNA lesions and TDP1 is poly (ADP)-ribosylated by PARP1 in this pathway (Das et al., 2014). However, a recent study demonstrated a lack of apparent epistasis between TDP1 and PARP1 for the repair of sapacitabine, a chain-terminating nucleoside analogs (CTNA) (Abo et al., 2017). This suggests that a differential mechanism exists that allows PARP1 to modulate TDP1's function in response to some types of modified ends but not others. Additionally, PARP1 is a key component in the alternative non-homologous end joining (A-NHEJ) pathway for the repair of DNA DSBs (Mansour, Rhein, & Dahm-Daphi, 2010). Thus, to investigate the functional interaction between TDP1, Artemis and PARP1 for the repair of NCS-induced 3'-PG terminated DSBs, clonogenic survival assays were performed using the PARP inhibitor, AZD-2281 (Olaparib). Unlike WT cells, all the mutants showed an increase in sensitivity to NCS upon PARP inhibition (Fig. 4-25) suggesting that TDP1 and Artemis are not epistatic with PARP1 but are involved in a pathway parallel to the PARP1-dependent repair of NCS-induced 3'-PG terminated DSBs.

ATM kinase is a critical DSB repair protein that phosphorylates a plethora of substrates facilitating DSB repair (Blackford & Jackson, 2017). ATM and Artemis are epistatic for the repair

of a subset of IR-induced DSBs (Riballo et al., 2004). On the other hand, ATM phosphorylates TDP1 for its optimal function at camptothecin-induced breaks (Das et al., 2009). Thus, to investigate the role of ATM in the epistasis between Artemis and TDP1, clonogenic survival assays were performed using NCS in the presence of an ATM inhibitor KU-60019. WT cells showed an increased sensitivity to NCS upon ATM inhibition suggesting an important role for ATM in the repair of 3'-PG DSBs (Fig. 4-26). Additional TDP1-depletion in these cells enhanced the sensitivity even further suggesting that ATM and TDP1 are involved in parallel pathways for the repair of NCS-induced DSBs (Fig. 4-26A). Interestingly, compared to ATM-inhibited WT cells, inhibition of ATM in Artemis^{-/-} single and Artemis^{-/-}•shTDP1#2 double mutants led to an increase in sensitivity only at high doses of NCS (Fig. 4-26B, C).

Thus, taken together, these data indicate that TDP1 and Artemis perform both complementary and parallel functions in human DNA DSB repair.

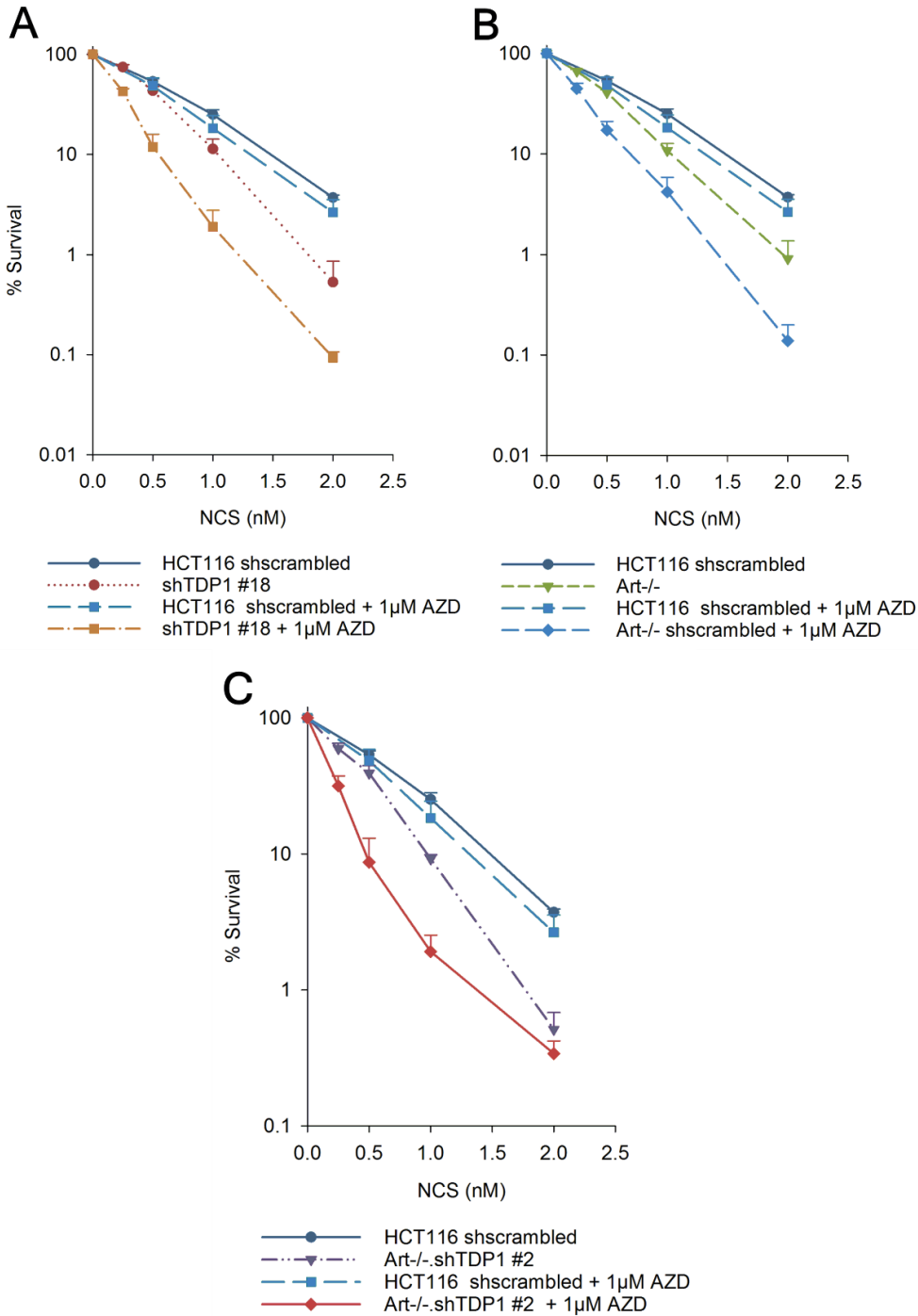


Figure 4-25: Artemis and TDP1 function in parallel with PARP1 in response to NCS-induced DSBs.

Clonogenic survival assays were performed on isogenic HCT116 WT, TDP1-deficient, Artemis-deficient, and TDP1/Artemis double-deficient cells treated with NCS in the presence of Olaparib. Error bars represent SEM. n=4.

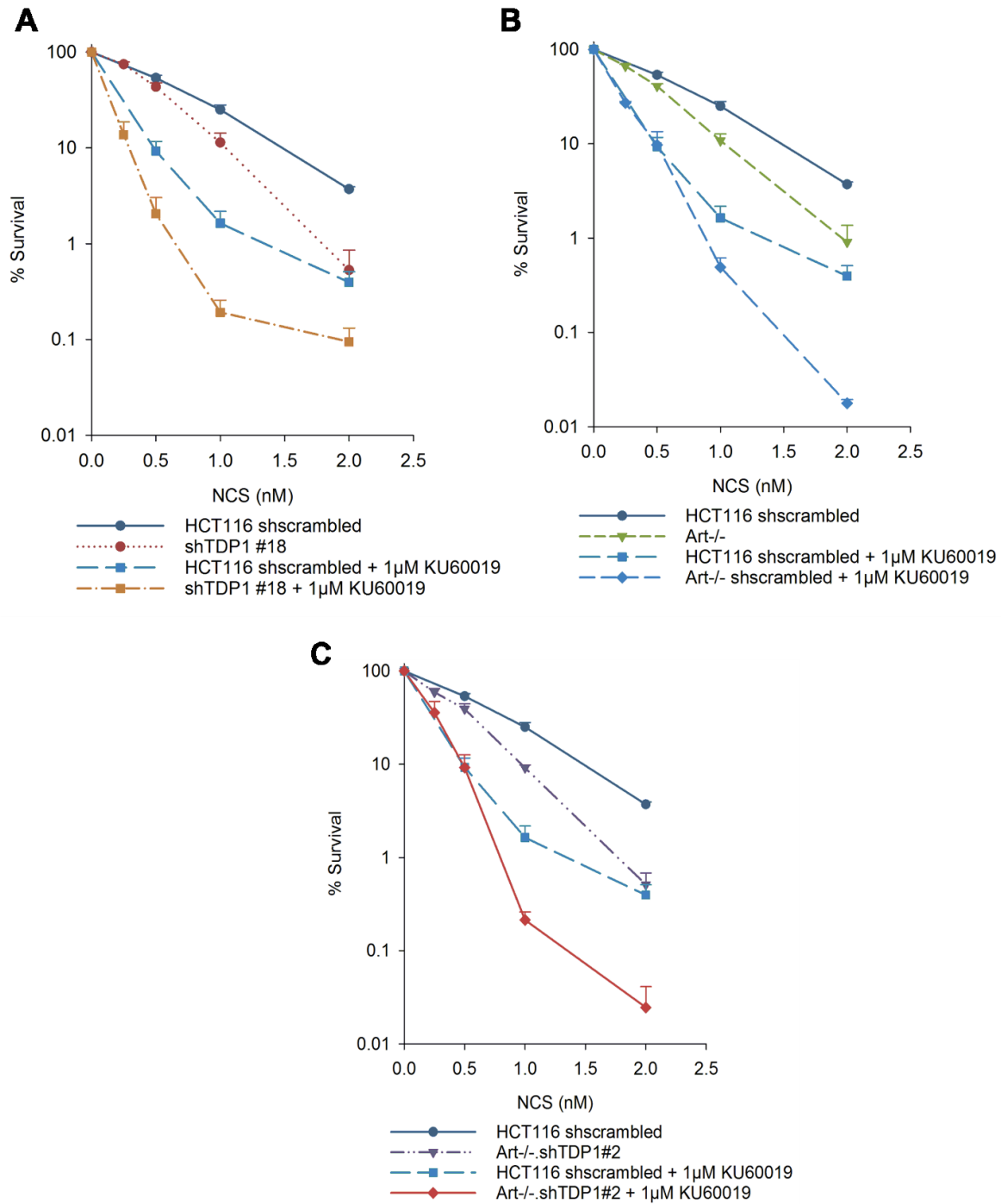


Figure 4-26: TDP1 and Artemis function in parallel to ATM in response to NCS-induced DSBs.

Clonogenic survival assays were performed on isogenic HCT116 WT, TDP1-deficient, Artemis-deficient, and TDP1/Artemis double-deficient cells treated with NCS in the presence of ATM inhibitor, Ku-60019. Error bars represent SEM. $n=4$.

4.9 PNKP-deficient cells display enhanced hypersensitivity to NCS

Polynucleotide Kinase/ Phosphatase is a bifunctional enzyme that processes 3'-phosphates and 5'-hydroxyl moieties on the DNA (Weinfeld et al., 2011). To investigate the biological significance of PNKP in response to these modification, PNKP was knocked out in HCT116 and HeLa cells in the lab of Dr. Michael Weinfeld, University of Alberta. Absence of PNKP in HCT116 cells was confirmed by a western blotting experiment. PNKP levels were too low to be detected and hence, cyto-nuclear fractionation was performed. A band corresponding to PNKP was observed in WT nuclear extract that was lacking in PNKP^{-/-} nuclear extract (Fig. 4-27).

Previously, it has been shown that shRNA-mediated knockdown of PNKP in A549 lung carcinoma cells conferred significant sensitivity to radiation and NCS (Rasouli-Nia, Karimi-Busheri, & Weinfeld, 2004; Segal-Raz et al., 2011). To more clearly evaluate the cytotoxicity of 3'-phosphates in the absence of PNKP, clonogenic survival assays were performed in HCT116 as well as HeLa cells. PNKP-deficient derivatives of HCT116 and HeLa cells showed enhanced sensitivity to both radiation and NCS (Fig. 4-28). In HCT116 cells, PNKP^{-/-} cells were considerably more sensitive to NCS, which specifically induces DSBs bearing protruding 3'-phosphate-terminated DSBs (DMF = 2.5) than to radiation (DMF = 1.5), suggesting that PNKP deficiency confers a specific sensitivity to 3'-phosphate-terminated DSBs, consistent with a possible deficiency in processing and repair of such lesions. However, in HeLa cells PNKP^{-/-} were equally as sensitive to NCS as to radiation (DMF = 1.37), suggesting the presence of more robust alternative PNKP-independent DSB repair pathway(s) in HeLa cells than in HCT116.

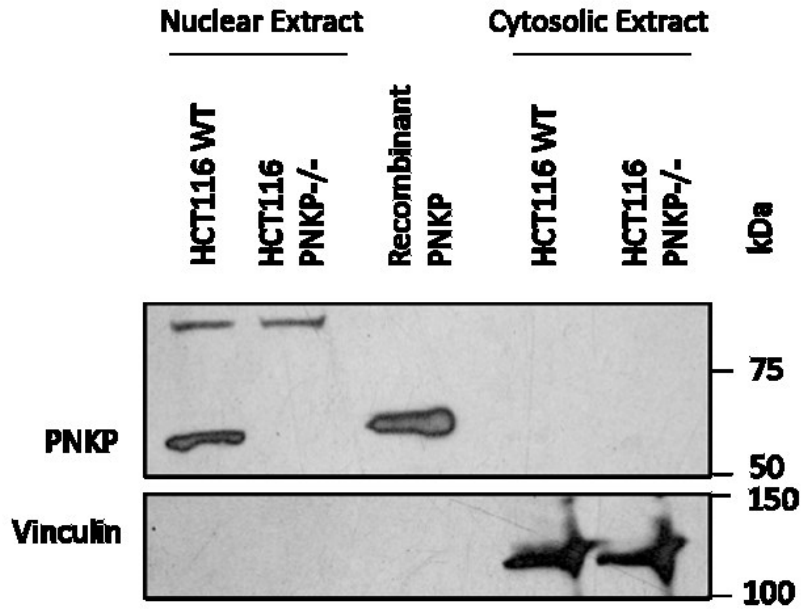


Figure 4-27: Absence of PNKP in nuclear extracts of PNKP^{-/-} HCT116 cells.

Lack of detectable PNKP in PNKP^{-/-} HCT116 nuclear extracts as probed with an N-terminal H101 antibody. A non-specific band at ~ 90 kDa serves as a loading control. rPNKP=50 ng His-tagged recombinant human PNKP. Vinculin is used as a fractionation control observed only in the cytoplasmic fraction.

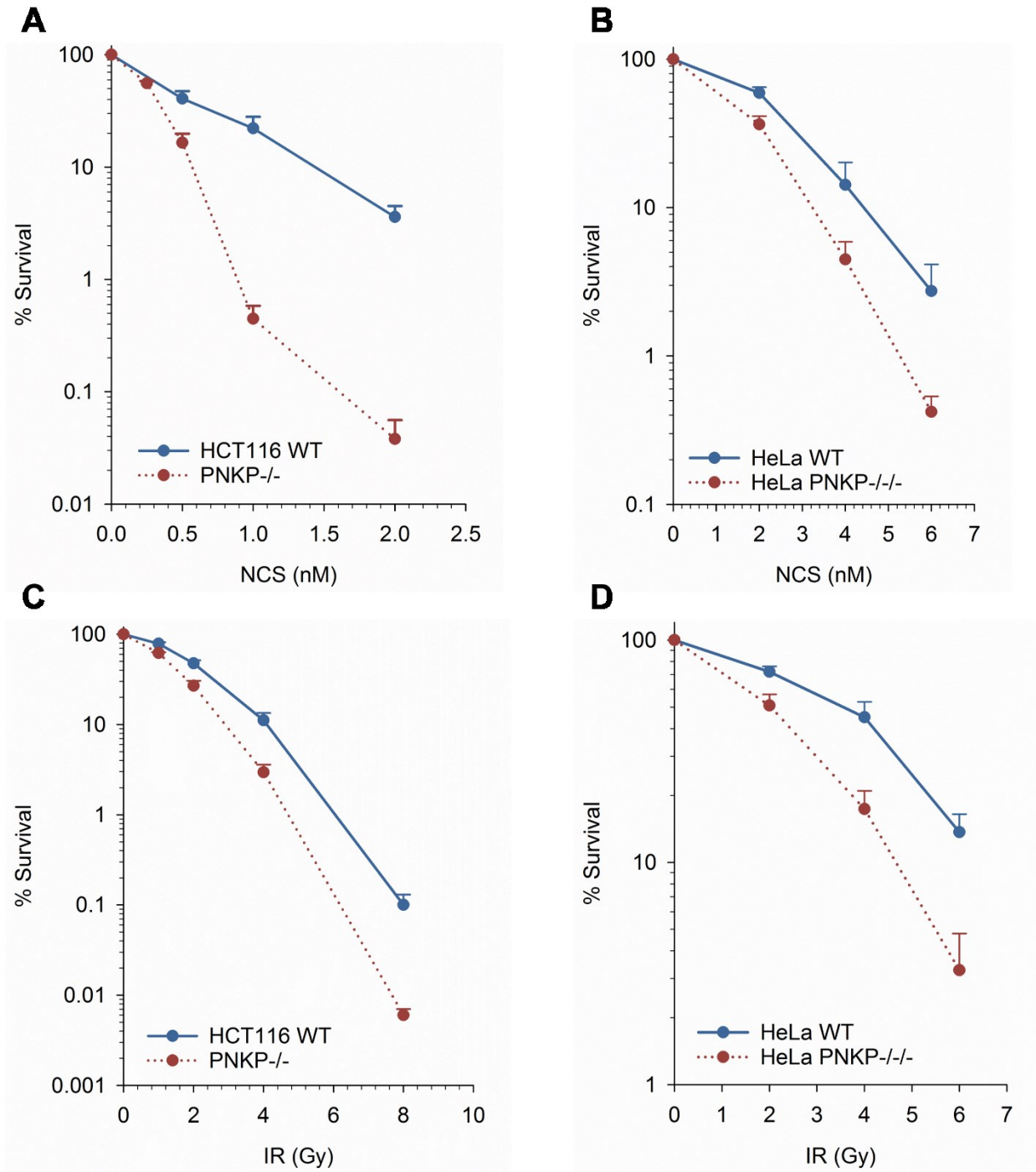


Figure 4-28: PNKP-deficient cells are hypersensitive to NCS and radiation

Clonogenic survival assays were performed on isogenic HCT116 WT and PNKP^{-/-} cells (A & C) as well as HeLa WT and PNKP^{-/-} cells (B & D) treated with NCS (A,B) or radiation (C,D). Error bars represent SEM. n=3.

4.10 Interplay between PNKP and other DNA repair factors

PNKP is phosphorylated at S114 and S126 by ATM and DNA-PK in response to DSB production and S114A/S126A phosphomutant PNKP proteins show decreased 3'-phosphatase activity (Segal-Raz et al., 2011). To examine the interplay between PNKP and the DNA damage response to NCS, survival of HCT116 WT and PNKP^{-/-} cells was assessed following treatment with NCS in the presence of an inhibitor of DNA-PK, ATM kinase, or both. DNA-PK is a critical factor in NHEJ (Jette & Lees-Miller, 2015), while ATM is important for DSB repair by homologous recombination as well as for repair of a subset of DSBs by NHEJ (Beucher et al., 2009; Kocher et al., 2012; Riballo et al., 2004). NU7441 (DNA-PKi) and KU60019 (ATMi) equally sensitized WT HCT116 cells, although at the highest NCS concentration, ATMi was more potent (Fig. 4-29). Intriguingly, at low NCS concentrations, each inhibitor was more deleterious to survival than was PNKP deficiency, but at the highest concentration, PNKP deficiency was more deleterious than the inhibitors, either alone or in combination. Furthermore, at high levels of damage, DNA-PKi had almost no effect on survival of PNKP^{-/-} cells (Fig. 4-29). These results are consistent with the presence of some alternative process or enzyme that can substitute for PNKP in NHEJ, but that saturates at very low levels of damage. Thus, in severely damaged cells, repair of NCS-induced DSBs by NHEJ becomes almost completely dependent on PNKP, so that DNA-PKi has little effect on PNKP^{-/-} survival. In the presence of low-level damage, DSBs would be repaired by NHEJ despite PNKP deficiency, so that DNA-PKi markedly reduces survival of PNKP^{-/-} cells. The additive effects of ATMi and PNKP deficiency on survival are likely to result from ATM's role in DSB repair by homologous recombination, which does not require PNKP (Karimi-Busheri, Rasouli-Nia, Allalunis-Turner, & Weinfeld, 2007).

Poly(ADP-ribose) polymerase (PARP) adds poly(ADP-ribose) chains to a variety of nuclear proteins when DNA is damaged (Rouleau et al., 2010), and is essential for efficient SSB repair, as well as for an alternative Ku-independent end joining pathway involving XRCC1, DNA ligase III and DNA polymerase theta (Audebert, Salles, & Calsou, 2004; Black, Kashkina, Kent, & Pomerantz, 2016; Wood & Doublet, 2016). In most genetic backgrounds, PARP inhibitors confer a replication-dependent radiosensitivity by inhibiting SSB repair and by inappropriately channeling the resulting single-ended DSBs into NHEJ (Patel, Sarkaria, & Kaufmann, 2011). However, radiosensitivity can be replication-independent when Ku-dependent NHEJ is compromised (Hochegger et al., 2006). Previous work showed that HCT116 cells were radiosensitized by the PARP inhibitor Olaparib (Alotaibi et al., 2016; Shelton et al., 2013). However, in the current study, Olaparib did not sensitize HCT116 WT cells to NCS, suggesting that the relatively small number of NCS-induced SSBs do not contribute significantly to cytotoxicity even when PARP is inhibited. Furthermore, neither Olaparib nor Veliparib further sensitized PNKP^{-/-} cells (Fig. 4-29), despite showing clear inhibition of Poly (ADP)-Ribosylation in these cells (Fig. 4-30). This result is consistent with reports that PNKP is involved in end joining by both Ku-dependent NHEJ (Karimi-Busheri et al., 2007) and PARP-dependent Alt-NHEJ (Audebert, Salles, Weinfeld, & Calsou, 2006). Thus, both repair systems are already compromised in PNKP^{-/-} cells, so that blocking Alt-NHEJ with a PARP inhibitor would be expected to have little, if any effect.

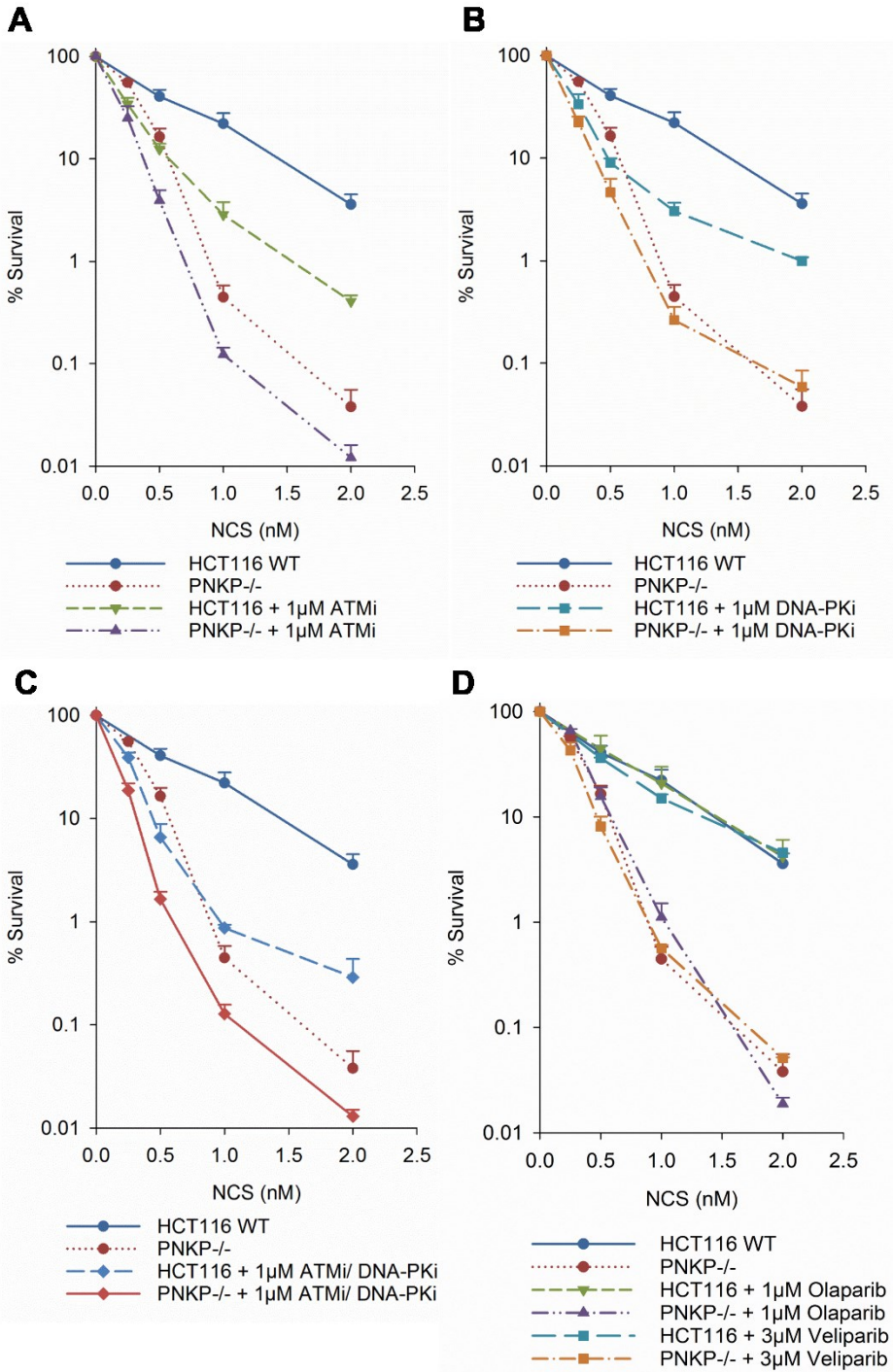


Figure 4-29: Interplay between PNKP and ATM, DNA-PK and PARP1 in response to NCS-induced DSBs

Clonogenic survival assays were performed on isogenic HCT116 WT and PNKP^{-/-} cells treated with NCS in the presence of inhibitors of ATM (A,C), DNA-PK (B,C) or PARP (D). Error bars represent SEM. n=3.

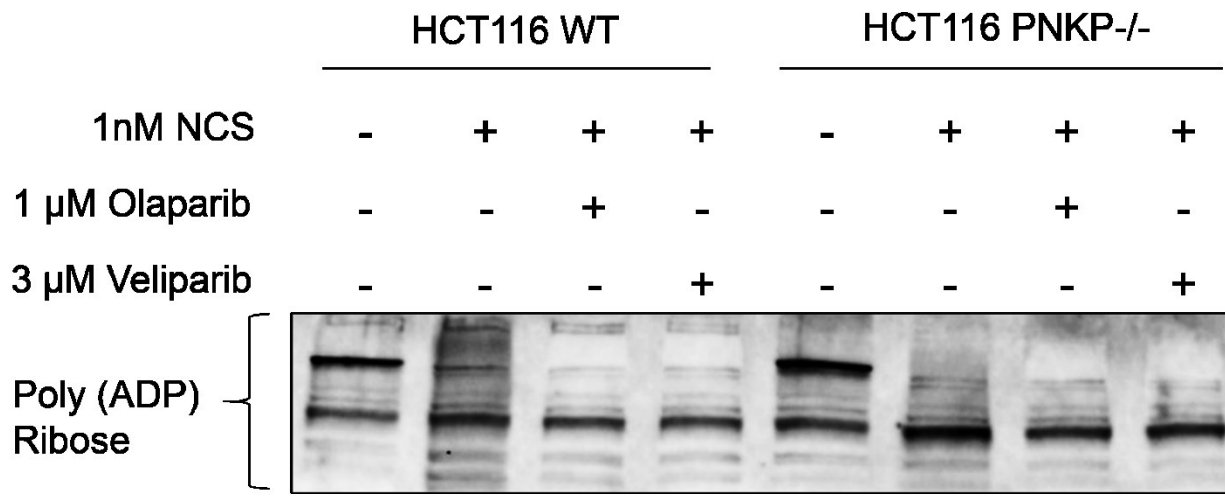


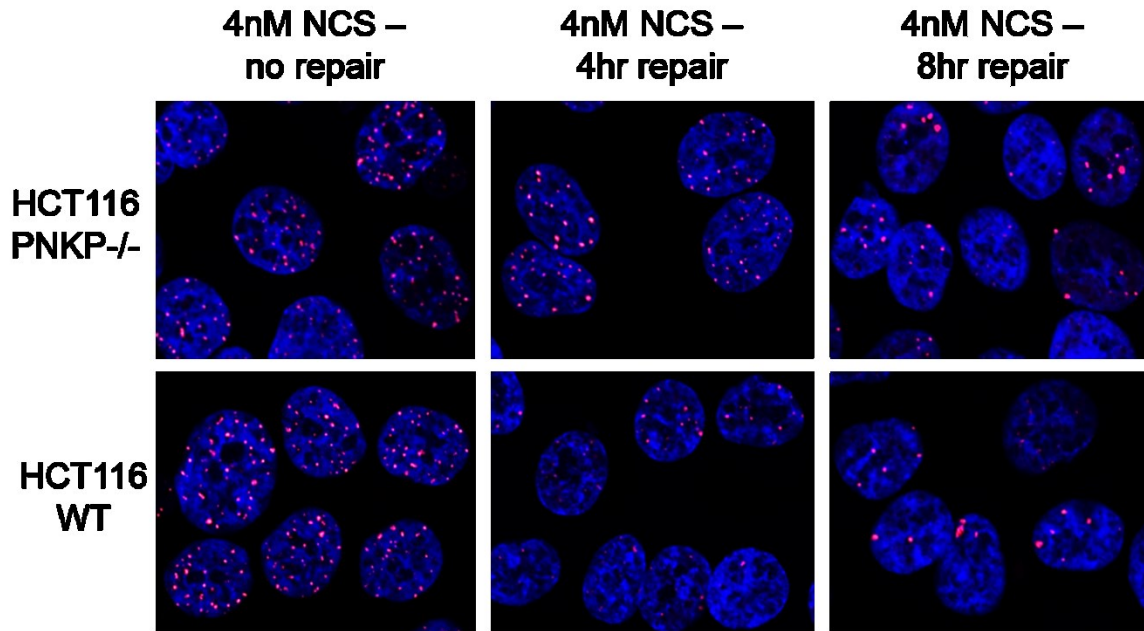
Figure 4-30: Confirmation of PARP inhibition using western blotting

4.10 PNKP is required for rejoining of 3'-P ended DSBs in cells.

To directly investigate whether the hypersensitivity shown by the mutants to NCS was attributable to a defect in repairing 3'-phosphate-ended DSBs, measurements of NCS-induced DSBs in cells, detected as 53BP1 foci, were performed. Serum-starved G1/G0 cells were used to specifically analyze DSB repair by NHEJ while avoiding spontaneous focus formation at stalled replication forks. As shown in Fig. 4-31, there were about twice as many residual DSBs in PNKP-deficient as in WT HCT116 cells at 4 and 8 hr after NCS treatment. This result is consistent with a model wherein increased persistence of 3'-phosphate termini due to lack of PNKP interferes with efficient DSB rejoining.

Since PNKP is critical for the removal of 3'-P from DSB ends during NHEJ and loss of PNKP significantly hampers DSB rejoining via NHEJ, we asked whether PNKP-deficient cells increase the use of Homologous Recombination for repairing these DSBs. Rad51 foci were analysed as HR markers in HCT116 WT and PNKP^{-/-} cells in conjunction with 53BP1 after NCS treatment since Rad51 foci indicate commitment to HR (Bunting et al., 2012; Krejci, Altmannova, Spirek, & Zhao, 2012; Tarsounas, Davies, & West, 2003). In WT cells, Rad51 foci increased slightly by 4 hours and remained steady over a period of 12 hours suggesting that in WT cells, majority of breaks are repaired by NHEJ requiring PNKP. In PNKP^{-/-} cells, increase in Rad51 foci was similar to WT at 4 hours (Fig. 4-32). However, their number kept increasing over a period of 12 hours, suggesting that in the absence of PNKP, cells resort to using HR for the repair of these 3'-phosphate ended DSBs. Interestingly, it was observed that although Rad51 and 53BP1 colocalize, 53BP1 appears to moves to the periphery allowing HR to proceed, presumably prior to resection initiation ultimately allowing Rad51 to load onto the ssDNA filaments and carry out the homology search (Fig. 4-31A).

A



B

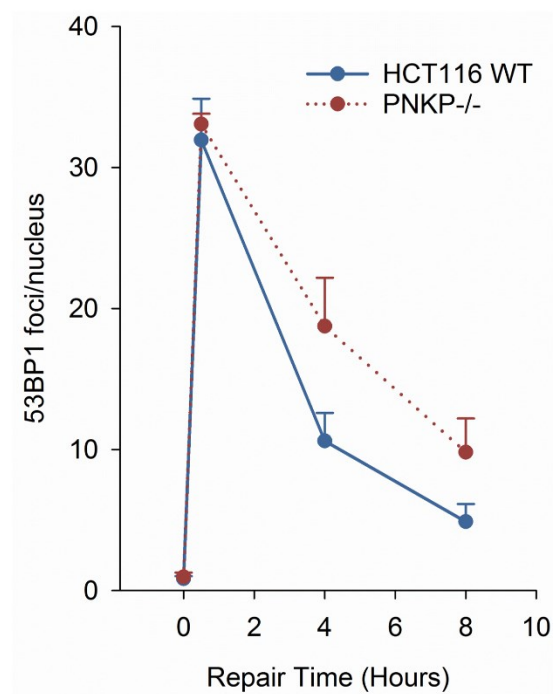


Figure 4-31: PNKP-deficient cells show a defect in 3'-P DSB rejoining

53BP1 foci were scored in serum-starved cells treated with 4 nM NCS for 1 hr and results plotted as number of 53BP1 foci per nucleus. Foci were counted using ImageJ whereas the counting of nuclei was done manually. Error bars represent SEM for $n=4$.

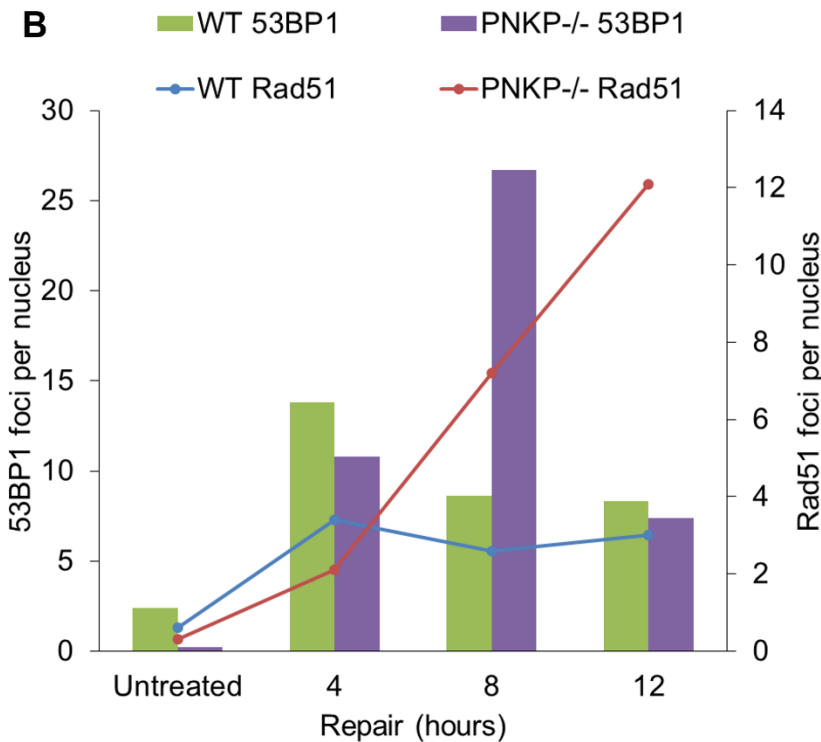
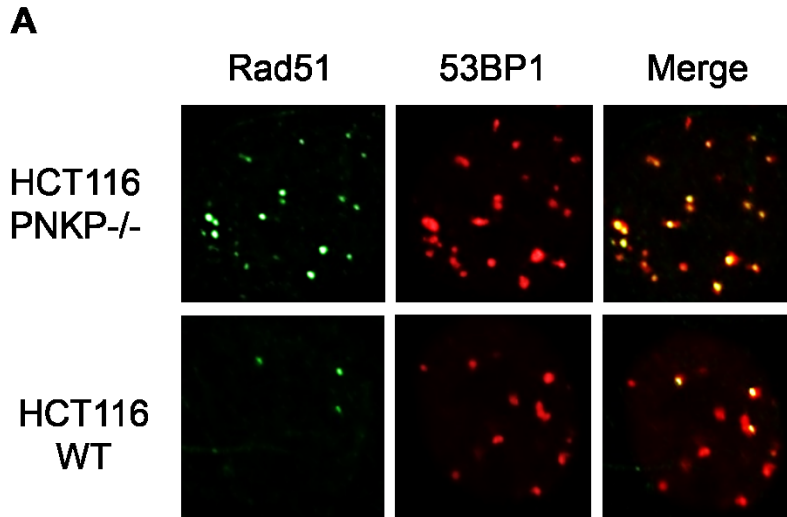


Figure 4-32: PNKP-/- cells show increased HR compared to WT cells for repairing 3'-P ended DSBs

53BP1 and Rad51 foci were scored at the indicated times after 4 nM NCS treatment for 1 hour. 0 hr indicates untreated sample. (A) Colocalization of Rad51 and 53BP1 foci in one representative nucleus in both WT and PNKP-/- cells. (B) Quantification of the respective markers. Left vertical axis indicates 53BP1 foci per nucleus represented by the bar graphs. Right vertical axis represents Rad51 foci per nucleus represented by the line graphs. Rad51 and 53BP1 foci were together analyzed only in 1 experiment.

5. DISCUSSION

Cytotoxic DNA damaging agents including ionizing radiation and radiomimetic natural compounds like NCS, CAL and bleomycin induce terminally-occluded DNA DSBs by free-radical mechanisms (Menon & Povirk, 2016). Although many 3'-blocked termini are unstable and spontaneously break down to 3'-phosphates, 3'-phosphoglycolates formed by fragmentation of the deoxyribose by oxidation of the C-4' position are stable and persistent (Povirk, 1996; Povirk, 2012). Gap-filling DNA polymerases and DNA ligases require 3'-hydroxyl DNA ends to efficiently add nucleotides and perform end ligation respectively, and therefore the resolution of a 3'-phosphoglycolate to a 3'-hydroxyl is an essential step in the repair of these DSBs. It is therefore not surprising that mammalian cells have evolved several enzymes — including TDP1, APE1 and Artemis — for such resolution (Zhou et al., 2005).

In the current study, NCS and CAL were used to investigate the role of TDP1 in the repair of 3'-phosphoglycolate DSBs. In contrast to radiation-induced DSBs which are heterogeneous and bear 3'-phosphoglycolate only on 10% of the total sugar oxidation products (B. Chen et al., 2007), about one in every four DSBs induced by CAL and NCS bear a 3'-phosphoglycolate, making these antitumor antibiotics more informative than IR in studying the repair of 3'-phosphoglycolate-DSBs (Povirk, 1996). Supporting established evidence of TDP1's critical role in 3'-phosphoglycolate

removal, TDP1-deficient cells were hypersensitive to both NCS and CAL (Hawkins et al., 2009; Inamdar et al., 2002; Zhou et al., 2009).

Scientists have used the principle of epistasis to delineate genes functioning in common or parallel DNA repair pathways (Glassner & Mortimer, 1994; Jensen, Ozes, Kim, Estep, & Kowalczykowski, 2013; Symington, 2002). According to the principle of epistasis, if the phenotypic impact of simultaneous deletion of 2 genes is equal in severity to that of the loss of function of individual genes, it may indicate that the genes function within a common pathway, possibly performing different roles in it (Ishii & Inoue, 1989). On the other hand, if the double deletion is phenotypically more severe than the individual deletions, it may result from the loss of compensatory repair pathways (Batenchuk, Tepliakova, & Kaern, 2010).

Elimination of Artemis, a DSB end-trimming nuclease that can also resolve 3'-phosphoglycolates (Povirk et al., 2007), likewise sensitized cells to NCS. Surprisingly, however, the toxicity of 3'-phosphoglycolate DSBs observed in cells simultaneously deficient in Artemis and TDP1 compared to cells with individual deficiencies in these genes was similar, indicating that these two proteins function in the same DSB repair pathway. Furthermore, as DSBs in G1-phase are repaired almost exclusively by NHEJ (Biehs et al., 2017), the epistasis between Artemis and TDP1 in cells synchronized in the G1-phase suggests an involvement of these two proteins in NHEJ. In addition, the increased toxicity of 3'-phosphoglycolate DSBs upon DNA-PK inhibition was not further enhanced by an additional deficiency in TDP1, Artemis or both. Thus, when C-NHEJ is suppressed, TDP1 and Artemis no longer contribute to survival after NCS treatment. Taken together, these data strongly support a functional involvement of Artemis and TDP1 in C-NHEJ for the repair of NCS-induced 3'-phosphoglycolate DSBs.

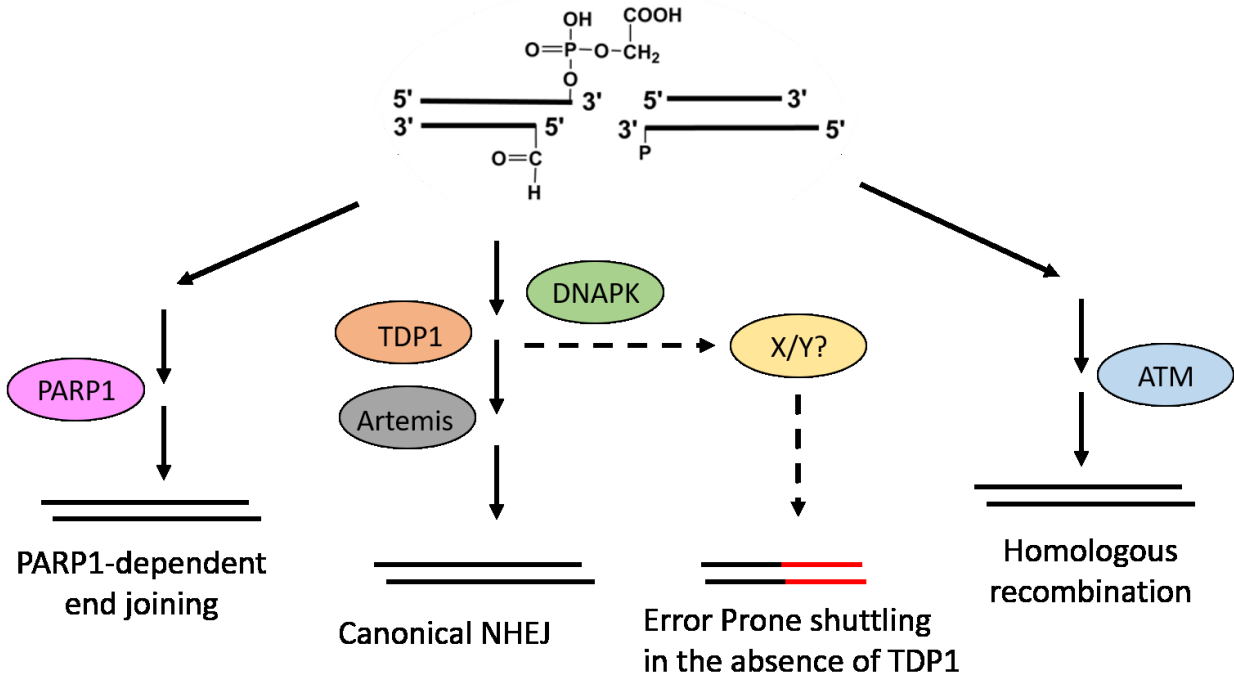


Figure 5-2: Model representing the DSB repair pathways and proteins analyzed in the study.

TDP1 and Artemis are in the same pathway for the repair of NCS-induced DSBs whereas ATM and PARP function in parallel. In the absence of TDP1, the breaks are shuttled to a more error-prone repair pathway regulated by the kinase activity of DNA-PK leading to misjoining of DSB ends. It is possible that the PARP1-dependent end joining pathway is actually the error-prone repair pathway promoting misjoining as has been previously shown.

The sensitivity of HEK293 TDP1^{-/-} cells to NCS was only partially rescued by complementing with recombinant TDP1 such that the complemented cells showed intermediate survival to WT and TDP1^{-/-} cells to NCS. This recombinant protein expressed in the complemented cell line has an N-terminal Flag tag. Since the N-terminal region of TDP1 is important for its recruitment to DSB sites, it is possible that this Flag tag interferes with the recruitment of TDP1 to DSB sites, thereby causing a partial rescue. This result is in agreement with previous reports where in one study, recombinant TDP1 only partially rescued the sensitivity of TDP1^{-/-} DT40 avian cells to ionizing radiation-induced DSBs (Abo et al., 2017). Another recent study reported that sensitivity HEK293 TDP1^{-/-} cells to camptothecin could be rescued at low, but not high doses of CPT by ectopically expressing WT TDP1 (J. Li et al., 2017).

The unexpected epistatic interplay between Artemis and TDP1 in survival of NCS treatment suggests that these two proteins perform non-overlapping roles in the repair of NCS-induced DSBs. This further implies that either Artemis or TDP1, but not both, are involved in the enzymatic processing of 3'-phosphoglycolates. Considering the well-documented role of TDP1 in clean 3'-phosphoglycolate removal, one likely possibility is that, upon NCS/CAL-induced DSB formation, the overhanging 3'-phosphoglycolate on one end of the DSB is a substrate for TDP1 whereas Artemis is required for removing the 5'-aldehyde formed on the other strand. Since the other end bears a 3'-phosphate which is the canonical substrate of PNKP, a critical end processing enzyme that interacts with the X-ray cross-complementing 4 (XRCC4)•LigaseIV complex in the context of C-NHEJ (Aceytuno et al., 2017), it is unlikely that either TDP1 or Artemis processes the 3'-phosphate ends. Alternatively, it can be surmised that if Artemis is important for 3'-phosphoglycolate end trimming via C-NHEJ, TDP1 might be playing a structural role in this pathway. Consistent with this possibility, TDP1 physically interacts with XLF and Ku70/80, key

proteins in the C-NHEJ pathway and stimulates binding of XLF and Ku70/80 to DNA (Heo et al., 2015). In this manner, a TDP1 deficiency would abrogate C-NHEJ-mediated DSB repair and the simultaneous absence of Artemis would have no additional effect. On the other hand, Artemis has been proposed to play a role in DSB repair pathway choice, directing breaks into C-NHEJ when appropriate (J. Wang et al., 2014). Loss of this function could lead to suboptimal repair regardless of whether 3'-phosphoglycolate termini are resolved. In the future, it will be interesting to explore these possibilities by tracking the processing of 3'-phosphoglycolate ends using ligation-mediated PCR (Akopiants et al., 2014) or complementing our mutant cell lines with either an endonuclease-deficient Artemis or a phosphodiesterase-deficient TDP1, respectively (J. Li et al., 2017; Mohapatra et al., 2011).

It is not uncommon for epistatic mutants with similar sensitivity to DNA damaging agents to show functional heterogeneity, evident from studies conducted on mutants belonging to the Rad52 epistasis group in *S. cerevisiae* (Petrini, Bressan, & Yao, 1997). Although scRad52, scRad51, scRad50 and scMre11 all are epistatic for IR sensitivity, the recombination phenotypes in mutants of these proteins are different. For example, meiosis-specific DSBs are formed by scMre11, scRad50 and scXrs2 to initiate recombination. These DSBs are formed in the scRad51 and scRad52 mutants, but the completion of recombination is severely impaired suggesting that these gene products are required at different stages of the recombination process (Petrini et al., 1997). Similarly, results from the current study show that although TDP1 and Artemis are epistatic for 3'-PG ended DSBs, they likely perform at different stages in the repair process.

In contrast to NCS and CAL, the repair of IR-induced breaks seems to require either TDP1 or Artemis as cells deficient in both are more radiosensitive than cells deficient in either individual protein. On one hand, it is known that the endonuclease function of Artemis is required in IR-

induced DSB repair (Mohapatra et al., 2011) and that Artemis is required for the repair of a subset of DSBs formed in heterochromatin (Beucher et al., 2009; Riballo et al., 2004). On the other hand, TDP1-mutant SCAN1 cells are defective in IR-induced SSB repair (El-Khamisy et al., 2007). Due to the heterogeneous nature of damage induced by radiation, TDP1 may thus be required for the repair of IR-induced SSBs while Artemis repairs the subset of DSBs in the heterochromatin. Accordingly, simultaneous absence of both proteins makes the cells more radiosensitive than their individual absence. Another possible basis for the positive epistasis is that phosphoglycolates formed on short overhangs (<3 bases) might be repaired by TDP1 whereas longer overhangs — due to clustered damage — might require Artemis (Povirk et al., 2007).

Another unanticipated finding was the apparent lack of a DSB rejoining defect in TDP1-depleted cells, despite their hypersensitivity to NCS. Assays of 53BP1 foci, a surrogate marker of unrepaired DSBs, indicated that these repair foci disappear with similar kinetics in WT and TDP1-depleted cells. Although this assay is standard for measuring the fraction of DSBs that remain unrejoined, it is limited by its inability to differentiate between DSB ends that are correctly rejoined, and DSB ends that are mis-joined to ends of other DSBs in the cell. Thus, it was hypothesized that TDP1-depleted cells might be hypersensitive to NCS due to inaccurate DSB joining and consequent formation of lethal chromosome aberrations. Indeed, C-FISH experiments demonstrated a significant increase in the number of dicentric chromosomes upon TDP1 depletion suggesting that, in these cells, many 3'-phosphoglycolate DSBs are mis-joined. Conversely, in agreement with a DSB rejoining defect observed in the 53BP1 assay, Artemis-deficient cells showed an increase in the level of acentric chromosomal fragments, representing unjoined DSBs, but not in dicentrics. The increased incidence of dicentrics in TDP1-depleted cells is reminiscent of increased dicentrics observed in TDP1-mutant SCAN1 cells following treatment with CAL.

The conclusion that TDP1 is involved predominately in mis-joining is consistent with a recent study that demonstrated that TDP1 is required for efficient C-NHEJ in human cells (J. Li et al., 2017). In this study, a deficiency of TDP1 reduced the fidelity of end joining with an increase in insertions at repair junctions of I-SceI-induced DSBs, which could be completely restored by WT TDP1 but only partially by catalytically-inactive TDP1^{H263A}. These insertions at DSB sites could reflect mis-joining of persistent DSB ends to small pieces of unrelated DNA. Even in yeast, in the absence of TDP1, restriction enzyme-induced DSBs are inaccurately repaired with an increase in C-NHEJ-dependent insertions possibly via the mutagenic polymerase, Pol IV (Bahmed et al., 2010).

In contrast to the recent findings that TDP1 knockout in HEK293 cells caused a decrease in end joining efficiency of I-SceI induced-DSBs, results in the current study do not show a DSB rejoining defect in TDP1-depleted cells. Possible explanations for this discrepancy include the difference in the nature and the number of breaks as well as the use of different cellular systems. DSBs induced by I-SceI contain unmodified, 3'-hydroxyl ends compared to those induced by NCS. In the absence of TDP1, the terminal nucleoside on the restriction enzyme-induced DSB ends would not be removed leading to insertions by mutagenic polymerases decreasing the overall end joining efficiency. Conversely, the 3'-modification in NCS-induced DSBs precludes the activity of these polymerases averting aberrant insertions and thus may prevent a DSB rejoining defect. Moreover, the use of different cellular systems impedes direct comparison of the results between the two studies.

In the context of C-NHEJ, inhibition of DNA-PK blocks its auto-phosphorylation and prevents its inward translocation from DSB ends and thereby restricts access of other end-processing enzymes to the DSB end. The finding that DNA-PK inhibition rescues mis-joining in

TDP1-depleted cells (both shTDP1#18 and Artemis^{-/-}•shTDP1#2) to levels seen in TDP1-proficient cells suggests that a TDP1 deficiency renders the C-NHEJ pathway more error-prone, rather than invoking a separate backup pathway. Although Artemis-mediated resection-dependent C-NHEJ can cause translocations (Biehs et al., 2017), in the current study, dicentric chromosomes were still persistent in Artemis^{-/-}•shTDP1#2 cells, refuting the role of Artemis in this error-prone mis-joining. The Alternative end-joining protein, C-terminal interacting protein (CtIP) is another possible candidate mediating error-prone joining in the absence of TDP1. Indeed, CtIP functions in parallel to TDP1 for the repair of Top1-induced SSBs and methyl methane sulfonate (MMS)-induced lesions (Murai et al., 2012). Moreover, CtIP is phosphorylated by Polo-like kinase 3 (Plk3) and promotes ionizing radiation-induced chromosomal translocations (Barton et al., 2014; Makharashvili & Paull, 2015). Depletion of CtIP has also been shown to decrease translocations in mouse cells (Helmink et al., 2011). Plk3 is phosphorylated by ATM in response to DNA-damage which is abrogated by caffeine treatment (Bahassi et al., 2002). Although there is no evidence yet of CtIP being a target of DNA-PK and since ATM and DNA-PK have redundant functions, it remains to be investigated whether in the absence of ATM, DNA-PK can phosphorylate Plk3 which in turn would activate CtIP-mediated end resection promoting translocations. Then, inhibition of DNA-PK would reduce the translocations as observed in the current study. Taken together, our results indicate that TDP1 is required for accurate joining of DSB ends and, in its absence, a more error-prone DNA-PK-dependent process inaccurately repairs NCS-induced DSBs.

Another interesting finding from the current study was the effect of the absence of TDP1 and Artemis on cell cycle progression in the presence of 3'-phosphoglycolate-ended DSBs. It is quite surprising that the role of TDP1 in cell cycle regulation, or its lack thereof, has never been

published. A few studies have investigated the role of Artemis in cell cycle (Kurosawa & Adachi, 2010). Artemis is phosphorylated by ATM and in response to ionizing radiation, is needed for recovery from the G2/M cell cycle checkpoint by regulation of Cdk1-Cyclin B (Geng et al., 2007). Artemis was shown to be phosphorylated by ATR at Ser516 and Ser645 in response to replication stress leading to ubiquitination and degradation of cyclin E, thus promoting recovery from S-phase checkpoint (H. Wang et al., 2009). The finding that Artemis deficiency prolongs DSB-induced G1-arrest in HCT116 cells has been shown for the first time and was expected as in the absence of Artemis, cells with increased proportion of un-rejoined breaks would be prevented from entering S-phase. Surprisingly, additional depletion of TDP1 released this DSB-induced G1-block with higher percent of Artemis^{-/-}•shTDP1#2 cells in the S-phase compared to the Artemis^{-/-} single mutants. One hypothesis explaining this discrepancy is the possibility of TDP1 being important for the DSB-induced G1-S checkpoint. In that scenario, the G1-arrest brought about by Artemis deficiency would be abrogated by an additional depletion of TDP1 as it would prevent the checkpoint from functioning and cells with unrepaired breaks would progress through the cell cycle accumulating damage, ultimately showing decreased survival. It would be interesting in future to investigate whether this observation holds true and if yes, the potential implications of TDP1 being a part of the G1-S checkpoint in therapy.

Survival assays performed to investigate the relationship between TDP1 and Artemis with ATM strongly suggest that ATM is critical for the repair of 3'-phosphoglycolate DSBs as WT cells show enhanced sensitivity to NCS upon ATM inhibition. ATM and TDP1 appear to function in parallel pathways for the repair of 3'-phosphoglycolate DSBs since TDP1-depleted cells showed increased sensitivity to NCS upon ATM inhibition compared to ATM inhibition in WT cells. More interestingly, compared to ATM inhibition in WT, ATM inhibition in Artemis-deficient cells (Art-

/- single mutants and Artemis-/-shTDP1#2 double mutants) did not sensitize them further to low doses of NCS. One possible explanation for this discrepancy is that, at lower doses of NCS, in the absence of ATM, Artemis drives the repair of 3'-phosphoglycolate DSBs towards a TDP1-dependent repair pathway. In this way, a combined absence of ATM and TDP1 would make the cells more sensitive than the absence of the individual proteins as both TDP1-dependent and ATM-dependent repair of 3'-phosphoglycolate DSBs would be abolished. However, in the absence of Artemis, the drive towards TDP1-dependent repair would be lost, allowing 3'-phosphoglycolate DSB repair via a backup repair pathway. This backup process would then prevent Artemis deficiency upon ATM inhibition from being more deleterious than ATM inhibition alone at low doses of NCS.

In contrast to a previous report showing radiosensitization of HCT116 WT cells by a PARP inhibitor (Alotaibi et al., 2016), PARP1 inhibition did not sensitize these cells to NCS. This differential response could be attributed to the type of damage induced by the different agents. Since PARP1 is a key protein in base excision repair (BER), PARP1 inhibition upon IR, which forms DSBs to SSBs at a ratio of around 1:20 in addition to base damage, would cause accumulation of residual SSBs and damaged bases that upon replication would be converted to one-ended DSBs (Povirk, 1996). Due to the higher proportion of DSBs formed by NCS (DSB/SSB ratio ~1:5) and the absence of base damage, PARP1 inhibition is less likely to significantly sensitize the cells through interference with SSB repair. The inference that SSBs contribute little to NCS cytotoxicity, even in PARP1-inhibited cells, provides further support for the conclusion that the NCS sensitivity of shTDP1 knockdown cells reflects a role for TDP1 in DSB repair, not its well-documented role in SSB repair. However, the toxicity of 3'-phosphoglycolate DSBs in PARP1-inhibited cells was slightly enhanced by a deficiency of TDP1, Artemis and both. This

relationship between PARP1 and TDP1/Artemis is consistent with PARP1-mediated DSB repair (*i.e.*, alternative end-joining) acting as a backup for NHEJ in the absence of TDP1 or Artemis.

Since PNKP is capable of dephosphorylating a variety of single- and double-strand substrates including DSB ends (Weinfeld et al., 2011) and is recruited to DSB ends by the core NHEJ protein XRCC4 (Aceytuno et al., 2017), a role for PNKP in resolving 3'-phosphate termini of free radical-mediated DSBs is highly likely but has never been explicitly demonstrated. In order to assess the importance of this function for DSB repair by NHEJ and to examine the fate of 3'-phosphate-terminated DSBs in the absence of PNKP, the PNKP gene was disrupted in HCT116 and in HeLa cells using CRISPR/CAS9. This is the first study, to our knowledge, reporting the generation of human PNKP knockout cells and suggests that PNKP is not an essential gene.

Supporting established evidence in the role of PNKP in removing 3'-phosphates on DSBs, PNKP-deficient HCT116 and HeLa cells were hypersensitive to both NCS as well as radiation. However, compared to HeLa cells, deficiency of PNKP in HCT116 cells was significantly more deleterious in response to NCS. As has been mentioned before, HCT116 cells show decreased expression of Mre11 (Sacho & Maizels, 2011). For the repair of Top1-induced breaks, PNKP functions downstream of TDP1 whereas Mre11 function in parallel to this TDP1-PNKP dependent pathway. Thus, deletion of PNKP in these cells potentially abrogates both the pathways possibly leading to the increased sensitization of these cells. Although involvement of PNKP in NHEJ, as well as radiosensitivity of PNKP knockdown cells had been demonstrated previously, the heterogeneous nature of radiation damage, the high ratio of single-strand breaks to DSBs, and the involvement of PNKP in multiple repair pathways including SSB repair, complicates interpretation of radiosensitivity data. Because NCS induces a much higher proportion of DSBs and all NCS-

induced DSBs have at least one 3'-phosphate end, the finding that PNKP-deficient HCT116 cells are more sensitive to NCS than to radiation strengthens the implication of PNKP in NHEJ.

The hypersensitivity seen in PNKP-deficient cells correlates with an increased persistence and a delayed disappearance of 53BP1 foci, observed as DSB markers. Given the bifunctional nature of PNKP, it is unclear whether this DSB rejoining defect seen in PNKP-deficient cells is as a result of a loss of its phosphatase activity, its kinase activity or a combination of both. However, since NCS-induced DSBs predominantly bear 3'-phosphate groups, it can be inferred that the DSB rejoining defect is specifically due to the absence of the phosphatase activity. 5'-hydroxyl DSB ends are usually not produced by NCS (Povirk, 1996).

Survival experiments performed using DNA-PK inhibitor showed that at low concentrations, inhibition of DNA-PK further sensitized PNKP^{-/-} cells to NCS. This data suggests that, in NHEJ, in the absence of PNKP, a DNA-PK-dependent repair factor can function as backup for repairing 3'-phosphate-ended DSBs at low NCS doses. Biochemical experiments performed have also shown a clear removal of the 3'-phosphate on model DSB substrates even in the extracts of PNKP-deficient cells. The identity of this apparent phosphatase is yet unknown and some candidates include Ape1, Mre11, Artemis, Aprataxin and APLF. Mre11 and Artemis are both known to trim >1 nucleotides via endonucleolytic trimming and hence, are unlikely to perform the clean phosphatase function observed in biochemical assays (Povirk et al., 2007; Sacho & Maizels, 2011). Although Ape1 has a weak 3'-phosphatase function (Demple & Harrison, 1994), it has not been shown to act on 3'-overhangs (Suh, Wilson, & Povirk, 1997). Aprataxin is a good candidate that has been shown to possess a clean 3'-phosphatase function (Takahashi et al., 2007). It will be interesting to construct double-mutants of PNKP and Aprataxin to study the relationship between

these two phosphatases in response to NCS-mediated DNA damage. Moreover, it seems unlikely that a broad-specificity phosphatase is performing this function as it is regulated by DNA-PK.

6. CONCLUSIONS AND FUTURE PERSPECTIVES

In conclusion, observations from this dissertation suggest a strong epistasis between Artemis and TDP1 for survival against the toxicity of 3'-phosphoglycolate terminated DSBs induced by NCS and CAL. Importantly, however, although Artemis and TDP1 are involved in the same pathway, they perform non-overlapping functions and thereby, mediate survival through different mechanisms. Artemis promotes survival by promoting DSB rejoining, whereas TDP1 promotes the accurate joining of the DSB ends. The inaccurate joining of 3'-PG DSB ends is mediated by the classical Non-Homologous End Joining Pathway as a small molecule inhibitor of DNA-PKcs eliminated the TDP1-loss-dependent misjoining. With respect to the role of Artemis and TDP1 in cell cycle regulation, Artemis is needed for a recovery from G1 → S cell cycle checkpoint upon 3'-PG DSB induction. TDP1 is important for the G1 → S cell cycle checkpoint and thus, an additional loss of TDP1 rescues the delayed recovery observed in Artemis-deficient cells. PARP1 functions in parallel to both TDP1 and Artemis in repairing 3'-PG DSBs. The interplay between ATM, Artemis and TDP1 is dose dependent. In the absence of ATM, TDP1 is more important at low concentrations whereas Artemis is critical at higher concentrations.

Experiments performed in PNKP-deficient cells showed that PNKP is critical for the repair of 3'-phosphate-terminated DSBs. The increased cytotoxicity is represented by a lack of

3'-phosphate-DSB rejoining. PARP1-dependent repair is a subset of PNKP-dependent repair pathways. ATM and PNKP function in parallel for repairing 3'-phosphate-ended DSBs. Despite the importance of PNKP, in its absence, a backup repair factor functions in a DNA-PK-dependent manner at low levels of 3'-phosphate DSBs. However, higher levels of 3'-phosphate DSBs require PNKP as this factor gets saturated.

It is important to note that since HCT116 Artemis^{-/-}TDP1^{-/-} cells were not available for the major part of the study and have been recently generated, most of the studies reported in this dissertation involve the use of TDP1-depleted cells. It is critical to reproduce the observations using these double-knockout cells. The involvement of TDP1 in NHEJ can be further confirmed by generating Ligase IV^{-/-} TDP1^{-/-} double mutants and performing these experiments in them. These cells will also be critical in understanding the role of NHEJ in misjoining of DSBs in the absence of TDP1.

Although TDP1 and Artemis are epistatic, it is unclear what roles do these proteins play at these DSBs. Complementing the deficient cells with endonuclease-deficient Artemis/ phosphodiesterase-deficient TDP1 will provide insights into these questions. In addition, a ligation mediated PCR assay will be performed to track the processing of NCS-induced modified ends in these mutants. Another important experiment that would provide completeness to the study will be to investigate this interplay in normal cells as opposed to cancer cells. Along those lines, CJ179- hTert Artemis-deficient fibroblasts will be used to eliminate TDP1 and survival experiments will be performed to analyze whether the epistasis is prevalent in normal cells.

Genomic instability is a hallmark of tumorigenesis, but its excess can limit cell survival. The nearly pervasive involvement of TDP1/PNKP in DNA repair makes them an attractive element for tumor cell sensitization. Indeed, inhibitors of several DNA repair proteins have

dominated the limelight in relation to cancer chemotherapy and the work has led to the development of the principle of synthetic lethality – largely selective toxicity of an inhibitor against tumor cells deficient in parallel repair pathways that are otherwise functional in normal cells. However, attempts toward developing potent inhibitors of TDP1 have met with resistance as none of the inhibitors have shown cellular activity. Elucidation of regulation of TDP1/PNKP and its functional interaction with other DNA repair proteins will add to our understanding of the complex web of networks to which DNA repair pathways belong, with the ultimate aim of making it easier to develop DNA repair inhibitors, functioning either clinically or in research to unravel the myriad DSB repair mechanisms.

7. BIBLIOGRAPHY

- Abo, M. A., Sasanuma, H., Liu, X., Rajapakse, V. N., Huang, S., Kiselev, E., . . . Pommier, Y. (2017). TDP1 is critical for the repair of DNA breaks induced by sapacitabine, a nucleoside also targeting ATM- and BRCA-deficient tumors. *Molecular Cancer Therapeutics*, *16*(11), 2543-2551. doi:10.1158/1535-7163.MCT-17-0110
- Aceytuno, R. D., Piett, C. G., Havali-Shahriari, Z., Edwards, R. A., Rey, M., Ye, R., . . . Glover, J. N. M. (2017). Structural and functional characterization of the PNKP-XRCC4-LigIV DNA repair complex. *Nucleic Acids Research*, *45*(10), 6238-6251. doi:10.1093/nar/gkx275 [doi]
- Akopiants, K., Mohapatra, S., Menon, V., Zhou, T., Valerie, K., & Povirk, L. F. (2014). Tracking the processing of damaged DNA double-strand break ends by ligation-mediated PCR: Increased persistence of 3'-phosphoglycolate termini in SCAN1 cells. *Nucleic Acids Research*, *42*(5), 3125-3137. doi:10.1093/nar/gkt1347 [doi]
- Akopiants, K., Zhou, R. Z., Mohapatra, S., Valerie, K., Lees-Miller, S. P., Lee, K. J., . . . Povirk, L. F. (2009). Requirement for XLF/cernunnos in alignment-based gap filling by DNA

polymerases lambda and mu for nonhomologous end joining in human whole-cell extracts. *Nucleic Acids Research*, 37(12), 4055-4062. doi:10.1093/nar/gkp283 [doi]

Alagoz, M., Wells, O. S., & El-Khamisy, S. F. (2014). TDP1 deficiency sensitizes human cells to base damage via distinct topoisomerase I and PARP mechanisms with potential applications for cancer therapy. *Nucleic Acids Research*, 42(5), 3089-3103. doi:10.1093/nar/gkt1260 [doi]

Alotaibi, M., Sharma, K., Saleh, T., Povirk, L. F., Hendrickson, E. A., & Gewirtz, D. A. (2016). Radiosensitization by PARP inhibition in DNA repair proficient and deficient tumor cells: Proliferative recovery in senescent cells. *Radiation Research*, 185(3), 229-245. doi:10.1667/RR14202.1 [doi]

Ashley, A. K., & Kemp, C. J. (2018). DNA-PK, ATM, and ATR: PIKKing on p53. *Cell Cycle (Georgetown, Tex.)*, , 1-2. doi:10.1080/15384101.2017.1412147 [doi]

Ashour, M. E., Atteya, R., & El-Khamisy, S. F. (2015). Topoisomerase-mediated chromosomal break repair: An emerging player in many games. *Nature Reviews.Cancer*, 15(3), 137-151. doi:10.1038/nrc3892 [doi]

Audebert, M., Salles, B., & Calsou, P. (2004). Involvement of poly(ADP-ribose) polymerase-1 and XRCC1/DNA ligase III in an alternative route for DNA double-strand breaks rejoining. *The Journal of Biological Chemistry*, 279(53), 55117-55126. doi:M404524200 [pii]

- Audebert, M., Salles, B., Weinfeld, M., & Calsou, P. (2006). Involvement of polynucleotide kinase in a poly(ADP-ribose) polymerase-1-dependent DNA double-strand breaks rejoining pathway. *Journal of Molecular Biology*, *356*(2), 257-265. doi:S0022-2836(05)01414-2 [pii]
- Bahassi el, M., Conn, C. W., Myer, D. L., Hennigan, R. F., McGowan, C. H., Sanchez, Y., & Stambrook, P. J. (2002). Mammalian polo-like kinase 3 (Plk3) is a multifunctional protein involved in stress response pathways. *Oncogene*, *21*(43), 6633-6640.
doi:10.1038/sj.onc.1205850 [doi]
- Bahmed, K., Nitiss, K. C., & Nitiss, J. L. (2010). Yeast Tdp1 regulates the fidelity of nonhomologous end joining. *Proceedings of the National Academy of Sciences of the United States of America*, *107*(9), 4057-4062. doi:10.1073/pnas.09099171107 [doi]
- Barthelmes, H. U., Habermeyer, M., Christensen, M. O., Mielke, C., Interthal, H., Pouliot, J. J., . . . Marko, D. (2004). TDP1 overexpression in human cells counteracts DNA damage mediated by topoisomerases I and II. *The Journal of Biological Chemistry*, *279*(53), 55618-55625. doi:M405042200 [pii]
- Barton, O., Naumann, S. C., Diemer-Biehs, R., Kunzel, J., Steinlage, M., Conrad, S., . . . Lobrich, M. (2014). Polo-like kinase 3 regulates CtIP during DNA double-strand break repair in G1. *The Journal of Cell Biology*, *206*(7), 877-894. doi:10.1083/jcb.201401146 [doi]

- Batenchuk, C., Tepliakova, L., & Kaern, M. (2010). Identification of response-modulated genetic interactions by sensitivity-based epistatic analysis. *BMC Genomics*, *11*, 493-2164-11-493. doi:10.1186/1471-2164-11-493 [doi]
- Bayer, R. A., Gaynor, E. R., & Fisher, R. I. (1992). Bleomycin in non-hodgkin's lymphoma. *Seminars in Oncology*, *19*(2 Suppl 5), 46-52; discussion 52-3.
- Beucher, A., Birraux, J., Tchouandong, L., Barton, O., Shibata, A., Conrad, S., . . . Lobrich, M. (2009). ATM and artemis promote homologous recombination of radiation-induced DNA double-strand breaks in G2. *The EMBO Journal*, *28*(21), 3413-3427. doi:10.1038/emboj.2009.276 [doi]
- Biehs, R., Steinlage, M., Barton, O., Juhasz, S., Kunzel, J., Spies, J., . . . Lobrich, M. (2017). DNA double-strand break resection occurs during non-homologous end joining in G1 but is distinct from resection during homologous recombination. *Molecular Cell*, *65*(4), 671-684.e5. doi:S1097-2765(16)30854-1 [pii]
- Black, S. J., Kashkina, E., Kent, T., & Pomerantz, R. T. (2016). DNA polymerase theta: A unique multifunctional end-joining machine. *Genes*, *7*(9), 10.3390/genes7090067. doi:10.3390/genes7090067 [doi]

- Blackford, A. N., & Jackson, S. P. (2017). ATM, ATR, and DNA-PK: The trinity at the heart of the DNA damage response. *Molecular Cell*, *66*(6), 801-817. doi:S1097-2765(17)30354-4 [pii]
- Borda, M. A., Palmitelli, M., Veron, G., Gonzalez-Cid, M., & de Campos Nebel, M. (2015). Tyrosyl-DNA-phosphodiesterase I (TDP1) participates in the removal and repair of stabilized-Top2alpha cleavage complexes in human cells. *Mutation Research*, *781*, 37-48. doi:10.1016/j.mrfmmm.2015.09.003 [doi]
- Breslin, C., Mani, R. S., Fanta, M., Hoch, N., Weinfeld, M., & Caldecott, K. W. (2017). The Rev1 interacting region (RIR) motif in the scaffold protein XRCC1 mediates a low-affinity interaction with polynucleotide kinase/phosphatase (PNKP) during DNA single-strand break repair. *The Journal of Biological Chemistry*, *292*(39), 16024-16031. doi:10.1074/jbc.M117.806638 [doi]
- Budanov, A. V., Sablina, A. A., Feinstein, E., Koonin, E. V., & Chumakov, P. M. (2004). Regeneration of peroxiredoxins by p53-regulated sestrins, homologs of bacterial AhpD. *Science (New York, N.Y.)*, *304*(5670), 596-600. doi:10.1126/science.1095569 [doi]
- Bunting, S. F., Callen, E., Kozak, M. L., Kim, J. M., Wong, N., Lopez-Contreras, A. J., . . . Nussenzweig, A. (2012). BRCA1 functions independently of homologous recombination in DNA interstrand crosslink repair. *Molecular Cell*, *46*(2), 125-135. doi:10.1016/j.molcel.2012.02.015 [doi]

Burma, S., Chen, B. P., Murphy, M., Kurimasa, A., & Chen, D. J. (2001). ATM phosphorylates histone H2AX in response to DNA double-strand breaks. *The Journal of Biological Chemistry*, 276(45), 42462-42467. doi:10.1074/jbc.C100466200 [doi]

Callebaut, I., Moshous, D., Mornon, J. P., & de Villartay, J. P. (2002). Metallo-beta-lactamase fold within nucleic acids processing enzymes: The beta-CASP family. *Nucleic Acids Research*, 30(16), 3592-3601.

Campeau, E., Ruhl, V. E., Rodier, F., Smith, C. L., Rahmberg, B. L., Fuss, J. O., . . . Kaufman, P. D. (2009). A versatile viral system for expression and depletion of proteins in mammalian cells. *PloS One*, 4(8), e6529. doi:10.1371/journal.pone.0006529 [doi]

Cavazzana-Calvo, M., Le Deist, F., De Saint Basile, G., Papadopoulo, D., De Villartay, J. P., & Fischer, A. (1993). Increased radiosensitivity of granulocyte macrophage colony-forming units and skin fibroblasts in human autosomal recessive severe combined immunodeficiency. *The Journal of Clinical Investigation*, 91(3), 1214-1218. doi:10.1172/JCI116282 [doi]

Ceccaldi, R., Rondinelli, B., & D'Andrea, A. D. (2016). Repair pathway choices and consequences at the double-strand break. *Trends in Cell Biology*, 26(1), 52-64. doi:10.1016/j.tcb.2015.07.009 [doi]

Chang, H., H. Y., & Lieber, M., R. (2016). Structure-specific nuclease activities of artemis and the artemis: DNA-PKcs complex. *Nucleic Acids Research*, *44*(11), 4991-4997.

doi:10.1093/nar/gkw456 [doi]

Chang, H. H., Watanabe, G., & Lieber, M. R. (2015). Unifying the DNA end-processing roles of the artemis nuclease: Ku-dependent artemis resection at blunt DNA ends. *The Journal of Biological Chemistry*, *290*(40), 24036-24050. doi:10.1074/jbc.M115.680900 [doi]

Chang, H. H. Y., Pannunzio, N. R., Adachi, N., & Lieber, M. R. (2017). Non-homologous DNA end joining and alternative pathways to double-strand break repair. *Nature Reviews.Molecular Cell Biology*, *18*(8), 495-506. doi:10.1038/nrm.2017.48 [doi]

Chanut, P., Britton, S., Coates, J., Jackson, S. P., & Calsou, P. (2016). Coordinated nuclease activities counteract ku at single-ended DNA double-strand breaks. *Nature Communications*, *7*, 12889. doi:10.1038/ncomms12889 [doi]

Chapman, J. R., Taylor, M. R., & Boulton, S. J. (2012). Playing the end game: DNA double-strand break repair pathway choice. *Molecular Cell*, *47*(4), 497-510.

doi:10.1016/j.molcel.2012.07.029 [doi]

Chaudhry, M. A., Dedon, P. C., Wilson, D. M., 3rd, Demple, B., & Weinfeld, M. (1999). Removal by human apurinic/aprimidinic endonuclease 1 (ape 1) and escherichia coli exonuclease III of 3'-phosphoglycolates from DNA treated with neocarzinostatin,

calicheamicin, and gamma-radiation. *Biochemical Pharmacology*, 57(5), 531-538.
doi:S0006-2952(98)00327-X [pii]

Chen, B., Zhou, X., Taghizadeh, K., Chen, J., Stubbe, J., & Dedon, P. C. (2007). GC/MS methods to quantify the 2-deoxypentose-4-ulose and 3'-phosphoglycolate pathways of 4' oxidation of 2-deoxyribose in DNA: Application to DNA damage produced by gamma radiation and bleomycin. *Chemical Research in Toxicology*, 20(11), 1701-1708.
doi:10.1021/tx700164y [doi]

Chen, J., & Stubbe, J. (2005). Bleomycins: Towards better therapeutics. *Nature Reviews.Cancer*, 5(2), 102-112. doi:nrc1547 [pii]

Chiang, S. C., Carroll, J., & El-Khamisy, S. F. (2010). TDP1 serine 81 promotes interaction with DNA ligase IIIalpha and facilitates cell survival following DNA damage. *Cell Cycle (Georgetown, Tex.)*, 9(3), 588-595. doi:10598 [pii]

Chumakov, S. P., Kravchenko, J. E., Prassolov, V. S., Frolova, E. I., & Chumakov, P. M. (2010). Efficient downregulation of multiple mRNA targets with a single shRNA-expressing lentiviral vector. *Plasmid*, 63(3), 143-149. doi:10.1016/j.plasmid.2009.12.003 [doi]

Ciccia, A., & Elledge, S. J. (2010). The DNA damage response: Making it safe to play with knives. *Molecular Cell*, 40(2), 179-204. doi:10.1016/j.molcel.2010.09.019 [doi]

- Cristini, A., Park, J. H., Capranico, G., Legube, G., Favre, G., & Sordet, O. (2016). DNA-PK triggers histone ubiquitination and signaling in response to DNA double-strand breaks produced during the repair of transcription-blocking topoisomerase I lesions. *Nucleic Acids Research*, *44*(3), 1161-1178. doi:10.1093/nar/gkv1196 [doi]
- Das, B. B., Antony, S., Gupta, S., Dexheimer, T. S., Redon, C. E., Garfield, S., . . . Pommier, Y. (2009). Optimal function of the DNA repair enzyme TDP1 requires its phosphorylation by ATM and/or DNA-PK. *The EMBO Journal*, *28*(23), 3667-3680. doi:10.1038/emboj.2009.302 [doi]
- Das, B. B., Huang, S. Y., Murai, J., Rehman, I., Ame, J. C., Sengupta, S., . . . Pommier, Y. (2014). PARP1-TDP1 coupling for the repair of topoisomerase I-induced DNA damage. *Nucleic Acids Research*, *42*(7), 4435-4449. doi:10.1093/nar/gku088 [doi]
- Davies, D., Interthal, H., Champoux, J., & Hol, W. (2002). The crystal structure of human tyrosyl-DNA phosphodiesterase, Tdp1. *Structure*, *10*, 237-248.
- Davies, D. R., Interthal, H., Champoux, J. J., & Hol, W. G. (2003). Crystal structure of a transition state mimic for Tdp1 assembled from vanadate, DNA, and a topoisomerase I-derived peptide. *Chemistry & Biology*, *10*(2), 139-147. doi:S1074552103000218 [pii]
- Davis, A. J., Chen, B. P., & Chen, D. J. (2014). DNA-PK: A dynamic enzyme in a versatile DSB repair pathway. *DNA Repair*, *17*, 21-29. doi:10.1016/j.dnarep.2014.02.020 [doi]

- Davis, A. J., & Chen, D. J. (2013). DNA double strand break repair via non-homologous end-joining. *Translational Cancer Research*, 2(3), 130-143. doi:10.3978/j.issn.2218-676X.2013.04.02 [doi]
- Dedon, P. C., & Goldberg, I. H. (1992). Free-radical mechanisms involved in the formation of sequence-dependent bistranded DNA lesions by the antitumor antibiotics bleomycin, neocarzinostatin, and calicheamicin. *Chemical Research in Toxicology*, 5(3), 311-332.
- Demple, B., & Harrison, L. (1994). Repair of oxidative damage to DNA: Enzymology and biology. *Annual Review of Biochemistry*, 63, 915-948.
doi:10.1146/annurev.bi.63.070194.004411 [doi]
- Deriano, L., & Roth, D. B. (2013). Modernizing the nonhomologous end-joining repertoire: Alternative and classical NHEJ share the stage. *Annual Review of Genetics*, 47, 433-455.
doi:10.1146/annurev-genet-110711-155540 [doi]
- Dong, J., Ren, Y., Zhang, T., Wang, Z., Ling, C. C., Li, G. C., . . . Wen, B. (2018). Inactivation of DNA-PK by knockdown DNA-PKcs or NU7441 impairs non-homologous end-joining of radiation-induced double strand break repair. *Oncology Reports*, 39(3), 912-920.
doi:10.3892/or.2018.6217 [doi]

- Dong, J., Zhang, T., Ren, Y., Wang, Z., Ling, C. C., He, F., . . . Wen, B. (2017). Inhibiting DNA-PKcs in a non-homologous end-joining pathway in response to DNA double-strand breaks. *Oncotarget*, 8(14), 22662-22673. doi:10.18632/oncotarget.15153 [doi]
- Dumitrache, L. C., & McKinnon, P. J. (2017). Polynucleotide kinase-phosphatase (PNKP) mutations and neurologic disease. *Mechanisms of Ageing and Development*, 161(Pt A), 121-129. doi:S0047-6374(16)30051-3 [pii]
- Einhorn, L. H. (2002). Curing metastatic testicular cancer. *Proceedings of the National Academy of Sciences of the United States of America*, 99(7), 4592-4595. doi:10.1073/pnas.072067999 [doi]
- El-Khamisy, S. F., Hartsuiker, E., & Caldecott, K. W. (2007). TDP1 facilitates repair of ionizing radiation-induced DNA single-strand breaks. *DNA Repair*, 6(10), 1485-1495. doi:S1568-7864(07)00179-6 [pii]
- El-Khamisy, S. F., Saifi, G. M., Weinfeld, M., Johansson, F., Helleday, T., Lupski, J. R., & Caldecott, K. W. (2005). Defective DNA single-strand break repair in spinocerebellar ataxia with axonal neuropathy-1. *Nature*, 434(7029), 108-113. doi:nature03314 [pii]
- Escribano-Diaz, C., Orthwein, A., Fradet-Turcotte, A., Xing, M., Young, J. T., Tkac, J., . . . Durocher, D. (2013). A cell cycle-dependent regulatory circuit composed of 53BP1-RIF1

and BRCA1-CtIP controls DNA repair pathway choice. *Molecular Cell*, 49(5), 872-883.
doi:10.1016/j.molcel.2013.01.001 [doi]

Feng, L., & Chen, J. (2012). The E3 ligase RNF8 regulates KU80 removal and NHEJ repair. *Nature Structural & Molecular Biology*, 19(2), 201-206. doi:10.1038/nsmb.2211 [doi]

Freschauf, G. K., Karimi-Busheri, F., Ulaczyk-Lesanko, A., Mereniuk, T. R., Ahrens, A., Koshy, J. M., . . . Weinfeld, M. (2009). Identification of a small molecule inhibitor of the human DNA repair enzyme polynucleotide kinase/phosphatase. *Cancer Research*, 69(19), 7739-7746. doi:10.1158/0008-5472.CAN-09-1805 [doi]

Friedberg, E. C. (2008). A brief history of the DNA repair field. *Cell Research*, 18(1), 3-7.
doi:cr2007113 [pii]

Friedberg, E. C. (2015). A history of the DNA repair and mutagenesis field: I. the discovery of enzymatic photoreactivation. *DNA Repair*, 33, 35-42. doi:10.1016/j.dnarep.2015.06.007 [doi]

Gao, R., Das, B. B., Chatterjee, R., Abaan, O. D., Agama, K., Matuo, R., . . . Pommier, Y. (2014). Epigenetic and genetic inactivation of tyrosyl-DNA-phosphodiesterase 1 (TDP1) in human lung cancer cells from the NCI-60 panel. *DNA Repair*, 13, 1-9.
doi:10.1016/j.dnarep.2013.09.001 [doi]

- Geng, L., Zhang, X., Zheng, S., & Legerski, R. J. (2007). Artemis links ATM to G2/M checkpoint recovery via regulation of Cdk1-cyclin B. *Molecular and Cellular Biology*, 27(7), 2625-2635. doi:MCB.02072-06 [pii]
- Glassner, B. J., & Mortimer, R. K. (1994). Synergistic interactions between RAD5, RAD16 and RAD54, three partially homologous yeast DNA repair genes each in a different repair pathway. *Radiation Research*, 139(1), 24-33.
- Gottlin, E. B., Rudolph, A. E., Zhao, Y., Matthews, H. R., & Dixon, J. E. (1998). Catalytic mechanism of the phospholipase D superfamily proceeds via a covalent phosphohistidine intermediate. *Proceedings of the National Academy of Sciences of the United States of America*, 95(16), 9202-9207.
- Hammel, M., Yu, Y., Radhakrishnan, S. K., Chokshi, C., Tsai, M. S., Matsumoto, Y., . . . Tainer, J. A. (2016). An intrinsically disordered APLF links ku, DNA-PKcs, and XRCC4-DNA ligase IV in an extended flexible non-homologous end joining complex. *The Journal of Biological Chemistry*, 291(53), 26987-27006. doi:10.1074/jbc.M116.751867 [doi]
- Hanzlikova, H., Gittens, W., Krejcikova, K., Zeng, Z., & Caldecott, K. W. (2017). Overlapping roles for PARP1 and PARP2 in the recruitment of endogenous XRCC1 and PNKP into oxidized chromatin. *Nucleic Acids Research*, 45(5), 2546-2557. doi:10.1093/nar/gkw1246 [doi]

- Hawkins, A. J., Subler, M. A., Akopiants, K., Wiley, J. L., Taylor, S. M., Rice, A. C., . . . Povirk, L. F. (2009). In vitro complementation of Tdp1 deficiency indicates a stabilized enzyme-DNA adduct from tyrosyl but not glycolate lesions as a consequence of the SCAN1 mutation. *DNA Repair*, 8(5), 654-663. doi:<https://doi.org/10.1016/j.dnarep.2008.12.012>
- Helmink, B. A., Tubbs, A. T., Dorsett, Y., Bednarski, J. J., Walker, L. M., Feng, Z., . . . Sleckman, B. P. (2011). H2AX prevents CtIP-mediated DNA end resection and aberrant repair in G1-phase lymphocytes. *Nature*, 469(7329), 245-249. doi:10.1038/nature09585 [doi]
- Heo, J., Li, J., Summerlin, M., Hays, A., Katyal, S., McKinnon, P. J., . . . Hanakahi, L. A. (2015). TDP1 promotes assembly of non-homologous end joining protein complexes on DNA. *DNA Repair*, 30, 28-37. doi:10.1016/j.dnarep.2015.03.003 [doi]
- Hohegger, H., Dejsuphong, D., Fukushima, T., Morrison, C., Sonoda, E., Schreiber, V., . . . Takeda, S. (2006). Parp-1 protects homologous recombination from interference by ku and ligase IV in vertebrate cells. *The EMBO Journal*, 25(6), 1305-1314. doi:7601015 [pii]
- Huang, S. Y., Murai, J., Dalla Rosa, I., Dexheimer, T. S., Naumova, A., Gmeiner, W. H., & Pommier, Y. (2013). TDP1 repairs nuclear and mitochondrial DNA damage induced by chain-terminating anticancer and antiviral nucleoside analogs. *Nucleic Acids Research*, 41(16), 7793-7803. doi:10.1093/nar/gkt483 [doi]

- Inamdar, K. V., Pouliot, J. J., Zhou, T., Lees-Miller, S. P., Rasouli-Nia, A., & Povirk, L. F. (2002). Conversion of phosphoglycolate to phosphate termini on 3' overhangs of DNA double strand breaks by the human tyrosyl-DNA phosphodiesterase hTdp1. *The Journal of Biological Chemistry*, 277(30), 27162-27168. doi:10.1074/jbc.M204688200 [doi]
- Interthal, H., Pouliot, J., & Champoux, J. (2001). The tyrosyl-DNA phosphodiesterase Tdp1 is a member of the phospholipase D superfamily. *Pnas*, 98(21), 12009-12014.
- Interthal, H., Chen, H. J., & Champoux, J. J. (2005). Human Tdp1 cleaves a broad spectrum of substrates, including phosphoamide linkages. *The Journal of Biological Chemistry*, 280(43), 36518-36528. doi:M508898200 [pii]
- Interthal, H., Chen, H. J., Kehl-Fie, T. E., Zotzmann, J., Leppard, J. B., & Champoux, J. J. (2005). SCAN1 mutant Tdp1 accumulates the enzyme--DNA intermediate and causes camptothecin hypersensitivity. *The EMBO Journal*, 24(12), 2224-2233. doi:7600694 [pii]
- Ishii, C., & Inoue, H. (1989). Epistasis, photoreactivation and mutagen sensitivity of DNA repair mutants upr-1 and mus-26 in neurospora crassa. *Mutation Research*, 218(2), 95-103. doi:0921-8777(89)90015-3 [pii]
- Jeggo, P. A., & Lobrich, M. (2005). Artemis links ATM to double strand break rejoining. *Cell Cycle (Georgetown, Tex.)*, 4(3), 359-362. doi:1527 [pii]

- Jensen, R. B., Ozes, A., Kim, T., Estep, A., & Kowalczykowski, S. C. (2013). BRCA2 is epistatic to the RAD51 paralogs in response to DNA damage. *DNA Repair*, 12(4), 306-311. doi:10.1016/j.dnarep.2012.12.007 [doi]
- Jette, N., & Lees-Miller, S. P. (2015). The DNA-dependent protein kinase: A multifunctional protein kinase with roles in DNA double strand break repair and mitosis. *Progress in Biophysics and Molecular Biology*, 117(2-3), 194-205. doi:10.1016/j.pbiomolbio.2014.12.003 [doi]
- Jilani, A., Ramotar, D., Slack, C., Ong, C., Yang, X. M., Scherer, S. W., & Lasko, D. D. (1999). Molecular cloning of the human gene, PNKP, encoding a polynucleotide kinase 3'-phosphatase and evidence for its role in repair of DNA strand breaks caused by oxidative damage. *The Journal of Biological Chemistry*, 274(34), 24176-24186.
- Karimi-Busheri, F., Rasouli-Nia, A., Allalunis-Turner, J., & Weinfeld, M. (2007). Human polynucleotide kinase participates in repair of DNA double-strand breaks by nonhomologous end joining but not homologous recombination. *Cancer Research*, 67(14), 6619-6625. doi:67/14/6619 [pii]
- Kawale, A.,S., & Povirk, L.,F. (2018). Tyrosyl-DNA phosphodiesterases: Rescuing the genome from the risks of relaxation. *Nucleic Acids Res.*, 46(2), 520-537. doi:10.1093/nar/gkx1219 [doi]

- Kocher, S., Rieckmann, T., Rohaly, G., Mansour, W. Y., Dikomey, E., Dornreiter, I., & Dahm-Daphi, J. (2012). Radiation-induced double-strand breaks require ATM but not artemis for homologous recombination during S-phase. *Nucleic Acids Research*, *40*(17), 8336-8347. doi:gks604 [pii]
- Krejci, Lumir, Altmannova, Veronika, Spirek, Mario, & Zhao, Xiaolan. (2012). Homologous recombination and its regulation. *Nucleic Acids Research*, *40*(13), 5795-5818. doi:10.1093/nar/gks270 [doi]
- Kurosawa, A., & Adachi, N. (2010). Functions and regulation of artemis: A goddess in the maintenance of genome integrity. *Journal of Radiation Research*, *51*(5), 503-509. doi:JST.JSTAGE/jrr/10017 [pii]
- Lee, S. E., Mitchell, R. A., Cheng, A., & Hendrickson, E. A. (1997). Evidence for DNA-PK-dependent and -independent DNA double-strand break repair pathways in mammalian cells as a function of the cell cycle. *Molecular and Cellular Biology*, *17*(3), 1425-1433.
- Lee, S. H., & Kim, C. H. (2002). DNA-dependent protein kinase complex: A multifunctional protein in DNA repair and damage checkpoint. *Molecules and Cells*, *13*(2), 159-166.
- Li, J., Summerlin, M., Nitiss, K. C., Nitiss, J. L., & Hanakahi, L. A. (2017). TDP1 is required for efficient non-homologous end joining in human cells. *DNA Repair*, *60*(Supplement C), 40-49. doi:<https://doi.org/10.1016/j.dnarep.2017.10.003>

Li, L., Moshous, D., Zhou, Y., Wang, J., Xie, G., Salido, E., . . . Cowan, M. J. (2002). A founder mutation in artemis, an SNM1-like protein, causes SCID in athabaskan-speaking native americans. *Journal of Immunology (Baltimore, Md.: 1950)*, *168*(12), 6323-6329.

Lieber, M. R. (2010). The mechanism of double-strand DNA break repair by the nonhomologous DNA end-joining pathway. *Annual Review of Biochemistry*, *79*, 181-211.

doi:10.1146/annurev.biochem.052308.093131 [doi]

Lieber, M. R., Ma, Y., Pannicke, U., & Schwarz, K. (2003). Mechanism and regulation of human non-homologous DNA end-joining. *Nature Reviews.Molecular Cell Biology*, *4*(9), 712-720.

doi:10.1038/nrm1202 [doi]

Liu,Chao, Vyas,Aditi, Kassab, M.,A., Singh, A.,K., & Yu,Xiaochun. (2017). The role of poly ADP-ribosylation in the first wave of DNA damage response. *Nucleic Acids Research*, *45*(14), 8129-8141. doi:10.1093/nar/gkx565 [doi]

Lobrich, M., & Jeggo, P. (2017). A process of resection-dependent nonhomologous end joining involving the goddess artemis. *Trends in Biochemical Sciences*, *42*(9), 690-701. doi:S0968-0004(17)30129-9 [pii]

Ma, Y., Schwarz, K., & Lieber, M. R. (2005). The artemis:DNA-PKcs endonuclease cleaves DNA loops, flaps, and gaps. *DNA Repair*, *4*(7), 845-851. doi:S1568-7864(05)00097-2 [pii]

Ma, Y., Pannicke, U., Schwarz, K., & Lieber, M. R. (2002). Hairpin opening and overhang processing by an artemis/DNA-dependent protein kinase complex in nonhomologous end joining and V(D)J recombination. *Cell*, *108*(6), 781-794. doi:[https://doi.org/10.1016/S0092-8674\(02\)00671-2](https://doi.org/10.1016/S0092-8674(02)00671-2)

Makharashvili, N., & Paull, T. T. (2015). CtIP: A DNA damage response protein at the intersection of DNA metabolism. *DNA Repair*, *32*, 75-81.
doi:<https://doi.org/10.1016/j.dnarep.2015.04.016>

Mali, P., Yang, L., Esvelt, K. M., Aach, J., Guell, M., DiCarlo, J. E., . . . Church, G. M. (2013). RNA-guided human genome engineering via Cas9. *Science (New York, N.Y.)*, *339*(6121), 823-826. doi:10.1126/science.1232033 [doi]

Mansour, W.,Y., Rhein,Tim, & Dahm-Daphi,Jochen. (2010). The alternative end-joining pathway for repair of DNA double-strand breaks requires PARP1 but is not dependent upon microhomologies. *Nucleic Acids Research*, *38*(18), 6065-6077. doi:10.1093/nar/gkq387 [doi]

Meisenberg, C., Gilbert, D. C., Chalmers, A., Haley, V., Gollins, S., Ward, S. E., & El-Khamisy, S. F. (2015). Clinical and cellular roles for TDP1 and TOP1 in modulating colorectal cancer response to irinotecan. *Molecular Cancer Therapeutics*, *14*(2), 575-585. doi:10.1158/1535-7163.MCT-14-0762 [doi]

- Menon, V., & Povirk, L. F. (2016). End-processing nucleases and phosphodiesterases: An elite supporting cast for the non-homologous end joining pathway of DNA double-strand break repair. *DNA Repair*, *43*, 57-68. doi:10.1016/j.dnarep.2016.05.011 [doi]
- Menon, V., & Povirk, L. F. (2017). XLF/cernunnos: An important but puzzling participant in the nonhomologous end joining DNA repair pathway. *DNA Repair*, *58*, 29-37. doi:S1568-7864(17)30173-8 [pii]
- Miao, Z. H., Agama, K., Sordet, O., Povirk, L., Kohn, K. W., & Pommier, Y. (2006). Hereditary ataxia SCAN1 cells are defective for the repair of transcription-dependent topoisomerase I cleavage complexes. *DNA Repair*, *5*(12), 1489-1494. doi:S1568-7864(06)00238-2 [pii]
- Mitelman, F., Johansson, B., & Mertens, F. (2007). The impact of translocations and gene fusions on cancer causation. *Nature Reviews.Cancer*, *7*(4), 233-245. doi:nrc2091 [pii]
- Mohapatra, S., Kawahara, M., Khan, I.,S., Yannone, S.,M., & Povirk, L.,F. (2011). Restoration of G1 chemo/radioresistance and double-strand-break repair proficiency by wild-type but not endonuclease-deficient artemis. *Nucleic Acids Research*, *39*(15), 6500-6510. doi:10.1093/nar/gkr257 [doi]
- Morales, J., Li, L., Fattah, F. J., Dong, Y., Bey, E. A., Patel, M., . . . Boothman, D. A. (2014). Review of poly (ADP-ribose) polymerase (PARP) mechanisms of action and rationale for

targeting in cancer and other diseases. *Critical Reviews in Eukaryotic Gene Expression*, 24(1), 15-28. doi:75feda1245856cd3,6aafae363655cefb [pii]

Moshous, D., Callebaut, I., de Chasseval, R., Corneo, B., Cavazzana-Calvo, M., Le Deist, F., . . . de Villartay, J. P. (2001). Artemis, a novel DNA double-strand break repair/V(D)J recombination protein, is mutated in human severe combined immune deficiency. *Cell*, 105(2), 177-186. doi:S0092-8674(01)00309-9 [pii]

Murai, J., Huang, S. N., Das, B. B., Dexheimer, T. S., Takeda, S., & Pommier, Y. (2012). Tyrosyl-DNA phosphodiesterase 1 (TDP1) repairs DNA damage induced by topoisomerases I and II and base alkylation in vertebrate cells. *The Journal of Biological Chemistry*, 287(16), 12848-12857. doi:M111.333963 [pii]

Nicolas, N., Moshous, D., Cavazzana-Calvo, M., Papadopoulo, D., de Chasseval, R., Le Deist, F., . . . de Villartay, J. P. (1998). A human severe combined immunodeficiency (SCID) condition with increased sensitivity to ionizing radiations and impaired V(D)J rearrangements defines a new DNA recombination/repair deficiency. *The Journal of Experimental Medicine*, 188(4), 627-634.

Niewolik, D., Pannicke, U., Lu, H., Ma, Y., Wang, L. C., Kulesza, P., . . . Schwarz, K. (2006). DNA-PKcs dependence of artemis endonucleolytic activity, differences between hairpins and 5' or 3' overhangs. *The Journal of Biological Chemistry*, 281(45), 33900-33909. doi:M606023200 [pii]

- Niewolik, D., Peter, I., Butscher, C., & Schwarz, K. (2017). Autoinhibition of the nuclease ARTEMIS is mediated by a physical interaction between its catalytic and C-terminal domains. *The Journal of Biological Chemistry*, 292(8), 3351-3365. doi:10.1074/jbc.M116.770461 [doi]
- O'Connor, M. J. (2015). Targeting the DNA damage response in cancer. *Molecular Cell*, 60(4), 547-560. doi:10.1016/j.molcel.2015.10.040 [doi]
- Panier, S., & Boulton, S. J. (2014). Double-strand break repair: 53BP1 comes into focus. *Nature Reviews.Molecular Cell Biology*, 15(1), 7-18. doi:10.1038/nrm3719 [doi]
- Pannicke, U., Ma, Y., Hopfner, K. P., Niewolik, D., Lieber, M. R., & Schwarz, K. (2004). Functional and biochemical dissection of the structure-specific nuclease ARTEMIS. *The EMBO Journal*, 23(9), 1987-1997. doi:10.1038/sj.emboj.7600206 [doi]
- Patel, A. G., Sarkaria, J. N., & Kaufmann, S. H. (2011). Nonhomologous end joining drives poly(ADP-ribose) polymerase (PARP) inhibitor lethality in homologous recombination-deficient cells. *Proceedings of the National Academy of Sciences of the United States of America*, 108(8), 3406-3411. doi:10.1073/pnas.1013715108 [doi]
- Paull, T. T. (2015). Mechanisms of ATM activation. *Annual Review of Biochemistry*, 84, 711-738. doi:10.1146/annurev-biochem-060614-034335 [doi]

- Petrini, J. H., Bressan, D. A., & Yao, M. S. (1997). The RAD52 epistasis group in mammalian double strand break repair. *Seminars in Immunology*, *9*(3), 181-188. doi:S1044-5323(97)90067-1 [pii]
- Pheiffer, B. H., & Zimmerman, S. B. (1982). 3'-phosphatase activity of the DNA kinase from rat liver. *Biochemical and Biophysical Research Communications*, *109*(4), 1297-1302. doi:0006-291X(82)91918-0 [pii]
- Plo, I., Liao, Z. Y., Barcelo, J. M., Kohlhagen, G., Caldecott, K. W., Weinfeld, M., & Pommier, Y. (2003). Association of XRCC1 and tyrosyl DNA phosphodiesterase (Tdp1) for the repair of topoisomerase I-mediated DNA lesions. *DNA Repair*, *2*(10), 1087-1100. doi:S1568786403001162 [pii]
- Pommier, Y. (2013). Drugging topoisomerases: Lessons and challenges. *ACS Chemical Biology*, *8*(1), 82-95. doi:10.1021/cb300648v [doi]
- Pommier, Y., Huang, S. Y., Gao, R., Das, B. B., Murai, J., & Marchand, C. (2014). Tyrosyl-DNA-phosphodiesterases (TDP1 and TDP2). *DNA Repair*, *19*, 114-129. doi:10.1016/j.dnarep.2014.03.020 [doi]
- Postow, L., & Funabiki, H. (2013). An SCF complex containing Fbx12 mediates DNA damage-induced Ku80 ubiquitylation. *Cell Cycle (Georgetown, Tex.)*, *12*(4), 587-595. doi:10.4161/cc.23408 [doi]

Pouliot, J. J., Yao, K. C., Robertson, C. A., & Nash, H. A. (1999). Yeast gene for a tyr-DNA phosphodiesterase that repairs topoisomerase I complexes. *Science (New York, N.Y.)*, 286(5439), 552-555. doi:7897 [pii]

Povirk, L. F. (1996). DNA damage and mutagenesis by radiomimetic DNA-cleaving agents: Bleomycin, neocarzinostatin and other enediynes. *Mutation Research*, 355(1-2), 71-89. doi:0027-5107(96)00023-1 [pii]

Povirk, L. F. (2012). Processing of damaged DNA ends for double-strand break repair in mammalian cells. *ISRN Molecular Biology*, 2012, 10.5402/2012/345805. doi:10.5402/2012/345805 [doi]

Povirk, L. F., Zhou, T., Zhou, R., Cowan, M. J., & Yannone, S. M. (2007). Processing of 3'-phosphoglycolate-terminated DNA double strand breaks by artemis nuclease. *Journal of Biological Chemistry*, 282(6), 3547-3558. doi:10.1074/jbc.M607745200

Price, B. D., & D'Andrea, A. D. (2013). Chromatin remodeling at DNA double-strand breaks. *Cell*, 152(6), 1344-1354. doi:10.1016/j.cell.2013.02.011 [doi]

Rasouli-Nia, A., Karimi-Busheri, F., & Weinfeld, M. (2004). Stable down-regulation of human polynucleotide kinase enhances spontaneous mutation frequency and sensitizes cells to genotoxic agents. *Proceedings of the National Academy of Sciences of the United States of America*, 101(18), 6905-6910. doi:10.1073/pnas.0400099101 [doi]

- Riballo, E., Kuhne, M., Rief, N., Doherty, A., Smith, G. C., Recio, M. J., . . . Lobrich, M. (2004). A pathway of double-strand break rejoining dependent upon ATM, artemis, and proteins locating to gamma-H2AX foci. *Molecular Cell*, *16*(5), 715-724. doi:S1097-2765(04)00654-9 [pii]
- Rogakou, E. P., Pilch, D. R., Orr, A. H., Ivanova, V. S., & Bonner, W. M. (1998). DNA double-stranded breaks induce histone H2AX phosphorylation on serine 139. *The Journal of Biological Chemistry*, *273*(10), 5858-5868.
- Roth, D. B. (2014). V(D)J recombination: Mechanism, errors, and fidelity. *Microbiology Spectrum*, *2*(6), 10.1128/microbiolspec.MDNA3-0041-2014. doi:10.1128/microbiolspec.MDNA3-0041-2014 [doi]
- Rouleau, M., Patel, A., Hendzel, M. J., Kaufmann, S. H., & Poirier, G. G. (2010). PARP inhibition: PARP1 and beyond. *Nature Reviews.Cancer*, *10*(4), 293-301. doi:10.1038/nrc2812 [doi]
- Sacho, E. J., & Maizels, N. (2011). DNA repair factor MRE11/RAD50 cleaves 3'-phosphotyrosyl bonds and resects DNA to repair damage caused by topoisomerase 1 poisons. *The Journal of Biological Chemistry*, *286*(52), 44945-44951. doi:10.1074/jbc.M111.299347 [doi]

Schorl, C., & Sedivy, J. M. (2007). Analysis of cell cycle phases and progression in cultured mammalian cells. *Methods (San Diego, Calif.)*, *41*(2), 143-150. doi:S1046-2023(06)00171-X [pii]

Schwarz, K., Gauss, G. H., Ludwig, L., Pannicke, U., Li, Z., Lindner, D., . . . Bartram, C. R. (1996). RAG mutations in human B cell-negative SCID. *Science (New York, N.Y.)*, *274*(5284), 97-99.

Segal-Raz, H., Mass, G., Baranes-Bachar, K., Lerenthal, Y., Wang, S. Y., Chung, Y. M., . . . Shiloh, Y. (2011). ATM-mediated phosphorylation of polynucleotide kinase/phosphatase is required for effective DNA double-strand break repair. *EMBO Reports*, *12*(7), 713-719. doi:10.1038/embor.2011.96 [doi]

Shelton, J. W., Waxweiler, T. V., Landry, J., Gao, H., Xu, Y., Wang, L., . . . Shu, H. K. (2013). In vitro and in vivo enhancement of chemoradiation using the oral PARP inhibitor ABT-888 in colorectal cancer cells. *International Journal of Radiation Oncology, Biology, Physics*, *86*(3), 469-476. doi:10.1016/j.ijrobp.2013.02.015 [doi]

Sishc, B. J., & Davis, A. J. (2017). The role of the core non-homologous end joining factors in carcinogenesis and cancer. *Cancers*, *9*(7), 10.3390/cancers9070081. doi:E81 [pii]

- Staples, C. J., Barone, G., Myers, K. N., Ganesh, A., Gibbs-Seymour, I., Patil, A. A., . . . Collis, S. J. (2016). MRNIP/C5orf45 interacts with the MRN complex and contributes to the DNA damage response. *Cell Reports*, *16*(10), 2565-2575. doi:S2211-1247(16)31050-6 [pii]
- Suh, D., Wilson, D. M., & Povirk, L. F. (1997). 3'-phosphodiesterase activity of human apurinic/aprimidinic endonuclease at DNA double-strand break ends. *Nucleic Acids Research*, *25*(12), 2495-2500.
- Sulli, G., Di Micco, R., & d'Adda di Fagagna, F. (2012). Crosstalk between chromatin state and DNA damage response in cellular senescence and cancer. *Nature Reviews.Cancer*, *12*(10), 709-720. doi:10.1038/nrc3344 [doi]
- Symington, L. S. (2002). Role of RAD52 epistasis group genes in homologous recombination and double-strand break repair. *Microbiology and Molecular Biology Reviews : MMBR*, *66*(4), 630-70, table of contents.
- Tada, K., Kobayashi, M., Takiuchi, Y., Iwai, F., Sakamoto, T., Nagata, K., . . . Takaori-Kondo, A. (2015). Abacavir, an anti-HIV-1 drug, targets TDP1-deficient adult T cell leukemia. *Science Advances*, *1*(3), e1400203. doi:10.1126/sciadv.1400203 [doi]
- Takahashi, T., Tada, M., Igarashi, S., Koyama, A., Date, H., Yokoseki, A., . . . Onodera, O. (2007). Aprataxin, causative gene product for EAOH/AOA1, repairs DNA single-strand

- breaks with damaged 3'-phosphate and 3'-phosphoglycolate ends. *Nucleic Acids Research*, 35(11), 3797-3809. doi:gkm158 [pii]
- Takashima, H., Boerkoel, C., John, J., Saifi, G. M., Salih, M., Armstrong, D., . . . Lupski, J. (2002). Mutation of *TDPI*, encoding a topoisomerase i-dependent DNA damage repair enzyme, in spinocerebellar ataxia with axonal neuropathy. *Nat Genet.*, 32, 267-272.
- Takemura, H., Rao, V. A., Sordet, O., Furuta, T., Miao, Z. H., Meng, L., . . . Pommier, Y. (2006). Defective Mre11-dependent activation of Chk2 by ataxia telangiectasia mutated in colorectal carcinoma cells in response to replication-dependent DNA double strand breaks. *The Journal of Biological Chemistry*, 281(41), 30814-30823. doi:M603747200 [pii]
- Tarsounas, M., Davies, D., & West, S. C. (2003). BRCA2-dependent and independent formation of RAD51 nuclear foci. *Oncogene*, 22(8), 1115-1123. doi:10.1038/sj.onc.1206263 [doi]
- Tomkinson, A. E., & Sallmyr, A. (2013). Structure and function of the DNA ligases encoded by the mammalian LIG3 gene. *Gene*, 531(2), 150-157. doi:10.1016/j.gene.2013.08.061 [doi]
- Uematsu, N., Weterings, E., Yano, K., Morotomi-Yano, K., Jakob, B., Taucher-Scholz, G., . . . Chen, D. J. (2007). Autophosphorylation of DNA-PKCS regulates its dynamics at DNA double-strand breaks. *The Journal of Cell Biology*, 177(2), 219-229. doi:jcb.200608077 [pii]
- Umezawa, H., Maeda, K., Takeuchi, T., & Okami, Y. (1966). New antibiotics, bleomycin A and B. *The Journal of Antibiotics*, 19(5), 200-209.

- Valerie, K., & Povirk, L. F. (2003). Regulation and mechanisms of mammalian double-strand break repair. *Oncogene*, 22(37), 5792-5812. doi:10.1038/sj.onc.1206679 [doi]
- Wang, H., Zhang, X., Geng, L., Teng, L., & Legerski, R. J. (2009). Artemis regulates cell cycle recovery from the S phase checkpoint by promoting degradation of cyclin E. *The Journal of Biological Chemistry*, 284(27), 18236-18243. doi:10.1074/jbc.M109.002584 [doi]
- Wang, J., Aroumougame, A., Loblrich, M., Li, Y., Chen, D., Chen, J., & Gong, Z. (2014). PTIP associates with artemis to dictate DNA repair pathway choice. *Genes & Development*, 28(24), 2693-2698. doi:10.1101/gad.252478.114 [doi]
- WATSON, J. D., & CRICK, F. H. (1953). Molecular structure of nucleic acids; a structure for deoxyribose nucleic acid. *Nature*, 171(4356), 737-738.
- Weinfeld, M., Mani, R. S., Abdou, I., Aceytuno, R. D., & Glover, J. N. (2011). Tidying up loose ends: The role of polynucleotide kinase/phosphatase in DNA strand break repair. *Trends in Biochemical Sciences*, 36(5), 262-271. doi:10.1016/j.tibs.2011.01.006 [doi]
- Wood, R. D., & Doublet, S. (2016). DNA polymerase theta (POLQ), double-strand break repair, and cancer. *DNA Repair*, 44, 22-32. doi:S1568-7864(16)30081-7 [pii]
- Yang, S. W., Burgin, A. B., Jr, Huizenga, B. N., Robertson, C. A., Yao, K. C., & Nash, H. A. (1996). A eukaryotic enzyme that can disjoin dead-end covalent complexes between DNA

and type I topoisomerases. *Proceedings of the National Academy of Sciences of the United States of America*, 93(21), 11534-11539.

Zhou, T., Lee, J. W., Tatavarthi, H., Lupski, J. R., Valerie, K., & Povirk, L. F. (2005).

Deficiency in 3'-phosphoglycolate processing in human cells with a hereditary mutation in tyrosyl-DNA phosphodiesterase (TDP1). *Nucleic Acids Research*, 33(1), 289-297.

doi:33/1/289 [pii]

Zhou, T., Akopiants, K., Mohapatra, S., Lin, P., Valerie, K., Ramsden, D. A., . . . Povirk, L. F.

(2009). Tyrosyl-DNA phosphodiesterase and the repair of 3'-phosphoglycolate-terminated DNA double-strand breaks. *DNA Repair*, 8(8), 901-911.

doi:<https://doi.org/10.1016/j.dnarep.2009.05.003>

VITA

Ajinkya Sudhir Kawale was born on October 19th, 1990 in Nashik, India and is an Indian citizen. He received a Bachelor of Technology in Biotechnology from Dr. D. Y. Patil University, School of Biotechnology and Bioinformatics, Navi Mumbai, India in 2013 and subsequently came to the USA to pursue further studies. He received a Master of Science in Pharmacology and Toxicology with a concentration in Molecular Biology and Genetics from Virginia Commonwealth University in 2013. After completion of his PhD, he will be working as a Postdoctoral Associate in the lab of Dr. Patrick Sung at Yale University in the Department of Molecular Biophysics and Biochemistry.